

HYDRAULIC CONDUCTIVITY ASSESSMENT FOR A  
VARIABLY-SATURATED ROCK MATRIX

by  
Khayyun Amtair Rahi

---

A Thesis Submitted to the Faculty of the  
DEPARTMENT OF HYDROLOGY AND WATER RESOURCES  
In Partial Fulfillment of the Requirements  
For the Degree of  
MASTER OF SCIENCE  
WITH A MAJOR IN HYDROLOGY  
In the Graduate College  
THE UNIVERSITY OF ARIZONA

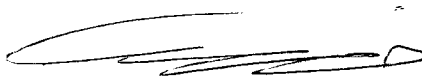
1 9 8 6

STATEMENT BY AUTHOR

This thesis has been submitted in partial fulfillment of requirements for an advanced degree at The University of Arizona and is deposited in the University Library to be made available to borrowers under rules of the Library.

Brief quotations from this thesis are allowable without special permission, provided that accurate acknowledgment of source is made. Requests for permission for extended quotation from or reproduction of this manuscript in whole or in part may be granted by the head of the major department or the Dean of the Graduate College when in his or her judgment the proposed use of the material is in the interests of scholarship. In all other instances, however, permission must be obtained from the author.

SIGNED: \_\_\_\_\_

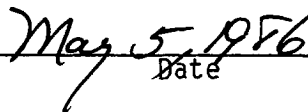


APPROVAL BY THESIS DIRECTOR

This thesis has been approved on the date shown below:

  
\_\_\_\_\_

Daniel D. Evans  
Professor of Hydrology  
and Water Resources

  
\_\_\_\_\_

Date

بِسْمِ اللّٰهِ الرَّحْمٰنِ الرَّحِیْمِ  
وَجَعَلْنَا مِنَ الْمَاءِ كُلِّ شَيْءٍ حَيٍّ  
صَدَقَ اللّٰهُ الْعَظِیْمُ

إلى والديّ الأكرم

To my parents

## ACKNOWLEDGMENTS

I would like to thank Dr. Daniel Evans for his patience, guidance, and support concerning this research project. I wish to thank also Dr. Arthur Warrick and Dr. Jim Yeh for their valuable comments and review of the manuscript.

I also gratefully acknowledge the student members of the unsaturated fractured rock group, especially Ingrid Anderson, for assistance and support. Special thanks are due to Dr. Rien van Genuchten, U.S. Salinity Laboratory, for his advice and permission to use the computer code RETC.

I would like to express my appreciation to Dr. Adnan Y. Mohammed, the Iraqi Cultural Attaché, and all the staff of the Iraqi Cultural Office, Washington, DC, for their support and encouragement during the course of my studies in the United States.

I am also grateful to Sally Adams, who helped with the typing of this manuscript, and Lorenzo Lujan, who helped build the equipment used for the study.

Finally, I would like to acknowledge both the Iraqi State Organization for Land Reclamation and the U.S. Nuclear Regulatory Commission for providing the financial support needed to accomplish this work.

## TABLE OF CONTENTS

	Page
LIST OF ILLUSTRATIONS . . . . .	vii
LIST OF TABLES . . . . .	x
ABSTRACT . . . . .	xi
1. INTRODUCTION . . . . .	1
2. LITERATURE REVIEW . . . . .	3
Prediction of Hydraulic Conductivity . . . . .	3
The Hydraulic Radius Approach . . . . .	3
The Statistical Approach . . . . .	7
Measurement of the Unsaturated Hydraulic Conductivity . . . . .	16
3. MATERIALS AND METHODS . . . . .	20
Sample Preparation . . . . .	20
Prediction of the Unsaturated Hydraulic Conductivity . . . . .	23
Determination of the Rock Water Retention Data . . . . .	25
The Pressure Plate Extractor Method . . . . .	25
The Tempe Cell . . . . .	28
The 15-bar Pressure Plate Extractor . . . . .	28
The Psychrometer Method . . . . .	28
Measurement of the Saturated Hydraulic Conductivity . . . . .	29
Measurement of the Unsaturated Hydraulic Conductivity . . . . .	31
4. RESULTS AND DISCUSSION . . . . .	35
Water Retention Data . . . . .	35
The Ceramic Plate Method . . . . .	35
The Psychrometer Method . . . . .	37
Discussion of the Water Retention Results . . . . .	45
The Outflow Method for Measuring K . . . . .	54
Measurement of Saturated Hydraulic Conductivity . . . . .	56
Prediction of the Unsaturated Hydraulic Conductivity . . . . .	56
Calculation of K Using the Water Retention and $K_s$ Data . . . . .	63
Calculation of K Using the Measured Water Retention, K, and $K_s$ Data . . . . .	69
Prediction of Diffusivity . . . . .	70

TABLE OF CONTENTS--Continued

	Page
5. SUMMARY AND CONCLUSIONS . . . . .	77
APPENDIX A: DERIVATION OF MUALEM'S EQUATION . . . . .	81
APPENDIX B: RETC COMPUTER CODE LISTING . . . . .	85
REFERENCES . . . . .	102

## LIST OF ILLUSTRATIONS

Figure	Page
1. Tempe cell . . . . .	26
2. 15-bar pressure plate extractor . . . . .	27
3. Modified Tempe cell used to measure the saturated hydraulic conductivity . . . . .	30
4. Tempe cell setting used to measure the unsaturated hydraulic conductivity . . . . .	32
5. Observed and fitted water retention curves for tuff sample T1 as defined by the pressure extractor method . . . . .	38
6. Observed and fitted water retention curves for tuff T2 as defined by the pressure extractor method . . . . .	39
7. Observed and fitted water retention curves for tuff T3 as defined by the pressure extractor method . . . . .	40
8. Observed and fitted water retention curves for tuff T4 as defined by the pressure extractor method . . . . .	41
9. Observed and fitted water retention curves for tuff T5 as defined by the pressure extractor method . . . . .	42
10. Observed and fitted water retention curves for sandstone S1 by the pressure extractor method . . . . .	43
11. Observed and fitted water retention curve for sandstone S2 by the pressure extractor method . . . . .	44
12. Observed and fitted water retention curves for tuff TS1B (subsample of T1) as defined by the psychrometer method . . . . .	47

LIST OF ILLUSTRATIONS--Continued

	Page
13. Observed and fitted water retention curves for tuff TS2A (subsample of T4) as defined by the psychrometer method . . . . .	48
14. Observed and fitted water retention curve for NTS G4 as defined by the psychrometer method . . . . .	49
15. Observed and fitted water retention curves for sample NTS GU3 by the psychrometer method . . . . .	50
16. Comparison of the water retention curves as defined by the pressure extractor and the psychrometer methods for tuff T1 . . . . .	52
17. Comparison of the water retention curves as defined by the pressure extractor and the psychrometer methods for tuff T4 . . . . .	53
18. Observed and fitted hydraulic conductivity curves for tuff T1 (pressure extractor method) . . . . .	57
19. Observed and fitted hydraulic conductivity curves for tuff T2 (pressure extractor method) . . . . .	58
20. Observed and fitted hydraulic conductivity curves for tuff T3 (pressure extractor method) . . . . .	59
21. Observed and fitted hydraulic conductivity curves for tuff T4 (pressure extractor method) . . . . .	60
22. Observed and fitted hydraulic conductivity curves for tuff T5 (pressure extractor method) . . . . .	61
23. Observed and fitted hydraulic conductivity curves for sandstone S1 (pressure extractor method) . . . . .	62
24. Comparison of fitted hydraulic conductivity curves from pressure extractor and from the psychrometer methods to the observed data for tuff T1 . . . . .	65
25. Comparison of fitted hydraulic conductivity curves from pressure extractor and from the psychrometer methods to the observed data for tuff T4 . . . . .	66

LIST OF ILLUSTRATIONS--Continued

	Page
26. Observed and fitted hydraulic conductivity (by modifying equation 21) for tuff T1 . . . . .	67
27. Observed and fitted hydraulic conductivity (by modifying equation 21) for tuff T4 . . . . .	68
28. Observed and fitted diffusivity curves for tuff T1 . . . . .	72
29. Fitted and observed diffusivity curves for tuff T2 . . . . .	73
30. Fitted and observed diffusivity curves for tuff T3 . . . . .	74
31. Observed and fitted diffusivity curves for tuff T4 . . . . .	75
32. Fitted and observed diffusivity curves for tuff T5 . . . . .	76

LIST OF TABLES

Table		Page
1.	Rock sample properties . . . . .	21
2.	The chemical composition of the water used to saturate the rock cores . . . . .	22
3.	List of the cores for which the water retention data were obtained by the pressure plate extractor method . . . . .	36
4.	Samples studied by the psychrometer method and their pressure ranges . . . . .	46

## ABSTRACT

Water flow through unsaturated rock has received increasing attention recently. In order to solve unsaturated flow problems, it is necessary to determine the unsaturated hydraulic conductivity,  $K$ . A model which predicts  $K$  from water retention data was evaluated for rock matrices. It includes three unknown parameters to be determined from experimental data. To verify the model,  $K$  was measured by the outflow method. Water retention data were determined by two methods, the pressure plate extractor and the psychrometer. Near saturation, the water retention curve was best estimated by the pressure extractor method. The outflow method gave reliable measurements of  $K$  at low negative pressure heads ( $\geq -1000$  cm of water). The predicted  $K$  deviated from the experimental values when only the water retention data were used to estimate the model parameters. When the measured  $K$  was incorporated in the parameter estimation process, the deviation was reduced considerably.

## CHAPTER 1

### INTRODUCTION

Fluid flow and mass transport in unsaturated fractured rock have received increasing attention in recent years. This can be attributed in part to the potential use of unsaturated rock as the host geologic medium for high level radioactive-waste disposal. Water flow through unsaturated rocks may be a principal mechanism for the transport of radioactive contaminants from the repository to the accessible environment. The flow occurs through the rock fractures as well as the rock matrix. However, fracture flow will not be considered here, and the terms rock, rock matrix, and consolidated porous medium will be used interchangeably to refer to the rock matrix.

The solution of ground-water flow problems in unsaturated porous media requires, among other things, that hydraulic conductivities be known in advance. Hydraulic conductivity usually varies spatially. Its direct measurement is difficult in the laboratory and even more difficult in situ. In addition, unsaturated hydraulic conductivity ( $K$ ) is a function of the degree of saturation. Therefore, investigators turn to the use of computational models to calculate  $K$  from the more easily measured water retention curve. A water retention curve is a plot of rock water content versus negative pressure head (or suction). The term pressure head will be used instead of negative

pressure head throughout this study, and its numerical values will be assumed positive for convenience.

The most widely used model is that of Mualem (1976), specifically the closed-form equations as given by Van Genuchten (1978 and 1980). The model calculates  $K$  as a function of water content or pressure head from the experimentally determined moisture retention curve. This model has been applied to nonconsolidated porous media and shows excellent agreements between the observed and calculated data (Van Genuchten, 1980; Yates, Van Genuchten and Warrick, 1984; and Van Genuchten and Nielsen, 1985).

Peters et al. (1984) were probably the first to apply the model to consolidated media (tuffaceous materials). Their experimental results for the rock retention data agrees reasonably with the model, but they did not measure  $K$  experimentally to verify the calculated data. The authors used a psychrometer to measure the water potential of different water contents to define the retention curve for their samples. As it will be shown later, the psychrometer method is not suitable to define the retention curve in the wet range.

The purpose of this study is to further examine the application of the model to consolidated media and to compare the calculated conductivities to those directly measured for the same rock cores. More consideration will be given to the wet range (pressure heads between 0 and 1000 cm). The rock retention data, which are needed to calculate  $K$ , are produced by a pressure extractor similar to the one that is used in soil physics applications.

## CHAPTER 2

### LITERATURE REVIEW

#### Prediction of Hydraulic Conductivity

There are two main approaches for the calculation of unsaturated hydraulic conductivity. The first is based on the concepts of hydraulic radius (the cross-sectional area divided by the wetted perimeter) and tortuosity. The Kozeny-Carmen equation (Carmen, 1939) and the Burdine theory (Burdine, 1953) fall into this category. The Burdine equation will be examined in more detail in this study.

The other approach is statistical and was first developed by Childs and Collis-George (1950). This approach is based on the probability of the continuity of pores in adjacent places within the porous medium. Sometimes this approach is called the cutting-rejoining model.

Both of these approaches depend on the pore size distribution, but the statistical approach (with the exception of the model developed by Mualem (1976)) does not take tortuosity into account explicitly.

In the following sections the two approaches will be labeled the hydraulic radius approach and the statistical approach.

#### The Hydraulic Radius Approach

The hydraulic radius concept was introduced by Blake (1922). He used the hydraulic radius ( $R$ ) to derive a permeability equation, assuming random packing, and considered  $R$  as the ratio of total

porosity to the surface area of the particles for a unit area of the porous medium. The Blake equation to calculate  $k_s$  can be written as

$$k_s = \frac{1}{bS_s^2} \frac{\phi^2}{(1-\phi)^2} \quad (1)$$

where  $k_s$  is the saturated permeability ( $L^2$ ),  $\phi$  is total porosity,  $b$  is a constant, and  $S_s$  is the specific surface of particles.

A similar equation was also derived by Kozeny (1927). Kozeny considered the porous medium to have a uniform pore-size distribution.

The general form of Kozeny's equation (follows from Poiseuille law) is given by:

$$k_s = \frac{\phi R^2}{C} \quad (2)$$

where  $C$  is a constant, and  $R$  is the hydraulic radius. An implicit account of tortuosity is included in the constant  $C$ .

Carmen (1939) refined equation (2) by introducing the concept of tortuosity,  $T$ , explicitly. He defined  $T$  by the following relation

$$T = \left(\frac{L_e}{L}\right)^2 \quad (3)$$

where  $L_e$  is the effective length of the flow path, and  $L$  is the length of the porous medium column. Carmen defined the Kozeny constant  $C$  as the product of  $T$  and a shape factor.

Later, Wyllie and Spangler (1952) measured tortuosity by means of electrical resistivity of the fluid-contained porous medium. They concluded that tortuosity for a consolidated medium is higher than that of nonconsolidated media by several orders of magnitude.

The application of the Kozeny type equation is limited to porous media with narrow pore size distribution. Serious difficulties arise when the equation is applied to material with broad pore size distributions, especially when numerous small particles, which contribute largely to surface area, may together act toward fluid flow as a single aggregate of much smaller area (Childs and Collis-George, 1952).

Burdine (1953) introduced a theory which views a porous medium as groups of parallel capillary tubes, each group with different permeability and uniform pore-size distribution. Unlike previous theories, Burdine's theory no longer assumes that air replaces water in all pores simultaneously, but assumes that portions are completely filled with air sequentially, beginning with the largest diameter portion. He concluded that tortuosity is a function of degree of saturation and is approximately equal to the square of the effective saturation  $S_e$ , where  $S_e$  is given by the following relationship:

$$S_e = \frac{\theta - \theta_r}{\theta_s - \theta_r} \quad (4)$$

where  $\theta$  is the porous medium water content by volume. The subscripts  $s$  and  $r$  refer to the saturated and residual water contents, respectively.

Burdine's equation for unsaturated hydraulic conductivity,  $K$ , is

$$K = K_s S_e^2 \frac{\int_0^{S_e} \frac{1}{h(x)^2} dx}{\int_0^1 \frac{1}{h(x)^2} dx} \quad (5)$$

where  $K_s$  is the saturated hydraulic conductivity, and  $h$  is the pressure head, which is a function of  $S_e$  ( $h$  is taken to be positive).

An empirical expression relating the effective saturation to pressure head was presented by Brooks and Corey (1964). It is of the form

$$h = [ \alpha S_e^{\frac{1}{n}} ]^{-1} \quad (6)$$

where  $\alpha$  and  $n$  are constant parameters to be determined from the experimental moisture retention data. Equation (6) is substituted in (5), and the latter is solved by Brooks and Corey (1964). Their solution is:

$$K = K_s (S_e)^{\frac{2+3n}{n}} \quad (7)$$

According to Brooks and Corey,  $n$  could have any value greater than zero, being small for media having broad pore-sized distribution and large for media with relatively uniform pore size. Thus, it was suggested that  $n$  be called the pore-size distribution index. However, Van Genuchten and Nielsen (1985) suggested that  $n$  should be more than or equal to two.

### The Statistical Approach

The statistical approach relates hydraulic conductivity to pore-size distribution. The pore-size distribution is derived from the interpretation of the retention curve of the porous medium. The theory behind this approach is based upon the probability of the continuation of pores of different sizes and the contribution of such connected pores to the conductivity of the porous medium.

Childs and Collis-George (1950) (referred to as CCG later) pioneered this approach. They developed an equation for the permeability,  $k$ , which takes into account the various sequences of pore sizes when the pores are randomly arranged. Their equation includes an empirical constant,  $M_0$  which has yet to be determined directly, and the equation is

$$k = M_0 \sum_{\rho=0}^{\rho=R_m} \sum_{\sigma=0}^{\sigma=R_m} \sigma^2 f(\rho) dr f(\sigma) dr \quad (8)$$

where  $f(\rho)dr$  is the cross-sectional area devoted to pores of radius  $\rho$  to  $\rho+dr$ ,  $\sigma$  and  $f(\sigma)dr$  is the cross-sectional area devoted to pores of radius  $\sigma$  to  $\sigma+dr$ . The summation is stopped at that pore size,  $R_m$ , of the largest pore that remains filled with water. The flow in each single pore, which consists of two sections in series, is assumed to be governed by the section with the smaller diameter. The constant  $M_0$  is determined by matching the calculated and experimental curves at a single point, usually taken as the value of the saturated hydraulic conductivity,  $K_s$ . Hence,  $M_0$  is given by

$$M_o = \frac{K_{sm}}{K_{sc}} \quad (9)$$

where the subscripts m and c refer to the measured and calculated values, respectively.

Marshall (1958) (referred to as M later) defined the following form of Poiseuille equation for porous medium

$$v = - \frac{\theta r_t^2}{8\mu} \frac{dH}{dL} \quad (10)$$

where  $v$  is mean velocity,  $\mu$  is viscosity,  $dH/dL$  is the potential gradient, and  $r_t$  is the radius of the equivalent tube that controls flow through porous material. He used the statistical model to calculate  $r_t^2$  to be:

$$r_t^2 = \frac{\theta}{N^2} [r_1^2 + 3r_2^2 + 5r_3^2 + \dots + (2N-1)r_N^2] \quad (11)$$

where  $N$  is the number of equal fractions of pore size classes filled with water, and  $r_1 > r_2 > \dots > r_n$  is the radius of a pore in the porous media. Therefore,  $v$  can be written as

$$v = - \frac{\theta^2}{8N^2\mu} \left( \frac{dH}{dL} \right) (r_1^2 + 3r_2^2 + 5r_3^2 + \dots + (2N-1)r_N^2) \quad (12)$$

By incorporating Darcy's law in equation (12), Marshall (1958) gave the following equation for  $k$ :

$$k = \frac{\theta^2}{8N^2} (r_1^2 + 3r_2^2 + 5r_3^2 + \dots + (2N-1)r_N^2) \quad (13)$$

Both of the previous models are based on the assumption that the effective area normal to the flow is equal to the liquid-filled porosity.

Millington and Quirk (1960) (referred to as MQ later) did away with the assumption that the effective area normal to the flow is equal to the liquid filled porosity. They derived an equation which takes into account area interaction as well as pore interaction, while CCG and M models consider the pore interaction only. The MQ equation to calculate  $k$  is given by

$$k = \frac{1}{8} \frac{\phi^{4/3}}{M_T} (r_1^2 + 3r_2^2 + 5r_3^2 + \dots + (2M_T-1)r_{M_T}^2) \quad (14)$$

where  $M_T$  is the total number of pore intervals. The effect of keeping  $M_T$  constant is to decrease the computed permeability at low water contents (Green and Corey, 1971).

The CCG, M, and MQ models assume isotropic conditions, random pore-size distribution and no shrinking or swelling of the porous medium. Each model was tested by its original authors through comparison of the calculated hydraulic conductivity  $K$  and measured  $K$  for sands and slate dust, and generally the results were satisfactory. The MQ model was also applied to consolidated porous media by its authors, but the results were in poor agreement with the experimental data. The deviation was attributed to the modification of the continuity of the original pore space by cementation, as well as to possible anisotropy resulting from downward compression of the consolidated porous media.

Nielsen, Kirkham, and Perrier (1960) compared values calculated with the CCG and M methods with measured values of K for four field soils over a pressure head range of 0 to 100 cm of water. They concluded that the CCG method with a constant value for matching factor yielded fairly reliable results for two of the four soils tested. These two soils could be considered as having a single grain structure. The other soils deviated from the CCG model because of their well established structure and their behavior as cemented material, violating one of the assumptions of the CCG model. They also found that the values of K obtained with the M method were greater than measured values. However, a better match between the measured and calculated K by the M method was obtained when a matching factor was introduced to the M equation.

Jackson, Reginato and Van Bavel (1965) compared the measured values of K with values calculated by the CCG, M, and MQ models for graded sand over a wide range of water contents. The CCG and M methods, with a matching factor for the latter, did not predict the shape of the conductivity curve (K vs  $\theta$ ).

The MQ method showed good results in terms of predicting the shape of the curve, but required a matching factor to predict the absolute shape of the curve. The matching factor as reported by the authors was the ratio of measured to calculated  $K_s$ .

Kunze, Uehara and Graham (1968) cited improvement in the MQ model when the parameter  $\phi$  is used instead of  $\phi^{4/3}$ . The modified version of equation (14) (Kunze et al., 1968) is written as

$$K(\theta)_i = \frac{K_{sm}}{K_{sc}} \frac{30\gamma^2 \phi}{\rho g \mu M_T^2} \sum_{j=1}^N [(2j + 1 - 2i) \frac{1}{h_j^2}] \quad i=1,2,\dots,N \quad (15)$$

where

$\gamma$  = surface tension of water

$\rho$  = density of water

$g$  = gravitational constant

In equation (15), the pore radius,  $r$ , is replaced by  $h$ . Jackson (1972) compared the M and MQ models with the matching factor. He concluded that the only difference between the two approaches is the exponent  $p$  in the following equation:

$$K(\theta)_i = K_s \left(\frac{\theta_i}{\theta_s}\right)^p \frac{\sum_{j=1}^N [(2j + 1 - 2i) h_j^{-2}]}{\sum_{j=1}^N [(2j - 1) h_j^{-2}]} \quad (16)$$

where  $p$  is 0 for the M method and 4/3 for the MQ method. The author estimated  $p$  to be 1 in average, which is consistent with the value suggested by Kunze et al. (1968).

Kunze et al. (1968) indicated that the matching factor may be a function of the bubbling pressure (air entry value), the range of pressure in the water retention curve, and soil texture, where it decreases as the textural size decreases.

Green and Corey (1971) revised the M method equation (12) by replacing  $\theta$  by  $\phi$  and  $N$  by  $M_T$  (the total number of pore-size classes). Hence, the M equation takes the form:

$$K(\theta)_i = \frac{K_s}{K_{sc}} \frac{30\gamma^2}{\rho g \mu} \frac{\phi}{M_T^2} \sum_{j=1}^N [(2j + 1 - 2i)h_j^{-2}] \quad i=1,2,\dots,N \quad (17)$$

Green and Cory compared measured values of  $K$  against calculated values using the M method with the matching factor (equation (13)), the MQ method with the matching factor (equation (16)), the MQ method (equation (14)), and the M method with the modification that they introduced (equation 17). The curves of  $K$  vs  $\theta$  produced showed that the M and MQ with all the modifications gave nearly the same results for a given porous medium, and there was little difference between the modified MQ equations (15) and (16). The revised M method (equation (17)) offered no advantages over the other methods.

The effect on the calculated conductivity of changing the number of pressure classes was investigated by Kunze et al. (1968) and Green and Corey (1971). Kunze et al. (1968) showed that a decrease in the number of pressure classes increased the conductivity and required a small matching factor for the MQ method. They also found that an increase of pressure classes gave greater deviation from the experimentally measured  $K$ -values. They recommended a number of pressure classes between five and ten. Green and Corey (1971) chose 20 pressure classes based on the evaluation of the effect of changes in the number (5, 10,

20, and 50) on the relation between predicted and measured  $K$  vs  $\theta$  curves. They found that it is difficult to accurately represent the water content-pressure head curves when the number is less than 10. Marshal (1958) suggested a large number of pressure head classes to improve the match between measured and calculated  $K$ .

The statistical model, as represented by the CCG method, ignores the effect of the larger pore in the sequence of two pores on the flow rate which overestimates the influence on the flow by the smaller pore (Childs and Collis-George, 1951). Mualem (1976) modified the CCG model by taking into account the effect of the larger pore section in the sequence. He assumed that the pore configuration may be replaced by a pair of capillary elements whose lengths are related to their radii by

$$\frac{L_1}{L_2} = \frac{r_1}{r_2} \quad (18)$$

where  $L$  is the length of the tube, and  $r$  is its radius. Since the radius of the pore is proportional to its length, a more important influence on  $K$  is given to the large pore by taking into account its length and not only its cross-section. Mualem's model shows that  $K$  varies with the product  $r_1 r_2$  instead of  $r_1^2$ , where  $r_1$  is the radius of the smaller section in the sequence.

After introducing a correction factor to account for partial correlation between pores in sequence and tortuosity, Mualem presented the following equation:

$$K(S_e) = K_s S_e^\lambda \left[ \frac{\int_0^{S_e} \frac{1}{h(x)} dx}{\int_0^1 \frac{1}{h(x)} dx} \right]^2 \quad (19)$$

The exponent  $\lambda$  in equation (19) (referred to as Mualem's equation later) was estimated by applying the equation to 45 soils and using the least squares method. It was found to be equal to 0.5 (Mualem, 1976). Yates, Van Genuchten and Warrick (1985) used a non-linear optimization technique to examine the exponent  $\lambda$  and also concluded that the value of 0.5 gave the best fit.

A closed-form solution for equation (19), with  $\lambda$  equal to 0.5, was presented by Van Genuchten (1978, 1980). The solution was achieved by substituting the following empirical relationship between  $S_e$  and  $h$

$$S_e = [1 + (\alpha h)^n]^{-m} \quad (20)$$

where  $\alpha$ ,  $n$  and  $m$  are parameters to be estimated from experimental data.

The Van Genuchten equation from equation (19) is

$$K(S_e) = K_s S_e^{\frac{1}{2}} \left[ 1 - (1 - S_e)^{\frac{1}{m}} \right]^2; \quad \begin{array}{l} m = 1 - \frac{1}{n} \\ 0 < m < 1 \\ n > 1 \end{array} \quad (21)$$

He also solved equation (19) by substituting into it the relation given by equation (5). In this case  $K$  is given by

$$K(S_e) = K_s S_e^{\frac{5}{2} + \frac{2}{n}} \quad (22)$$

When comparing (21) and (22), he found large deviation between the two models at or near the bubbling pressure. However, this deviation decreases substantially for  $K$  at large negative pressures.

The parameter  $n$  can be considered as the pore-size distribution index. It usually assumes higher values for porous media with narrow pore-size distributions. In this case,  $m$  would be close to one.

Yates et al. (1984) estimated  $\alpha$ ,  $m$ ,  $\theta_r$  and possibly  $\lambda$  in equations (19), (20), and (21) by minimizing the sum of square deviations between observed and calculated data. They showed that the overall accuracy in fitting the hydraulic parameters can be improved when the observed and calculated data for  $K$  and  $\theta$  are used for the minimization scheme. Mualem's exponent  $\lambda$  was shown to be equal to -2.

Van Genuchten (1978, 1980) solved equation (4) (Burdine Equation) by substituting equation (20) into it. The hydraulic conductivity becomes

$$K(S_e) = K_s S_e^2 \left[ 1 - \left( 1 - S_e^{\frac{1}{m}} \right)^m \right]^m ; \quad \begin{array}{l} m = 1 - \frac{2}{n} \\ 0 < m < 1 \\ n > 2 \end{array} \quad (23)$$

Because  $K$  as given by equation (23) will go to zero as  $n$  goes to two, the application of the Burdine model is very limited for porous media with broad pore-size distribution (i.e., material with  $n \leq 2$ ) (Van

Genuchten and Nielsen, 1984). And since tuffaceous materials, which are the subject of this study, usually have a broad size distribution, the Burdine model will not be considered hereafter.

Extensive review of the relationships that describe the soil water retention curve was presented by Van Genuchten and Nielsen (1985). They concluded that equation (20) with  $n > 1$  gives the best fit to the observed data, and that it contains five independent parameters:  $\theta_r$ ,  $\theta_s$ ,  $\alpha$ ,  $n$ , and  $m$ , where  $\theta_r$  and  $\theta_s$  are empirical parameters that can be determined by fitting the model to observed data. They indicated that the parameter  $\alpha$  is approximately equal to the inverse of the bubbling pressure when  $m/n$  is small and equal to the inverse of the pressure head at the inflection point when  $m/n$  is large. In addition, the product  $mn$  is found to be a function of soil texture.

As far as the relationship between  $n$  and  $m$  is concerned, the same authors suggested that variable  $n$  and  $m$  would give the best fit to experimental data as compared to the restriction cases on  $n$  and  $m$  ( $m = 1 - 1/n$  and  $m = 1 - 2/n$ ). Also, when  $1 < n < 2$  (i.e. broad pore-size distribution),  $K$  curves become sensitive to change in the slope of the retention curves, especially near saturation.

#### Measurement of the Unsaturated Hydraulic Conductivity

Various methods to measure the unsaturated hydraulic conductivity ( $K$ ) for porous media are described in the literature. Klute (1972) presented an extensive review of these methods.

Most of the methods were designed for use with unconsolidated porous media. Their usefulness for consolidated porous media is limited, and few can be adapted for this purpose. One of the promising methods is a method commonly known as the outflow method. By this method the hydraulic conductivity can be measured by desaturating a saturated rock core by placing it in a pressure cell and applying air pressure to it in small increments. The water is forced to flow out of the core through a porous plate under the pressure. The rate at which the water flows is recorded, and from it the hydraulic conductivity can be computed. Hence, the method is the solution of the inverse problem to calculate the conductivity of the material. More description of the outflow method will be given in the next chapter.

Gardner (1956) was the first to introduce the outflow method for estimating  $K$  from pressure plate outflow data. He solved the inverse water flow equation in one dimension. In order to solve the problem analytically, Gardner assumed that:

- 1) the effect of gravity is negligible,
- 2)  $K$  is constant for the outflow caused by applying small pressure increment to the sample,
- 3) the water content is a linear function of  $h$  over the small pressure increment,

and

- 4) the impedance of the pressure plate is neglected.

Miller and Elrick (1958) refined the outflow method by taking into account the plate impedance. Their method requires the experimental

determination of the plate impedance and neglects the effect of the hydraulic contact (between the sample and the pressure plate) impedance.

The method was further improved by Rijtema (1959) who did away with the need to experimentally determine the plate and the contact impedance. Instead, the plate and contact impedance can be determined from the plot of outflow volumes vs time. For more detail about the procedure, the interested reader should refer to the original paper.

Kunze and Kirkham (1962) considered the assumption of constant conductivity for a given pressure increment (assumption number 2 above) invalid. They assumed that  $K$  is approximately constant for the first 10-15 percent of the outflow for that increment, then  $K$  decreases dramatically as  $\theta$  decreases. Their approach reduces the time needed to accomplish the measurement, because only the flow rate during the first one to two hours and the total outflow for a given pressure increment needs to be recorded.

The theoretical and experimental aspects of the outflow method were examined by Jackson, Van Bavel and Reginato (1963). They concluded that the assumption of constant conductivity is invalid in most cases due to the difficulty of selecting a pressure increment small enough to make the assumption valid. They suggested the use of the outflow method as presented by Kunze and Kirkham (1962), when  $K$  is not constant and the plate impedance is negligible. Mualem and Klute (1984) suggested that the plate impedance is a function of water content of the sample, it increases as the water content decreases.

Considering the low permeability materials that were used in this study, the plate impedance could be neglected compared to the rock core impedance. Also,  $K$  could not be constant for a given pressure increment. However, the pressure increments used are considered reasonably small to assume that  $K$  is constant for the first 10-15 percent of the outflow.

Thus, the Kunze and Kirkham version of the outflow method will be followed in the course of this study.

## CHAPTER 3

### MATERIALS AND METHODS

#### Sample Preparation

Two types of rock were tested: Coconino sandstone from Strawberry, Arizona, and Apache Leap tuff from Superior, Arizona. The samples were obtained by core drilling using bits of different diameters (Table 1). Most of the samples were cut to lengths of about five centimeters. A total of nine samples were studied. Six samples (5 tuff and 1 sandstone) were tested for their hydraulic conductivity as well as their moisture retention data. The other 3 (2 tuff and 1 sandstone) were tested for their retention data only.

The samples were first dried, and their weight and volume were measured for the purpose of the bulk density ( $\rho_B$ ) determination. All cores were saturated by placing the oven-dried sample in a vacuum dessicator. A vacuum pump was used to evacuate the air in the dessicator for at least two hours. Tap water was introduced into the evacuated dessicator until most of the sample was immersed in water. Table 2 shows the chemical composition of the water used. A continuous vacuum was maintained for 4 to 6 hours. The vacuum pump was turned off, but the dessicator was sealed and retained the vacuum for an additional 12 to 24 hours. At this stage, the sample are assumed to be fully saturated. Then, the saturated weight was recorded and the water content at saturation was determined. The porosity ( $\phi$ ) of the sample

Table 1. Rock sample properties

Sample #	Rock Type	Diameter (cm)	Length (cm)	Porosity (percent)	Bulk Density (gm/cm <sup>3</sup> )	Grain Density (gm/cm <sup>3</sup> )
S1	sandstone	5.00	4.88	16.40	2.18	2.60
S2	sandstone	5.00	1.50	17.50	2.16	2.62
T1	tuff	7.63	4.84	18.60	2.09	2.57
T2	tuff	7.63	4.81	17.80	2.11	2.57
T3	tuff	7.63	4.84	17.76	2.12	2.57
T4	tuff	6.32	5.04	20.00	2.14	2.58
T5	tuff	6.32	5.01	17.00	2.15	2.59
TS1B	tuff	--	--	20.00	1.92	2.42
TS2A	tuff	--	--	18.60	2.03	2.52

Table 2. The chemical composition of the water used to saturate the rock cores\*

Components	Amount (ppm)
Hardness (ppm CaCO <sub>3</sub> )	128
Total dissolved solids (TDS)	315
Calcium	42
Magnesium	5.6
Sodium	41
Chloride	15
Sulfate	44
Alkalinity (as CaCO <sub>3</sub> )	140
pH	7.8

\*After Tucson Water (1984)

is assumed to be equal to the "saturated" water content. The grain density ( $\rho_s$ ) was calculated from the following relation:

$$\rho_s = \frac{\rho_B}{1-\phi} \quad (24)$$

The validity of this calculation relies on the degree of saturation that could be obtained. But it should be a good estimation if we consider the porosity of interest is the effective porosity (i.e., interconnected pores), and in this case the deadend pores are considered a part of the solid portion of the rock.

The grain density of some of the tuff samples were also determined by crushing the samples and sieving the resulting powder through a No. 500 sieve. Then,  $\rho_s$  was measured according to the procedure outlined by Blake (1965). Grain densities resulting from this method were less than those calculated by the method which assumes that  $\phi$  is equal to the saturated water content. This implies that the porosity would be less than the water content of the rock at saturation which makes the powdered rock values of  $\rho_s$  questionable.

#### Prediction of the Unsaturated Hydraulic Conductivity

Hydraulic conductivity as a function of water content was calculated by equation (21). The equation requires the knowledge of five parameters:  $\theta_s$ ,  $\theta_r$ ,  $\alpha$ ,  $n$  or  $m$ , and  $K_s$ . From these parameters,  $\theta_s$  and  $K_s$  are experimentally determined as explained in the previous

section for the former and will be outlined in a coming section for the latter.

The parameters  $\theta_r$ ,  $\alpha$ , and  $n$  were determined by fitting the experimental data of rock water retention using equation (20) (referred to as E1 optimization), or using the rock retention data as well as the hydraulic conductivity data by equations (20) and (21) (referred to as E2 optimization). The objective functions E1 and E2 to be minimized are of the form (Van Genuchten, 1985):

$$E1 = \sum_{i=1}^N [W_i(\theta_i - \hat{\theta}_i)]^2 \quad (25)$$

$$E2 = \sum_{i=1}^N [W_i(\theta_i - \hat{\theta}_i)]^2 + \sum_{i=N+1}^M [W_1 W_2 W_i [K_i - \hat{K}_i]]^2 \quad (26)$$

where  $\theta_i$  and  $\hat{\theta}_i$  are the observed and fitted water contents,  $K_i$  and  $\hat{K}_i$  are the observed and fitted conductivities,  $N$  is the number of retention data points and  $M$  is the total number of observed data points (retention plus conductivity data).

The weighting parameter  $W_i$  is intended to give more or less weight to a given observation point.  $W_1$  and  $W_2$  are also weighting factors. The optimization process is achieved by the computer code RETC (Van Genuchten, 1985) (Appendix B).

The prediction of  $K$  requires the determination of: a) rock water retention data and b) saturated hydraulic conductivity,  $K_s$ . The following is a discussion of the measurement of these rock hydraulic properties.

#### Determination of the Rock Water Retention Data

Two experimental techniques were used to obtain the water retention data.

##### The Pressure Plate Extractor Method

This technique is widely used to define the moisture retention curve for soils (Richards, 1965). To prepare samples for use on the ceramic plate extractor, the core samples were oven dried, weighed and saturated, as mentioned previously, and the saturated weight recorded. The samples were placed individually on a saturated ceramic plate. To assure good contact between the cores and the ceramic plate, a bentonite clay was used along the contact surface of the core and the ceramic plate. The ceramic plate and samples were sealed inside the extractor vessel and a pressure was applied within the vessel by means of nitrogen gas.

As the pressure was increased in the vessel, water in the saturated rock sample moved out of the sample through the ceramic plate and was collected in a burette outside the vessel. Two types of pressure plate extractors were used in this study: the Tempe pressure cell (Figure 1) and the 15-bar pressure plate extractor (Figure 2).

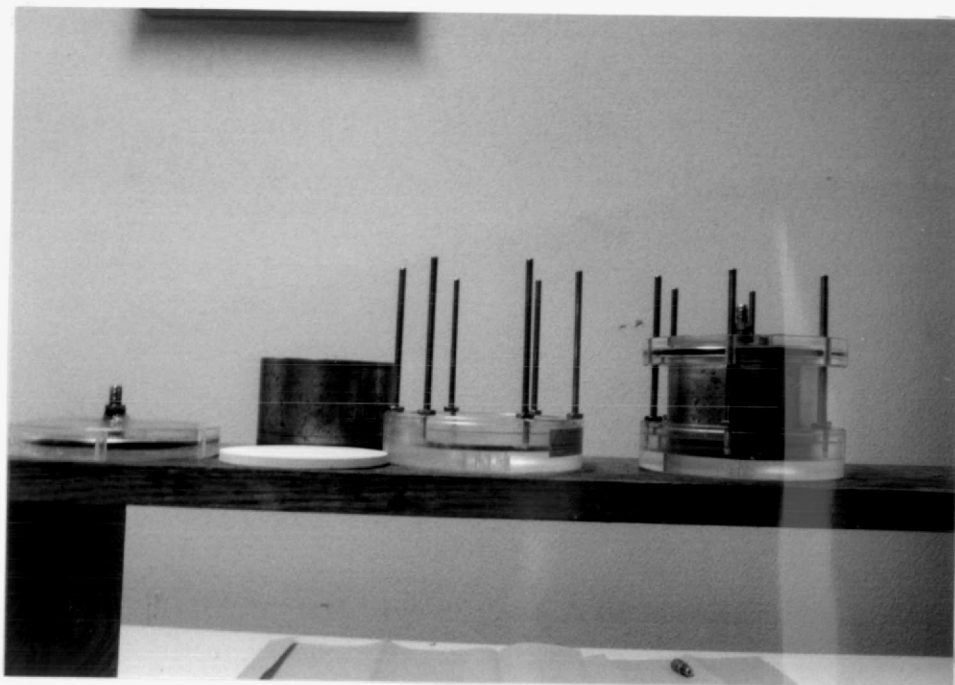


Figure 1. Tempe cell.



Figure 2. 15-bar pressure plate extractor.

The Tempe Cell. The Tempe cell was primarily used to measure  $K$  by the outflow method (see next section). However, moisture retention curve for the 0 to 1000 cm (about 0 to 1.0 bar) range of pressure head can also be determined by the Tempe Cell. The water content  $\theta$  after a given pressure increment is given by:

$$\theta = \theta_{in} - \frac{Q_0}{V_s} \quad (27)$$

where  $\theta_{in}$  is the initial water content,  $Q_0$  is the total volume of water extracted from the sample for a given pressure increment, and  $V_s$  is the bulk volume of the sample. Hence, every applied pressure head will be associated with the proper  $\theta$  to define the water retention curve.

The 15-Bar Pressure Plate Extractor. For this method, the equilibrium was achieved when the outflow water which was collected in the burette remains at constant level for several hours. The pressure was then released and the samples were taken out of the vessel immediately. The water content was determined gravimetrically. The samples were resaturated, replaced in the pressure vessel, and the procedure repeated until the desired range of pressure head values were obtained.

#### The Psychrometer Method

Water retention data for several tuff samples were also obtained using a Thermocouple Psychrometer SC-10A (Decagon Devices, Inc., Pullman, Washington). The psychrometer measures the relative humidity in a closed chamber directly above a moist sample. The water potential in the gas phase, which is assumed to be in equilibrium with

the water potential in the sample, is related to the relative humidity by the equation

$$\psi = \frac{R_g T}{M_w} \ln(RH) \quad (28)$$

where  $\psi$  is total water potential (expressed in pressure units),  $R_g$  is the gas constant,  $T$  is temperature in degrees Kelvin,  $M_w$  is molecular weight of water, and  $RH$  is relative humidity by fraction. Peters et al. (1984) conclude that when water of low salinity is used for the test,  $\psi$  is approximately equal to the matric potential or it is expressed in this investigation as pressure head. Samples which were tested by this method were about  $1 \text{ cm}^3$  in volume. All samples were vacuum saturated before testing with the thermocouple psychrometer. The samples were wiped clean of any free water, placed in the measuring cups of the psychrometer, weighed, and placed into a vapor-tight chamber in the sample changer of the psychrometer. After approximately 1 hour, during which time the samples were allowed to equilibrate thermally, the relative humidity associated with the sample was measured, and the water potential was computed by equation 28. The samples were removed, partially oven dried ( $105^\circ\text{C}$ ) for 5 to 10 minutes, allowed to cool and weighed again and the above process was then repeated. Moisture content was determined gravimetrically for every pressure head.

#### Measurement of the Saturated Hydraulic Conductivity

Saturated hydraulic conductivity,  $K_s$ , was measured with a modified Tempe Pressure Cell (Figure 3). The saturated sample was placed

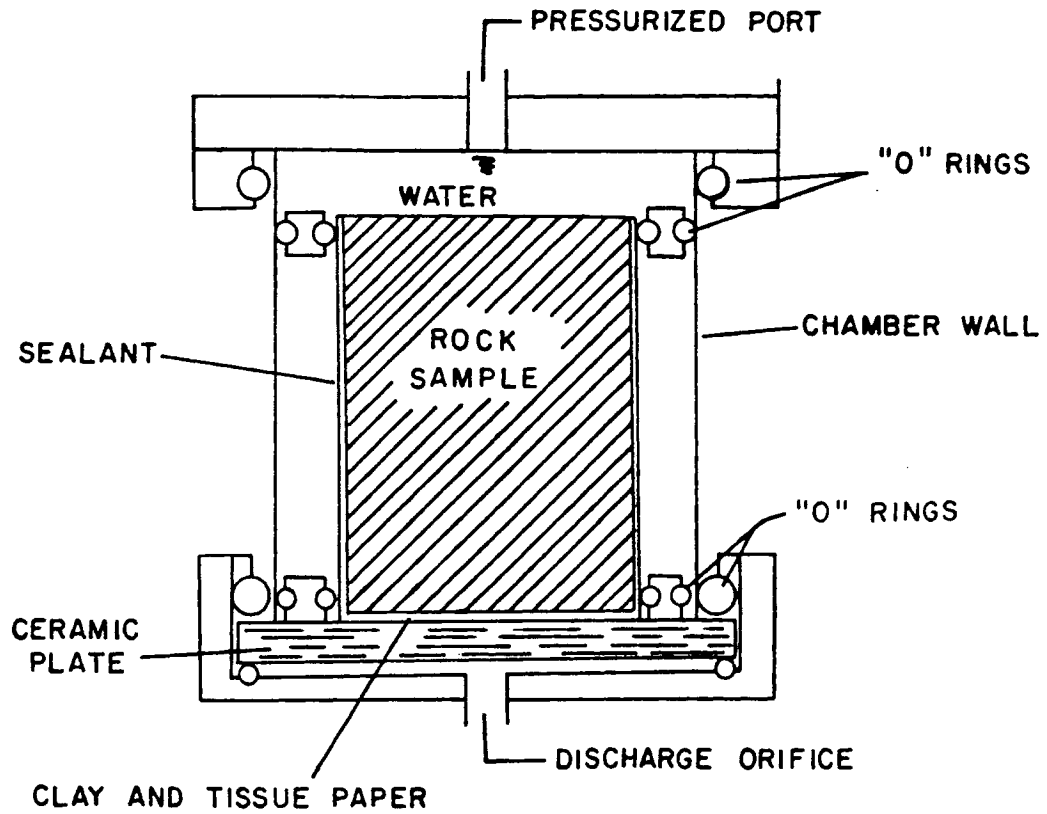


Figure 3. Modified Tempe cell used to measure the saturated hydraulic conductivity.

in the cell and confined by "O" rings on the top and the bottom. The sides of the sample between the "O" rings were sealed with a sealant to prevent flow along the sides. The cell was filled with water and a selected pressure applied. Outflow was collected in a graduated cylinder, and the time to collect  $10 \text{ cm}^3$  was recorded.  $K_s$  can be calculated by Darcy's Law

$$K_s = \frac{Q}{\Delta t} \frac{L}{\Delta h A} \quad (29)$$

where  $Q$  is the outflow volume,  $L$  is the length of the core,  $\Delta t$  is time required to collect  $Q$ ,  $\Delta h$  is the pressure head applied, and  $A$  is the cross-sectional area of the sample.

#### Measurement of the Unsaturated Hydraulic Conductivity

Unsaturated hydraulic conductivity,  $K$ , was measured by the outflow method. The saturated rock core was placed on the ceramic plate after spreading a thin clay layer between them, and the whole assembly was put within the Tempe pressure cell. Figure 4 shows the Tempe cell setting used to measure  $K$ . A pressure was applied, and the rate of water flow out of the sample was recorded. The rate measurement was taken for the first 10 to 15 percent of the total volume outflow,  $Q_0$ , resulting from a given pressure incremental change.

The outflow ratio  $Q/Q_0$ , where  $Q$  is the outflow at any time  $t$ , is plotted on log-log paper against time. The experimental plot is fitted to a set of theoretical type curves (Kunze and Kirkham, 1962). The data should match one of these curves which differ from each other

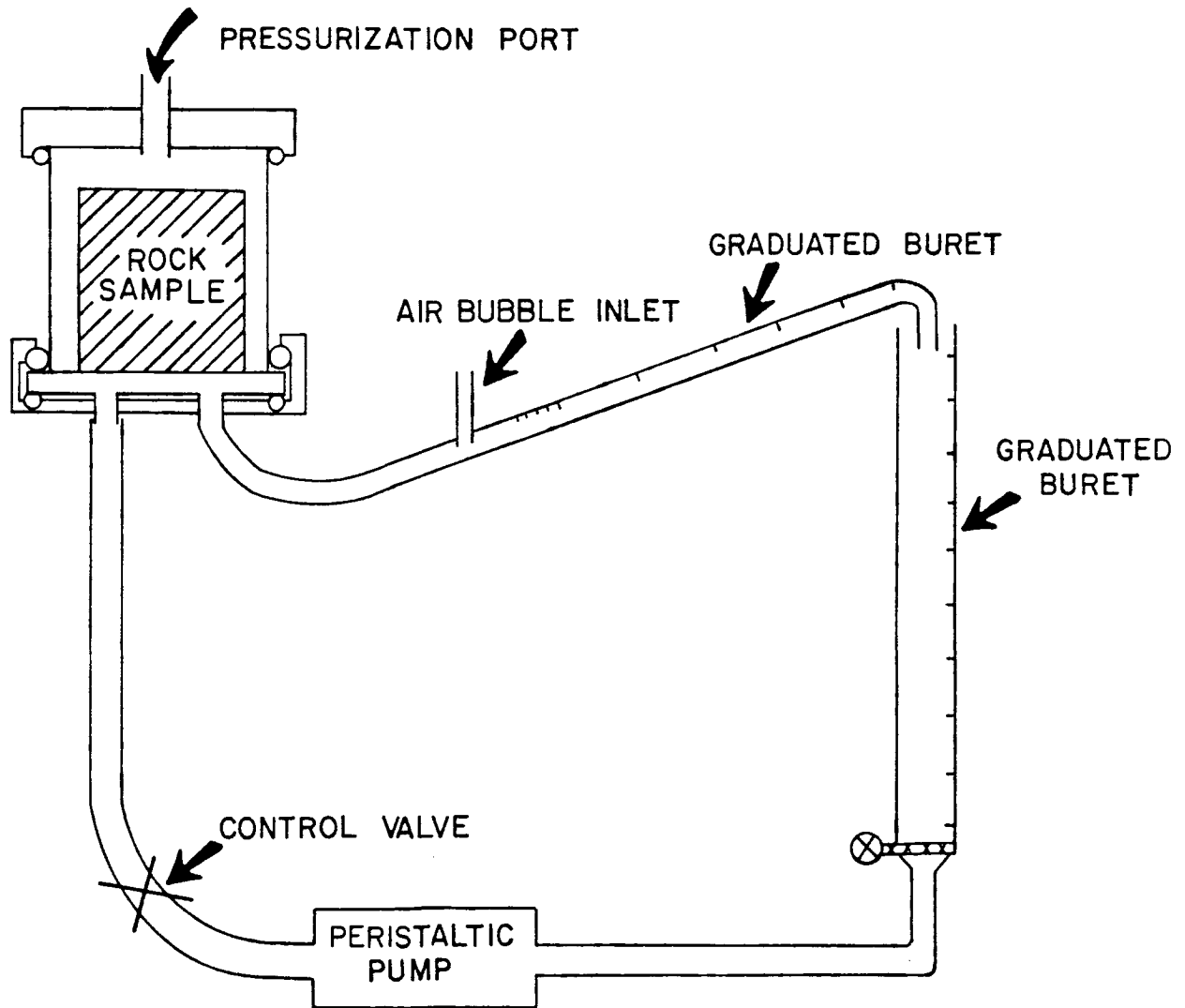


Figure 4. Tempe cell setting used to measure the unsaturated hydraulic conductivity.

by the magnitude of the plate impedance. Once the data are fitted to the proper curve, two parameters are read-- $t_{rp}$  and  $\beta_1^2$ . These parameters are used in the calculation of the rock diffusivity,  $D$ , as follows:

$$D = \frac{L^2}{\beta_1^2 t_{rp}} \quad (30)$$

$K$  is calculated from  $D$  through the relation:

$$K = D \frac{\Delta\theta}{\Delta h} \quad (31)$$

where  $\Delta\theta$  is the change of moisture content of the sample due to the application of a pressure head increment  $\Delta h$ .

When equilibrium was achieved (i.e. water ceased to flow out of the sample), the pressure was increased by a small increment and the above process was repeated. The measurement was stopped at a pressure head of near 1000 cm (1 bar).

The purpose of spreading a thin layer of bentonite clay between the sample and the ceramic plate is to improve the hydraulic contact. However, some extra outflow was introduced from the clay layer. To minimize the extra outflow, the clay was replaced by a "kleenex" tissue. The kleenex method appears to give satisfactory results and does not introduce any measureable extra outflow. But the tissue does not stay saturated for the whole range of pressures used, and a weak contact resulted when high pressure was applied (>600 cm of pressure

head). The best results were obtained when the tissue and a very thin layer of clay were used together.

All measurements described in this chapter were done at a room temperature of 19 to 21°C. The liquid used was tap water with the compositions given in Table 2. No account is taken for the chemical concentrations of the water or any other chemical considerations in the determination of D or K.

## CHAPTER 4

### RESULTS AND DISCUSSION

The results of the predicted K will be discussed after the discussion of the measured K rather than discussing it at the beginning of the chapter as was the case in the earlier chapters because it is more convenient.

#### Water Retention Data

##### The Ceramic Plate Method

The water retention data were obtained for seven cores (2 sandstone and 5 tuff) by the pressure plate extractor method. The pressure head range for which the data were determined varied between 0-1000 to 1-15000 cm (Table 3).

The retention data for all the samples but S2 were determined by the Tempe cell for the 0 to 1000 cm pressure head range. The 15-bar pressure plate was used for those samples which were subjected to pressure heads higher than 1000 cm. The samples were resaturated after being removed from the Tempe cell and then placed in the 15-bar pressure vessel. Data points for sample S2 were all obtained using the 15-bar pressure extractor.

The time required to obtain equilibrium varied from 4 to 7 days for pressure heads less than 1000 cm and as long as 10 days for higher

Table 3. List of the cores for which the water retention data were obtained by the pressure plate extractor method

Sample Code	Pressure Head Range (cm)
T1	0 - 9500
T2	0 - 1000
T3	0 - 4500
T4	0 - 1000
T5	0 - 1000
S1	0 - 1000
S2	0 - 14250

pressures. The long time required to attain equilibrium was a serious limitation to obtaining water retention data for higher pressures.

The measured water retention curves as determined by this method are shown in Figure 5 to 11. Also shown in these figures are two other curves: E1 and E2. E2 will be discussed later. E1 is the predicted water retention curve by equation 20. Figures 5 to 9 are the results of the tuffaceous samples. The fit, as can be seen, between the observed data and the model (E1) is reasonably good. Figures 10 and 11 are the results of the sandstone samples S1 and S2, respectively. Again, the fit between the model (E1) and the observed data is almost perfect. Therefore, the pressure extractor method is a suitable procedure to define the water retention curve for rocks, as is the case for soils. The long time that is required to obtain the measurement is a problem. However, the method may be worth the time invested when the accuracy in the wet side of the curve is of concern. Later discussion will show that the pressure extractor method has some advantages over the psychrometer method over the wet (near saturation) side of the water retention curve.

#### The Psychrometer Method

Water retention data for four tuff samples obtained by the thermocouple psychrometer method are presented here. Two of the samples were examined as a part of this study and their retention data were determined as described in Chapter 3. The results for the other two were presented by Peters et al. (1984) (referred to here as Nevada Test Site (NTS) samples). The data for the NTS samples were obtained

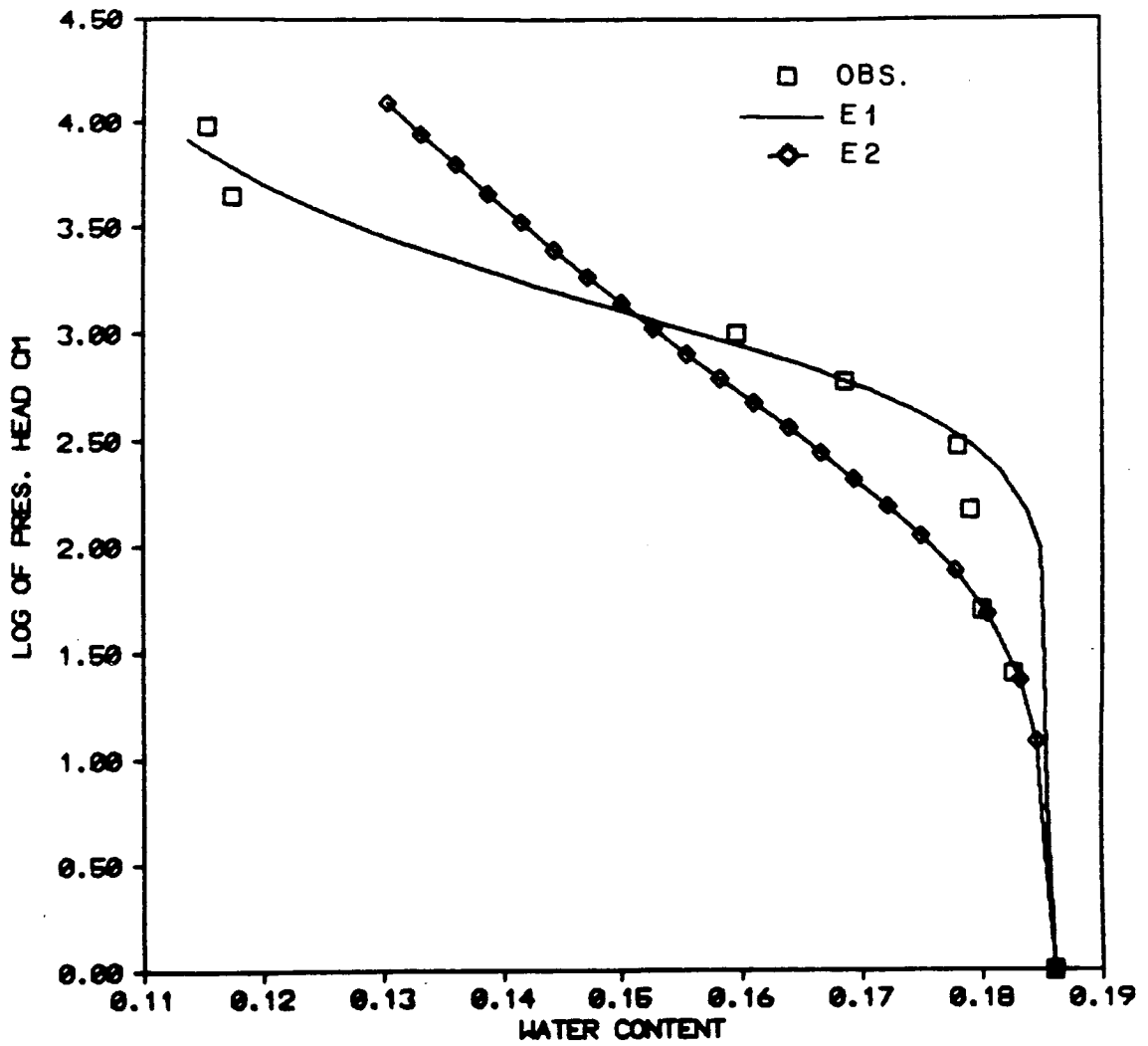


Figure 5. Observed and fitted water retention curves for tuff sample T1 as defined by the pressure extractor method.

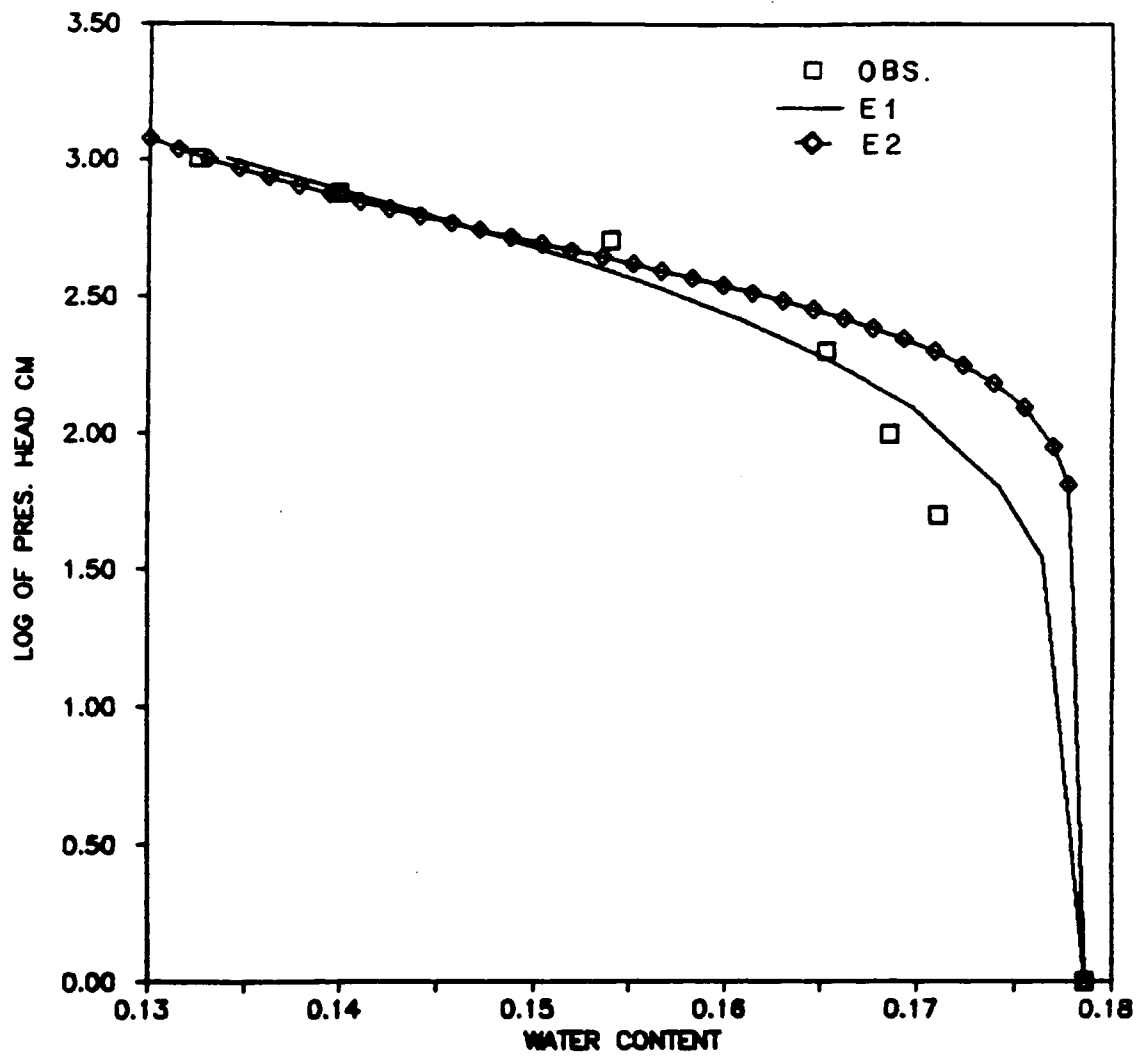


Figure 6. Observed and fitted water retention curves for tuff T2 as defined by the pressure extractor method.

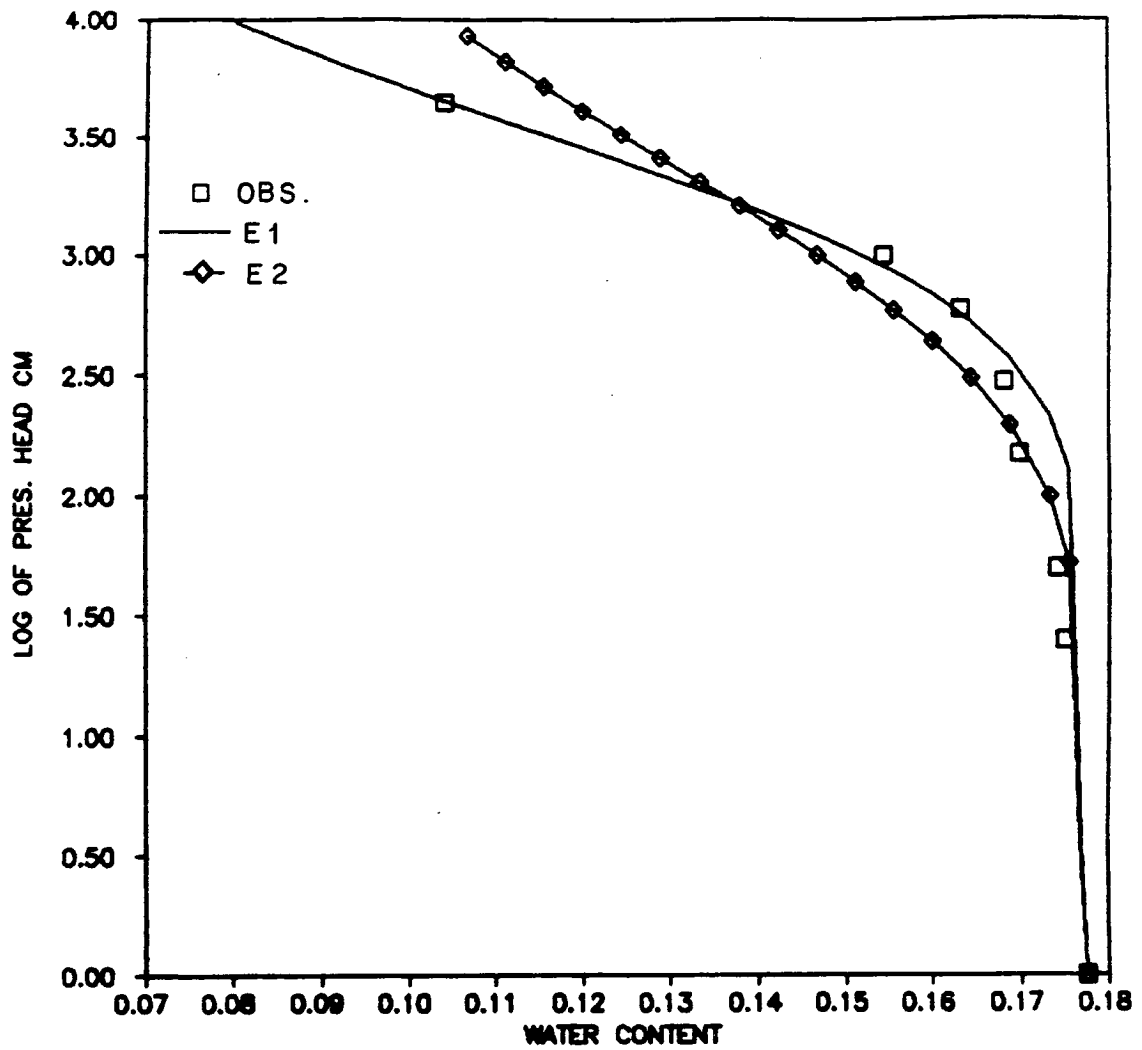


Figure 7. Observed and fitted water retention curves for tuff T3 as defined by the pressure extractor method.

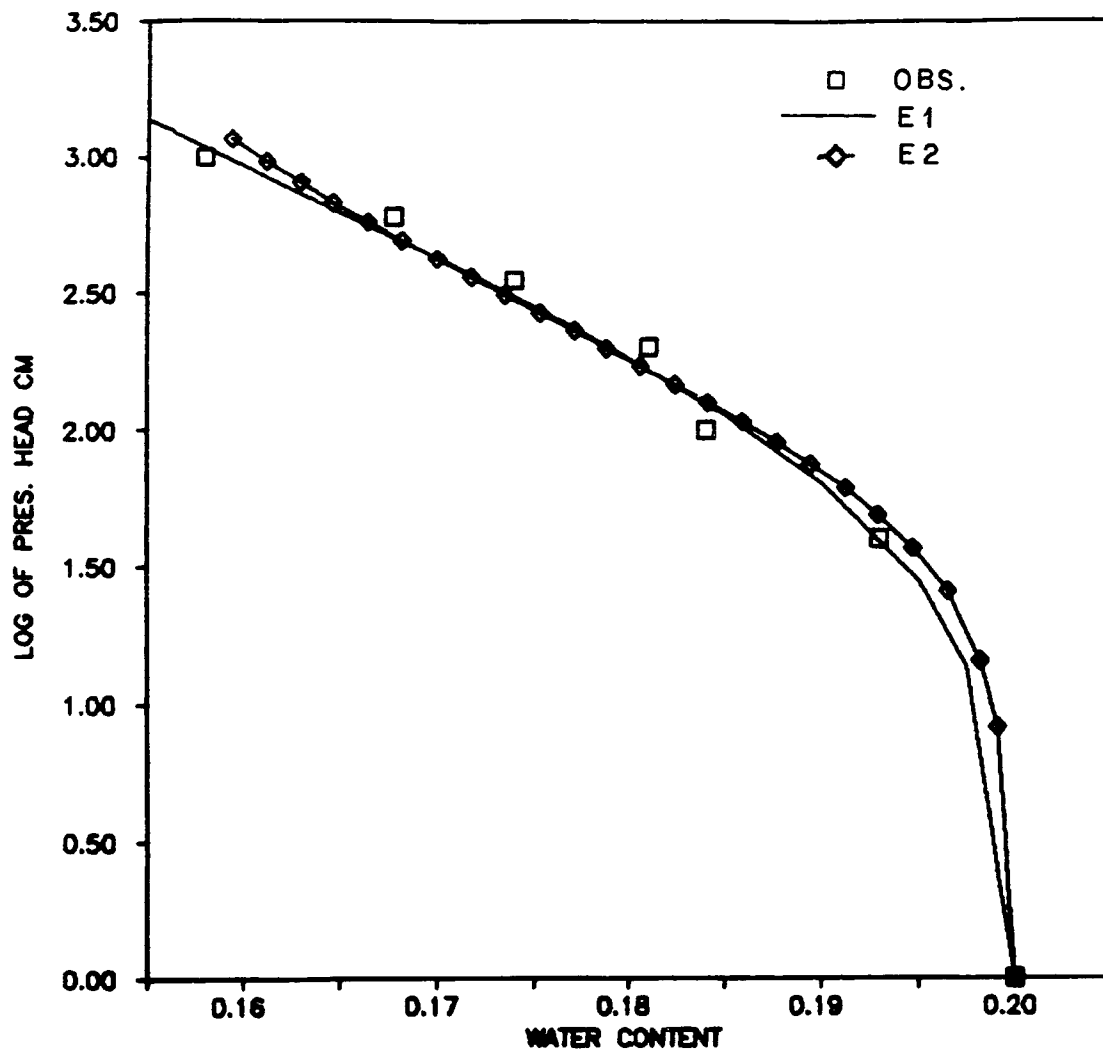


Figure 8. Observed and fitted water retention curves for tuff T4 as defined by the pressure extractor method.

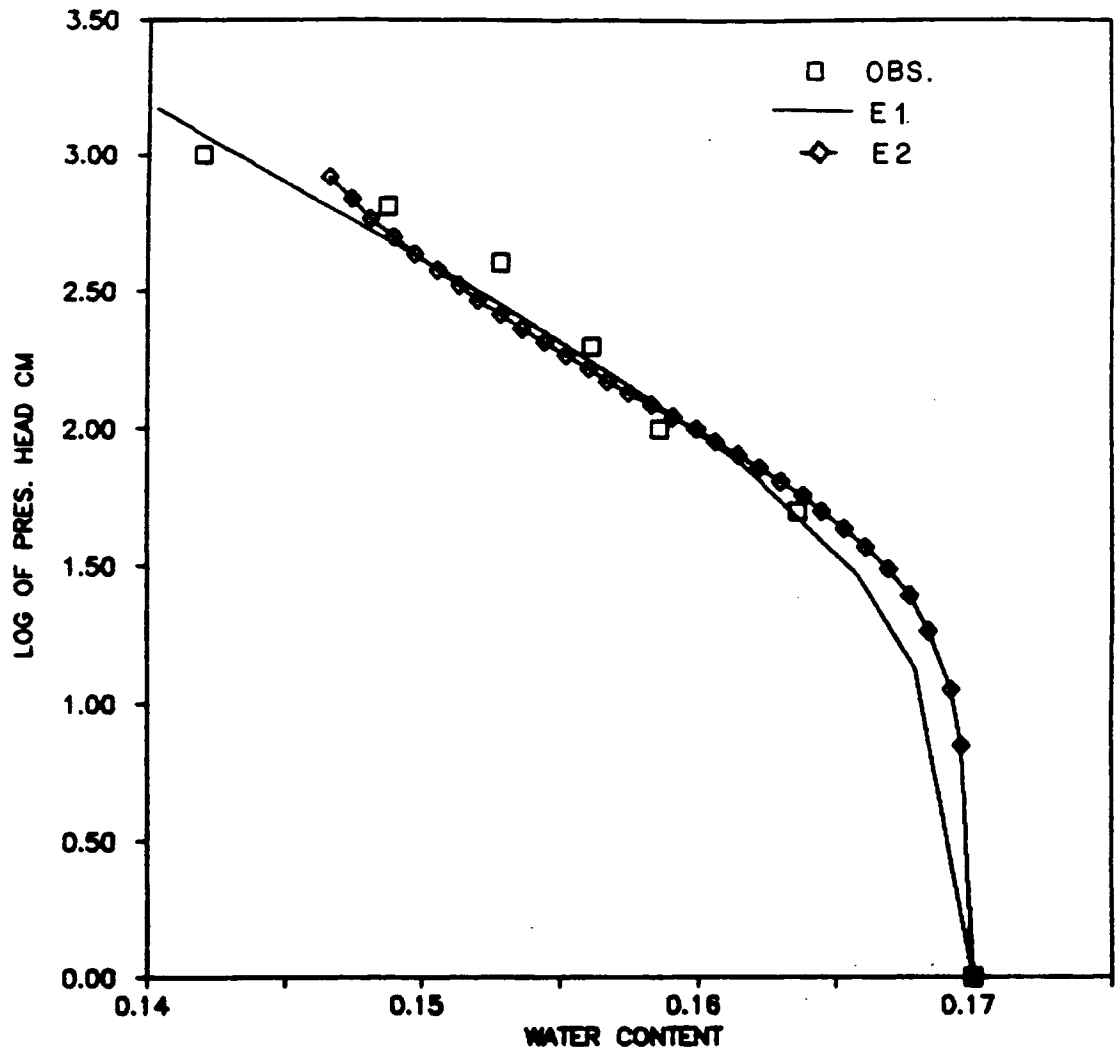


Figure 9. Observed and fitted water retention curves for tuff T5 as defined by the pressure extractor method.

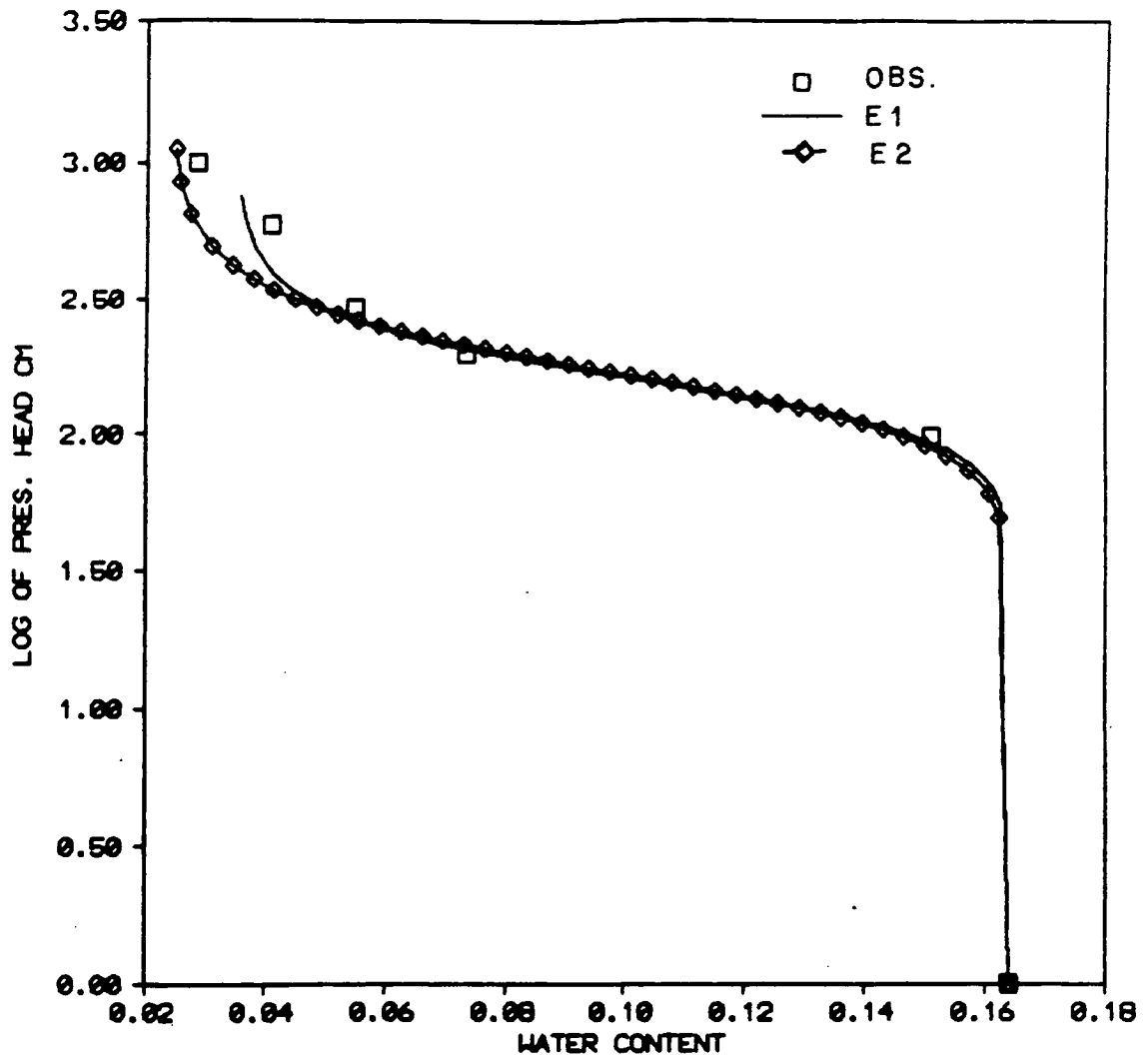


Figure 10. Observed and fitted water retention curve for sandstone S1 by the pressure extractor method.

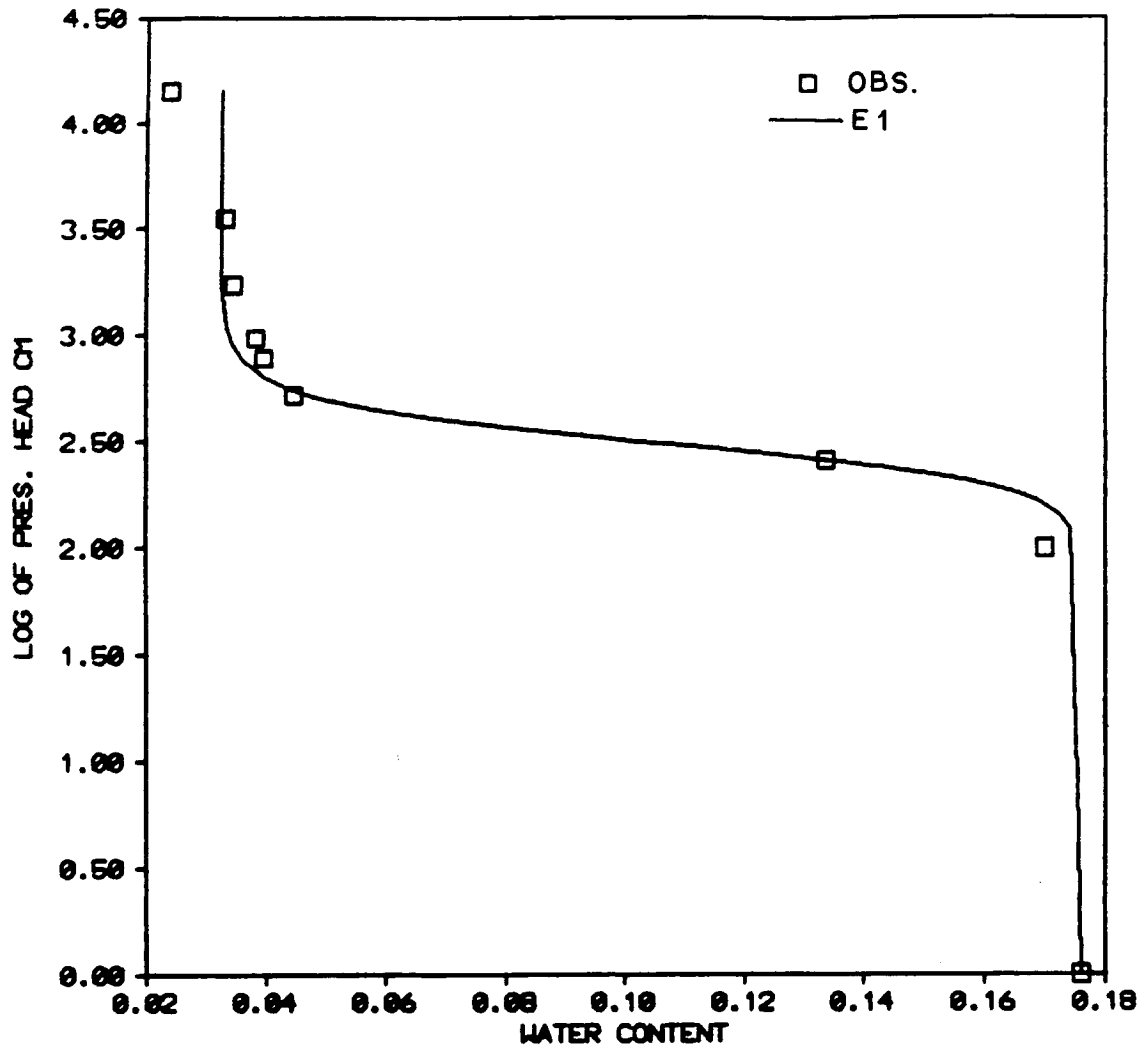


Figure 11. Observed and fitted water retention curve for sandstone S2 by the pressure extractor method.

in a similar fashion, as mentioned in this report, but the samples were dried in a microwave oven rather than in the ordinary oven, as used here. Table 4 shows the sample designations and the pressure range for each.

Figures 12 to 15 show the water retention curves resulting from the psychrometer method. In these curves, the observed data are compared to the model (equation 20). The model is represented by the curves that are labeled "E1 psych." Figures 12 and 13 show the results obtained from this study. Figures 14 and 15 were taken from Peters et al. (1984) for comparison purposes. For all samples, the observed data agree with the model reasonably well, as was the case with the pressure extractor method.

#### Discussion of the Water Retention Results

The water retention data obtained by the above two methods are discussed here in order to show the advantages and the disadvantages of each.

The psychrometer method seems to over-estimate the air entry value (the pressure head value at which first change in  $\theta$  from  $\theta_s$  is observed) when compared to the pressure extractor method. Also, the method did not show the expected broad pore-size distribution of the tuffaceous materials. These two conclusions are well illustrated by Figure 15, which shows the results of the NTS sample GU3. In this figure, the observed data as well as the model suggest almost a uniform pore-size distribution. Also, the air entry pressure head, read from the figure, is about 4700 cm, whereas the porosity of the sample is

Table 4. Samples studied by the psychrometer method  
and their pressure ranges

Sample Code	Pressure Head Range (cm)
TS1B	0 - 1,580,000
TS2A	0 - 2,310,000
NTS A4-6A Unit II	0 - 810,000
NTS Au3-7A Unit I-B	0 - 816,000

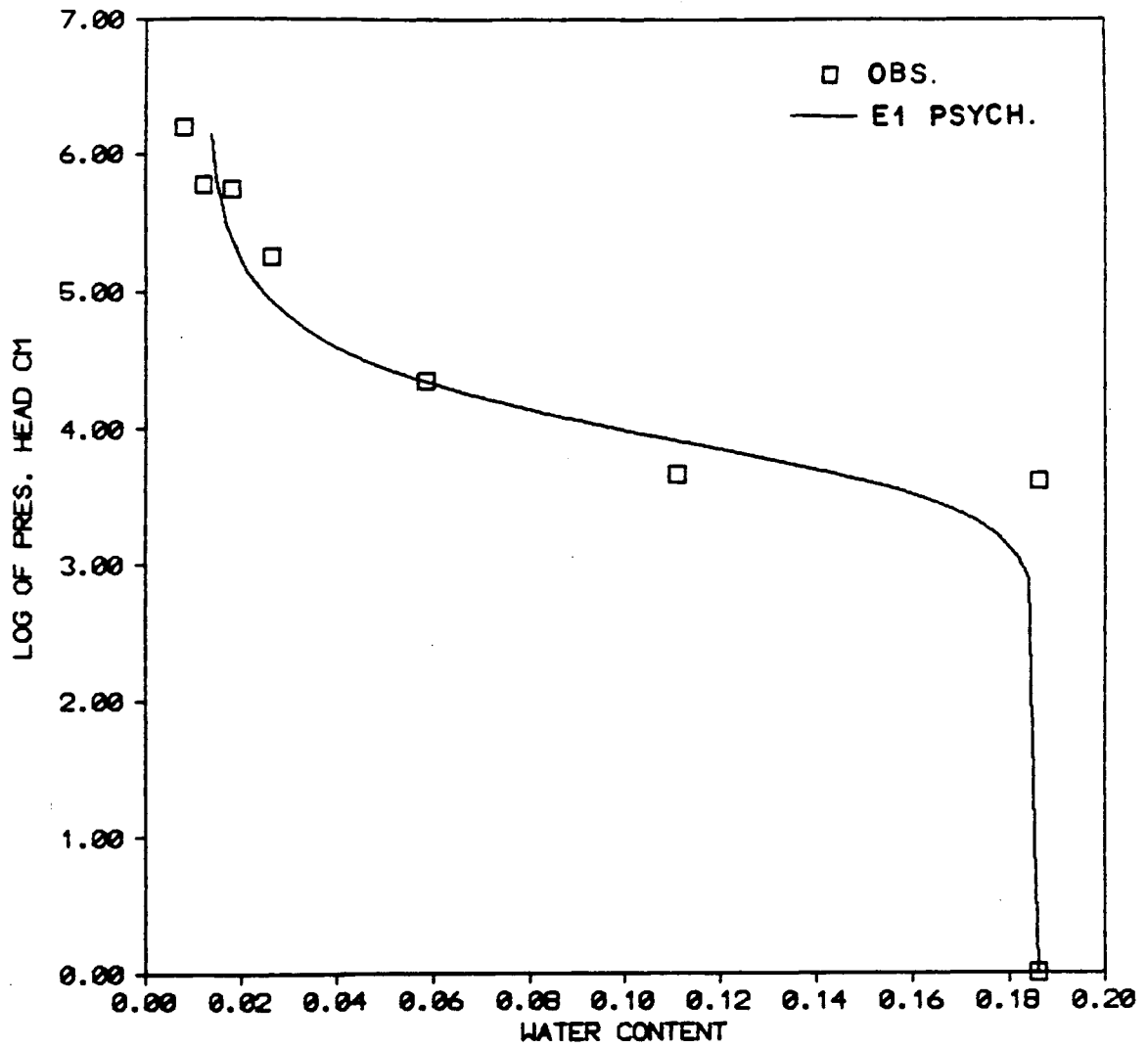


Figure 12. Observed and fitted water retention curves for tuff TS1B (subsample of T1) as defined by the psychrometer method.

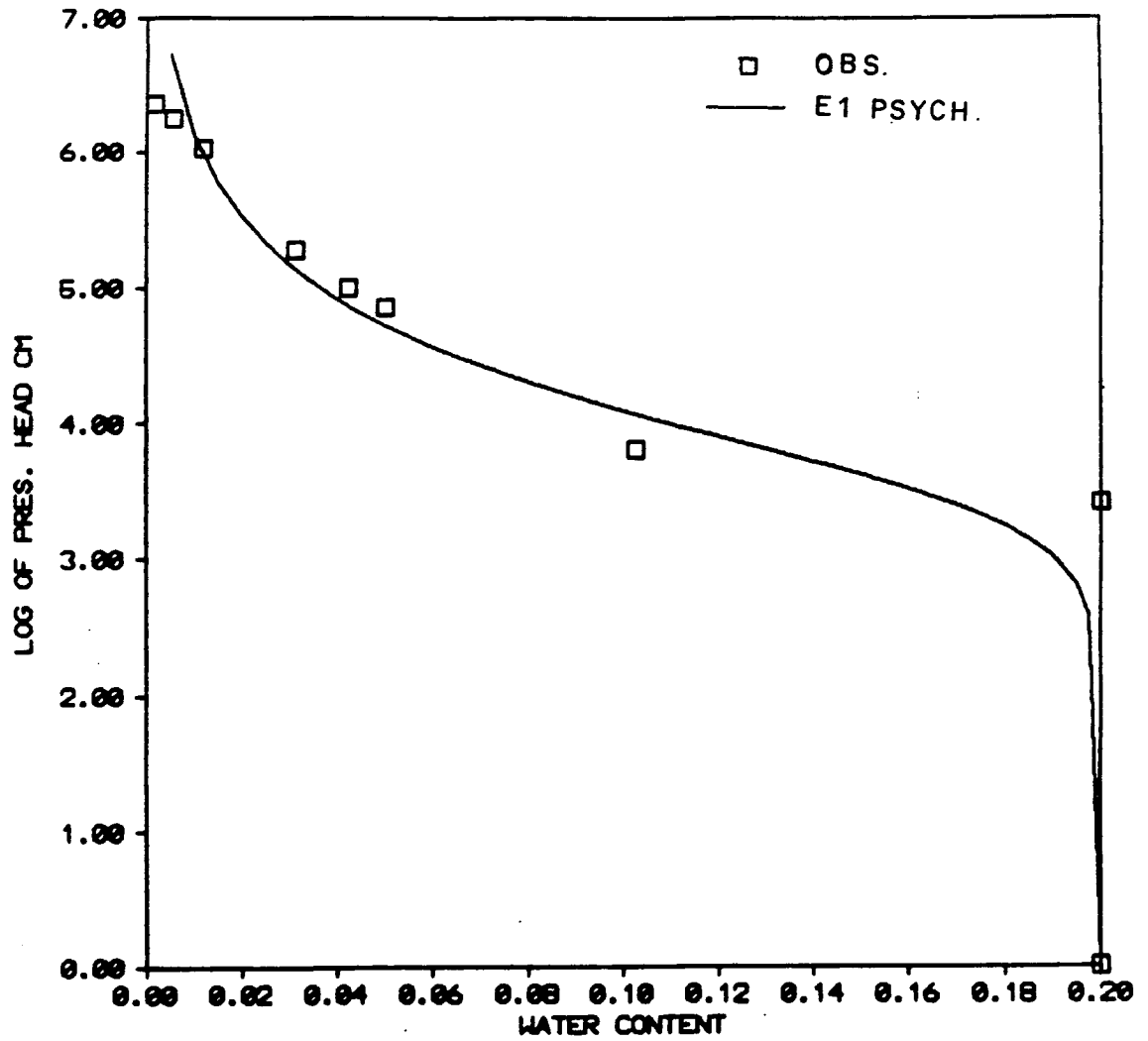


Figure 13. Observed and fitted water retention curves for tuff TS2A (subsample of T4) as defined by the psychrometer method.

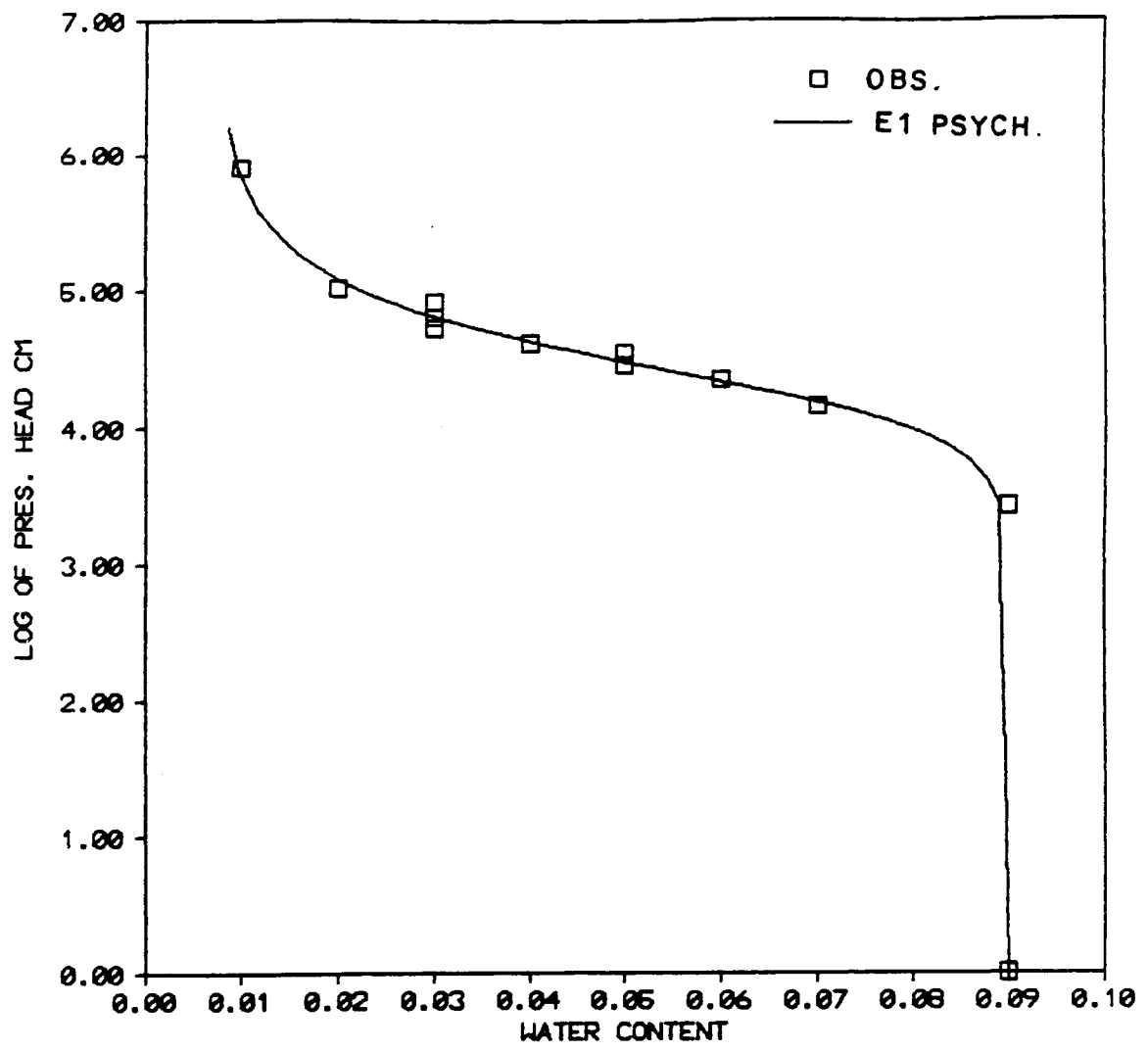


Figure 14. Observed and fitted water retention curve for NTS G4 as defined by the psychrometer method.

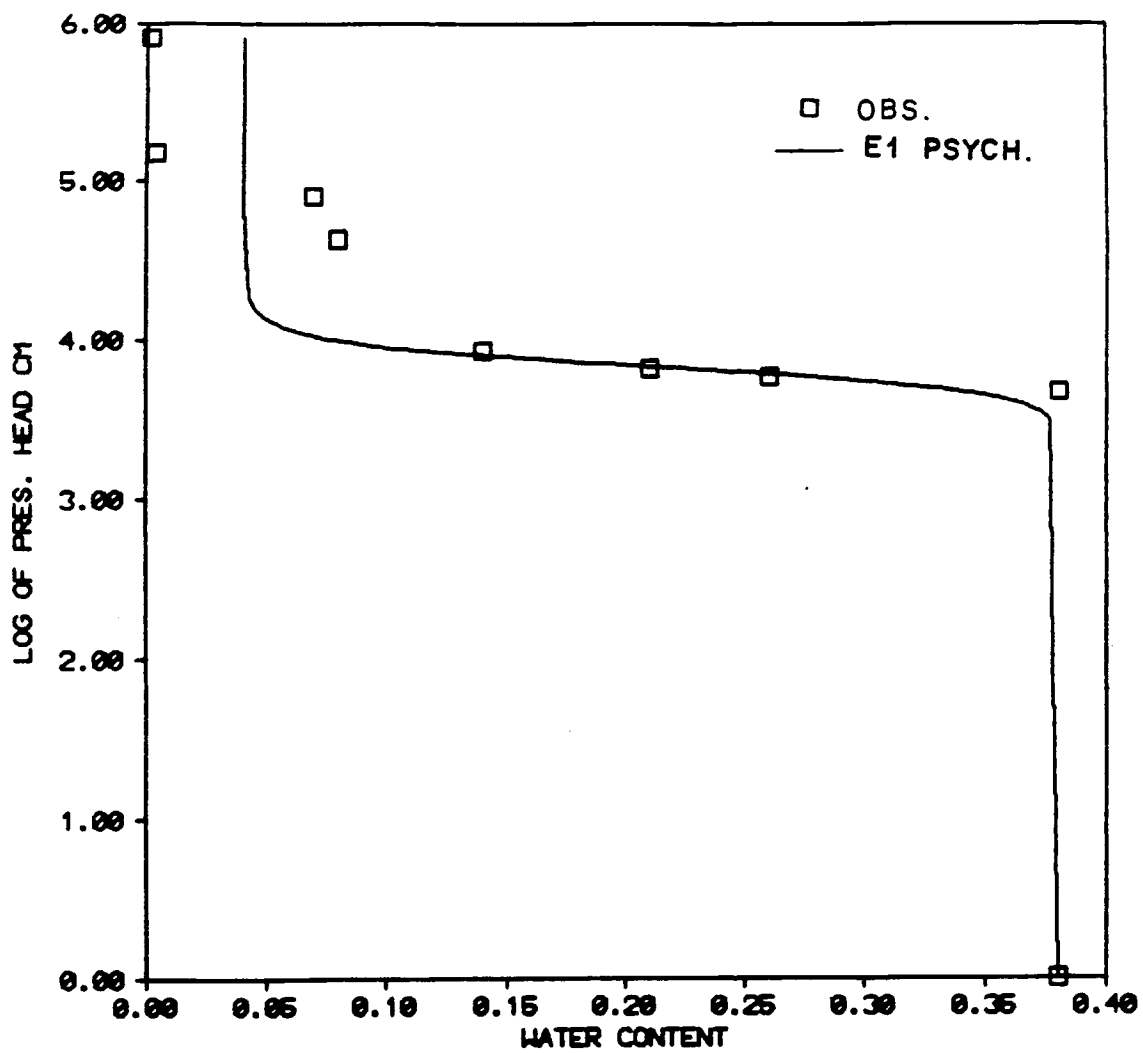


Figure 15. Observed and fitted water retention curves for sample NTS GU3 by the psychrometer method.

0.38 (Peters et al., 1984). In most cases, a porous medium with such high porosity is unlikely to have an air entry value higher than 100 cm, unless it is a certain type of compacted clay.

To explore these results further, twelve subsamples from the tuff samples T1 and T4 were studied by the psychrometer method (6 for each sample) in order to compare their results with those obtained by the pressure extractor method. Since there were no significant differences observed among the six subsamples which were taken from the same sample, the results of only two subsamples, one from each sample, will be discussed here. These results are presented in Figures 12 and 13, which were discussed earlier. Figures 16 and 17 show a comparison between the psychrometer and the pressure extractor methods. In these two figures, it is clearly shown that the psychrometer method overestimated the air entry value, which results from a lack of accuracy of the water retention curve near saturation.

The accuracy of the psychrometer method is reported to be in the order of 1000 cm (Peters et al., 1984). However, based on the results of the twelve samples studied by this method (during the course of this study), it seems that the accuracy of the method is in the order of 2000 to 4000 cm, especially near saturation. No conclusion could be drawn about the method for pressure heads higher than 4000 cm, because no other method is known to define the moisture retention curve for high pressure ranges.

An accurately defined water retention curve becomes even more important if the retention data are to be used to calculate  $K$ . Van

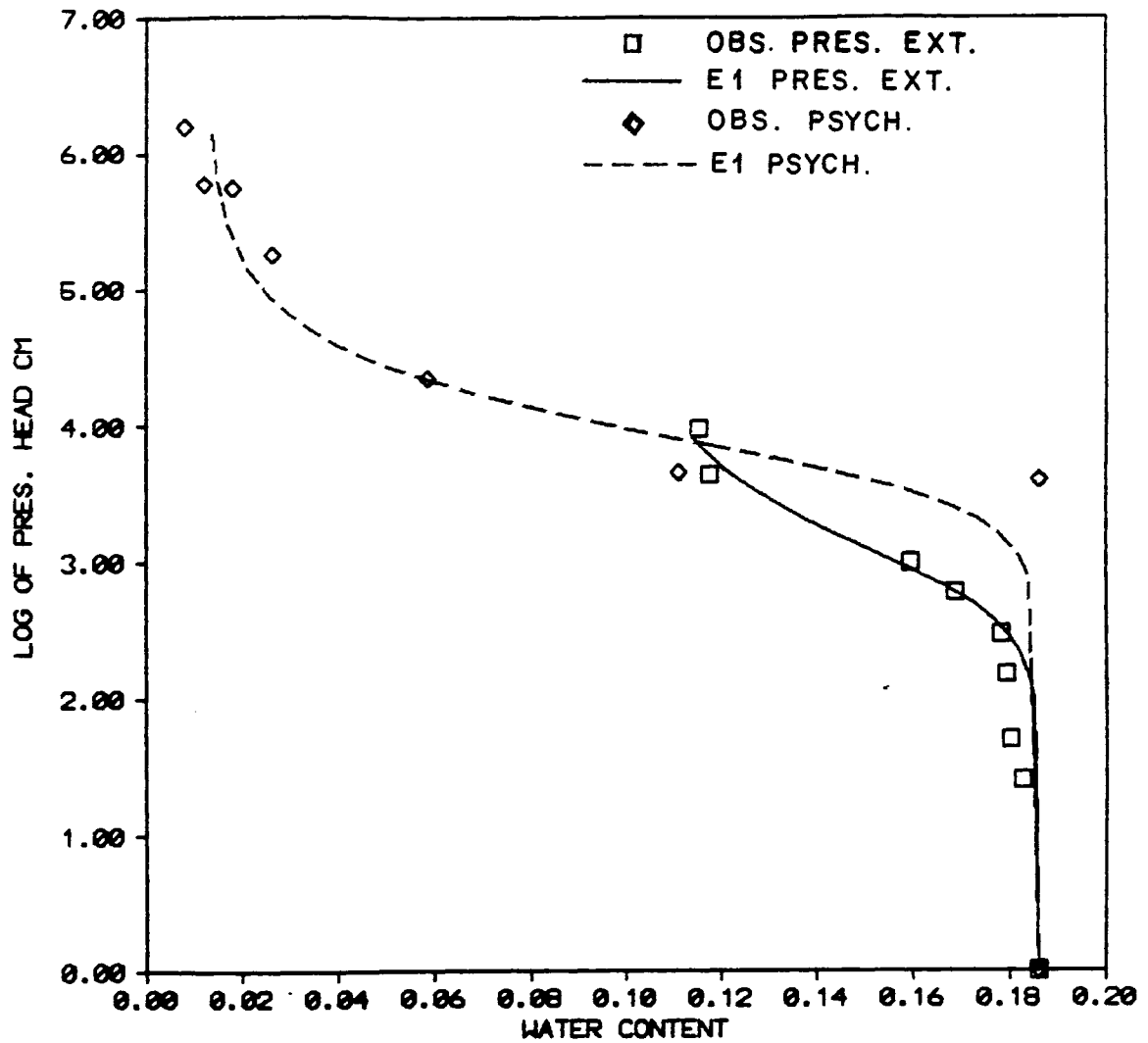


Figure 16. Comparison of the water retention curves as defined by the pressure extractor and the psychrometer methods for tuff T1.

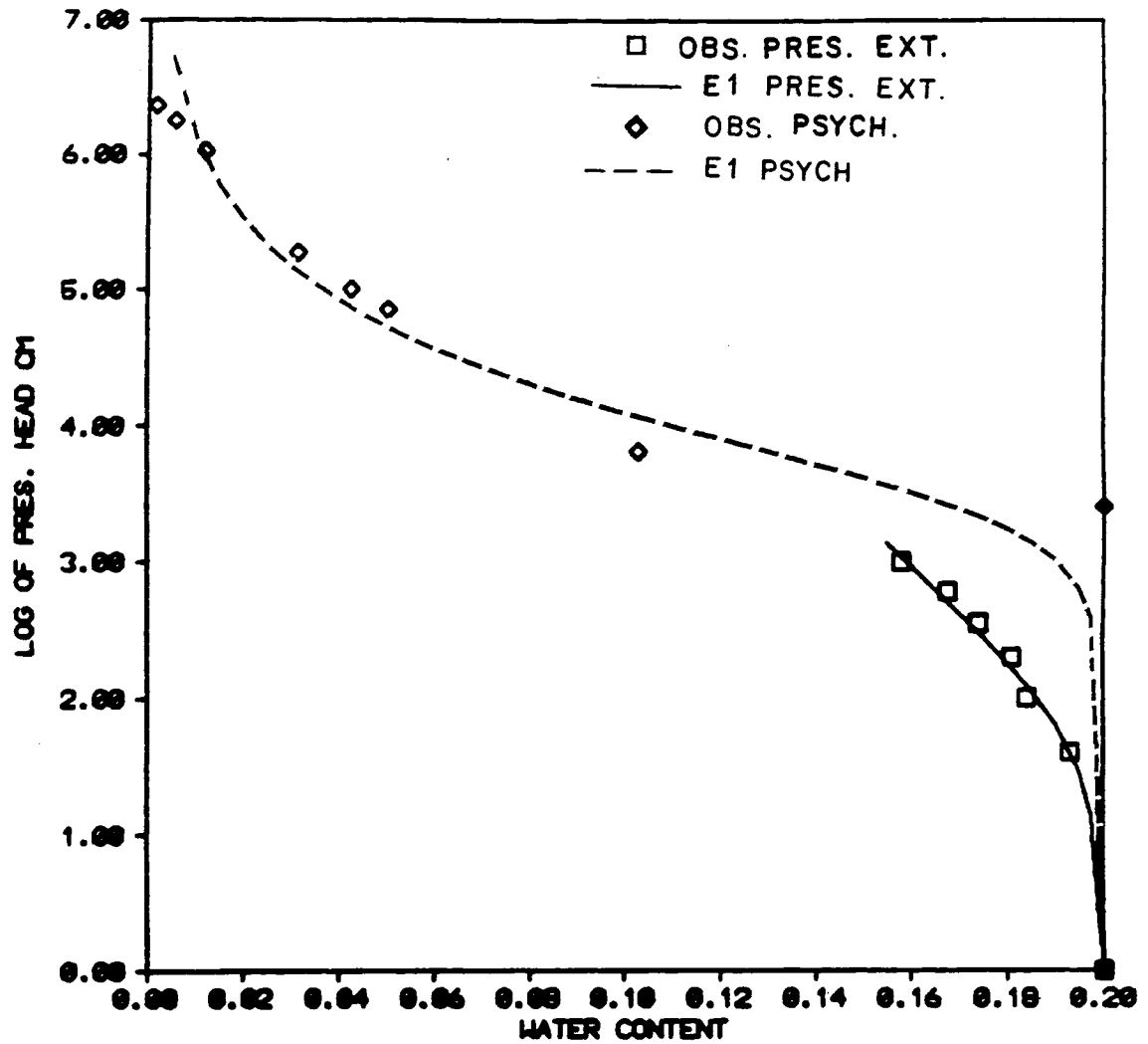


Figure 17. Comparison of the water retention curves as defined by the pressure extractor and the psychrometer methods for tuff T4.

Genuchten and Nielsen (1985) indicated that calculated  $K$  is very sensitive to the slope of the water retention curve, especially near saturation. Also, the results obtained in this study suggest that in most cases  $K$  is reduced 3 to 5 orders of magnitude with a reduction of 20 percent in the degree of saturation. Hence, careful consideration should be given to the moisture retention curve near saturation in order to use the water retention data for calculating  $K$ .

Even though the pressure extractor method showed better results, it has its limitations. One of these limitations is the long time needed to achieve the measurements, as mentioned earlier. The second is that it is very hard to extend the method for pressure heads higher than 10,000 cm (10 bars) because it becomes extremely difficult to maintain the hydraulic contact between the sample and the ceramic plate.

#### The Outflow Method for Measuring $K$

The outflow method was used to measure the unsaturated hydraulic conductivity and diffusivity of rock cores for the pressure head range of 0 to 1000 cm. The conductivity (and diffusivity) was measured for six cores; five of them were tuff and one was sandstone. These samples are T1, T2, T3, T4, T5 and S1; and their properties are listed in Table 1.

The total amount of water extracted from the tuffaceous samples during the measurement ranged from 13 to 25 percent of saturation. In the case of the sandstone sample, 82 percent of the saturation water was extracted. The measured  $K$  of the tuff samples dropped 3 to 5

Orders of magnitude during a drop of only 13 to 25 percent in the water content from saturation. This large drop in  $K$  for a relatively small drop in water content suggests that  $K$  may approach zero, while the sample was still 50 percent or more saturated. However, this should not be viewed as to underestimate the significance of water flow through the rock matrix when the saturation is reduced to 50 percent or less, especially when a long time period is involved, as is the case with contaminant transport.

As mentioned earlier, the outflow method required the use of a small amount of bentonite clay between the sample and the ceramic plate to maintain a hydraulic contact. The use of the clay introduced some extra outflow which introduced certain errors into the measured  $K$  values. The extra outflow measured was between 1 to 5 percent of the total amount of water extracted. Its effect on  $K$  values was neglected.

The outflow method appeared to be suitable to measure  $K$  for rock samples. It does not require the sample to be confined from the sides, and it is a simple laboratory procedure. The resultant  $K$  values near saturation which should be close to  $K_S$  are consistent with the  $K_S$  values for the tuff samples obtained by other investigators (see, for example, Peters et al., 1984).

However, the use of the method is limited to low pressures. It was used here for a pressure head range of 0 to 1000 cm, but it may be possible to extend the method to a pressure head range of 0 to 2000 cm. At pressure heads higher than 2000 cm, it would be difficult to maintain the hydraulic contact between the sample and the ceramic plate

without introducing sizable mounts of extra outflow, because at higher pressures more and more clay is needed to maintain the hydraulic contact.

The measured  $K$  values for the samples studied are shown in Figures 18 through 23. These figures will be discussed in more detail in a later section.

#### Measurement of Saturated Hydraulic Conductivity

The saturated hydraulic conductivity  $K_s$  was measured using the modified Tempe cell as described in Chapter 3.  $K_s$  was obtained for all the samples for which  $K$  vs  $\theta$  curves were determined. However, only the results of samples T1 and T3 were considered reliable and were used in the calculation. For the rest of the samples, the measured  $K_s$  turned out to be unrealistically high, possibly because water had leaked through the annular space between the sample and its container, and therefore were not used. Thus,  $K_s$  was estimated to be equal to the first value of the measured unsaturated hydraulic conductivity which was obtained while the sample was 95 percent saturated or higher. This approximation is valid (Kunze and Kirkham, 1962) as long as the pressure head increment applied to obtain the  $K$  value is small (pressure heads changes in this study were around 25 cm).

#### Prediction of the Unsaturated Hydraulic Conductivity

Hydraulic conductivity  $K$  results predicted by Equation 21 are discussed in this section. Since the unknown parameters in equation 21 were determined by two different optimization functions, E1 and E2, as

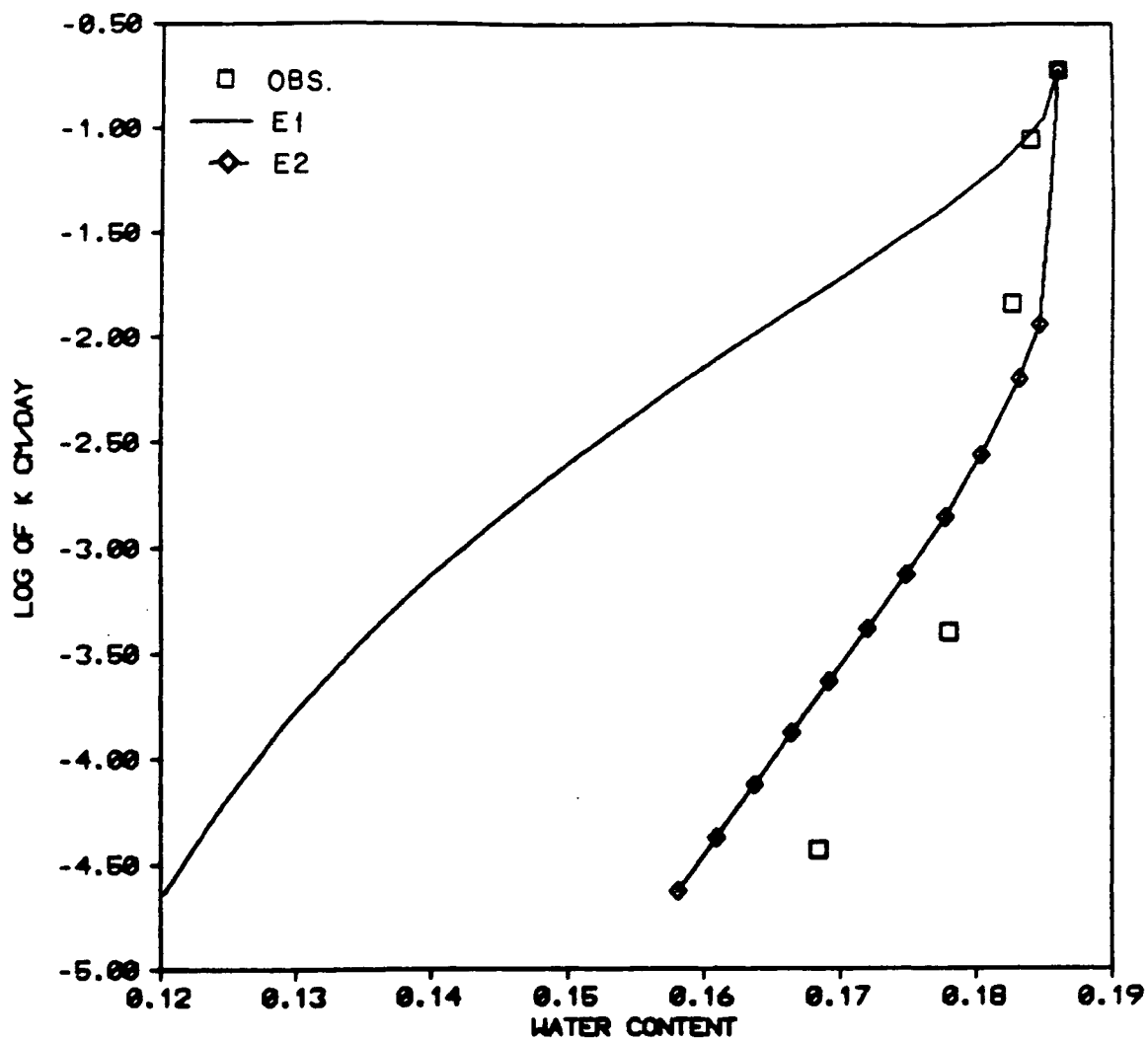


Figure 18. Observed and fitted hydraulic conductivity curves for tuff T1 (pressure extractor method).

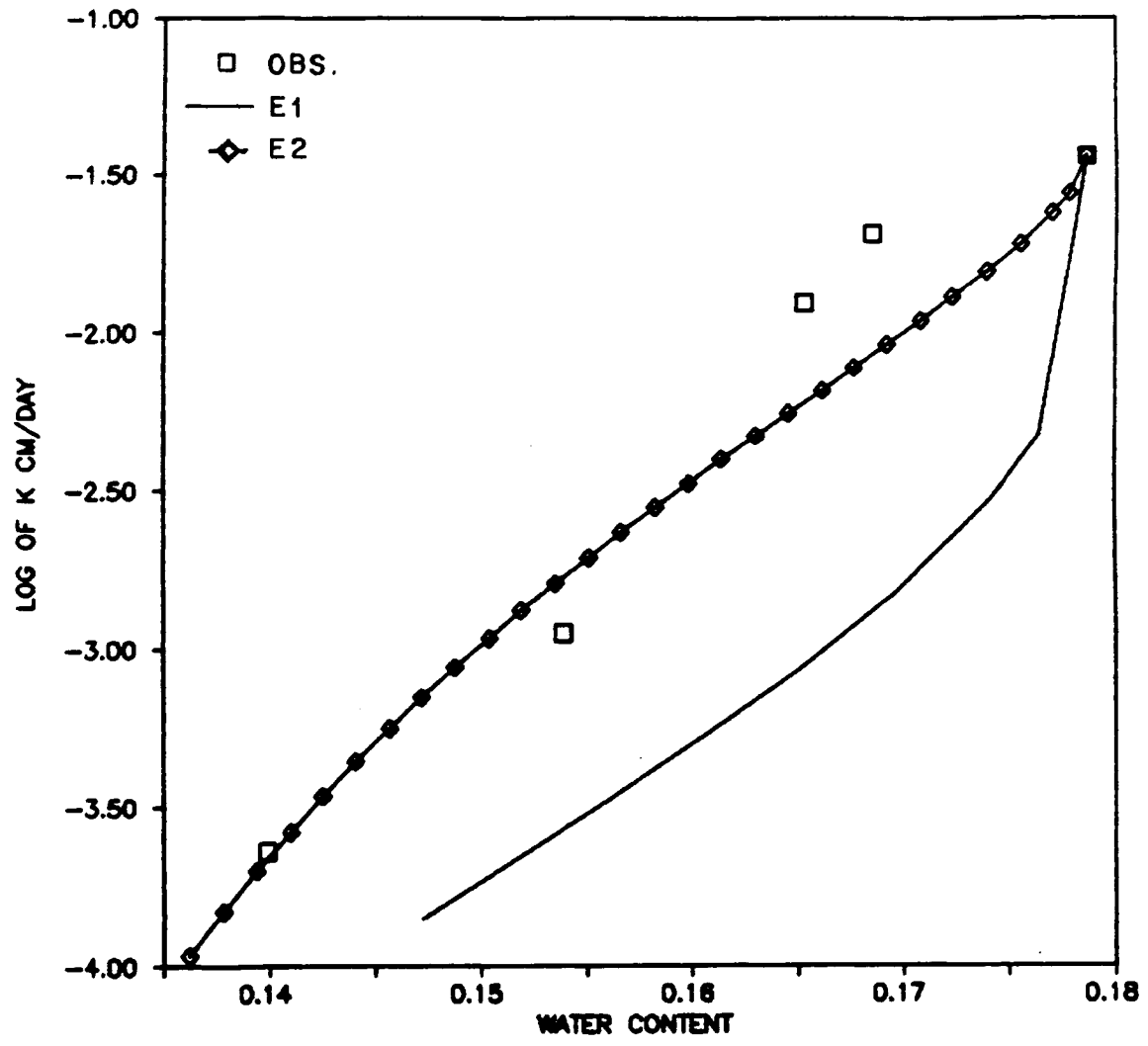


Figure 19. Observed and fitted hydraulic conductivity curves for tuff T2 (pressure extractor method).

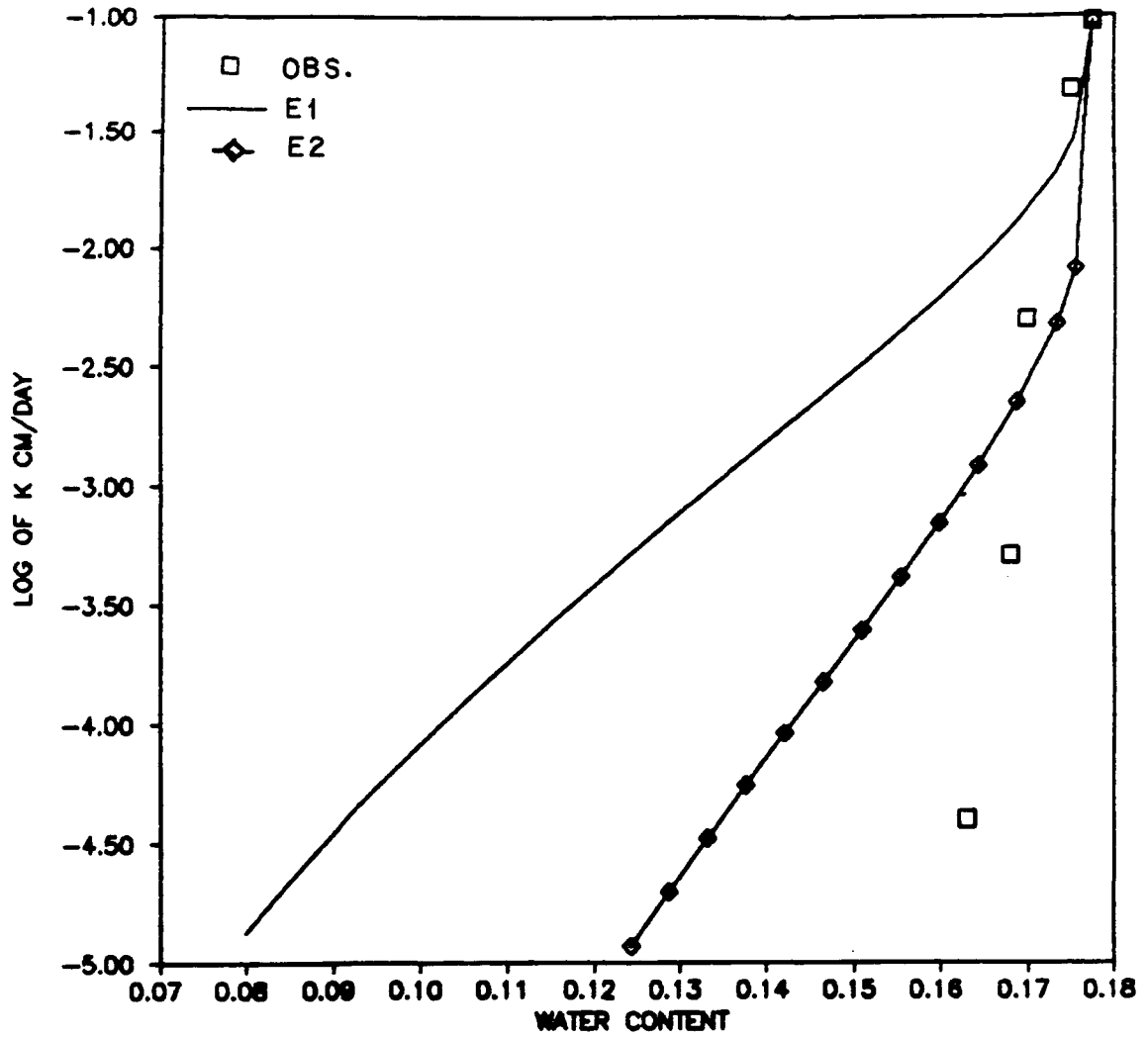


Figure 20. Observed and fitted hydraulic conductivity curves for tuff T3 (pressure extractor method).

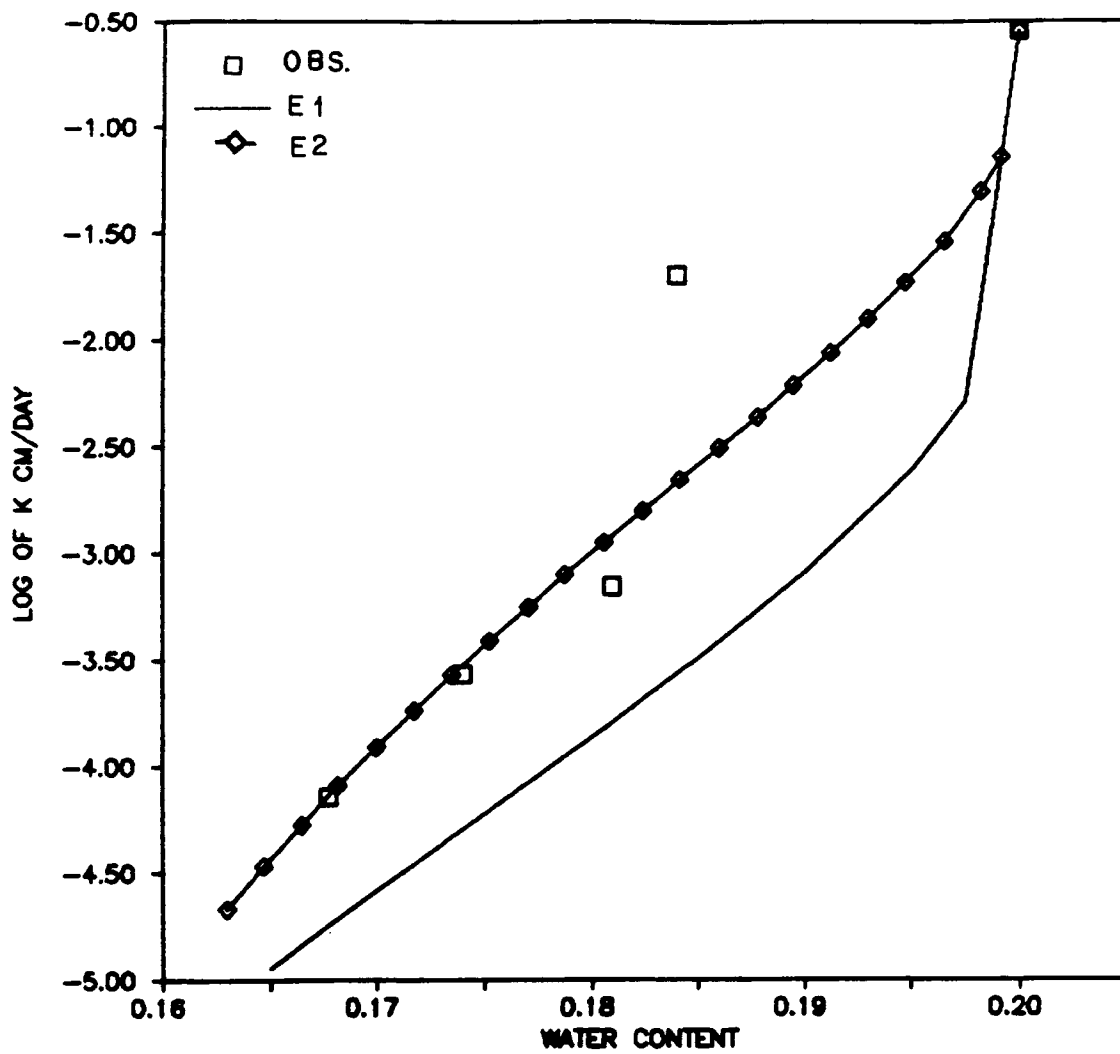


Figure 21. Observed and fitted hydraulic conductivity curves for tuff T4 (pressure extractor method).

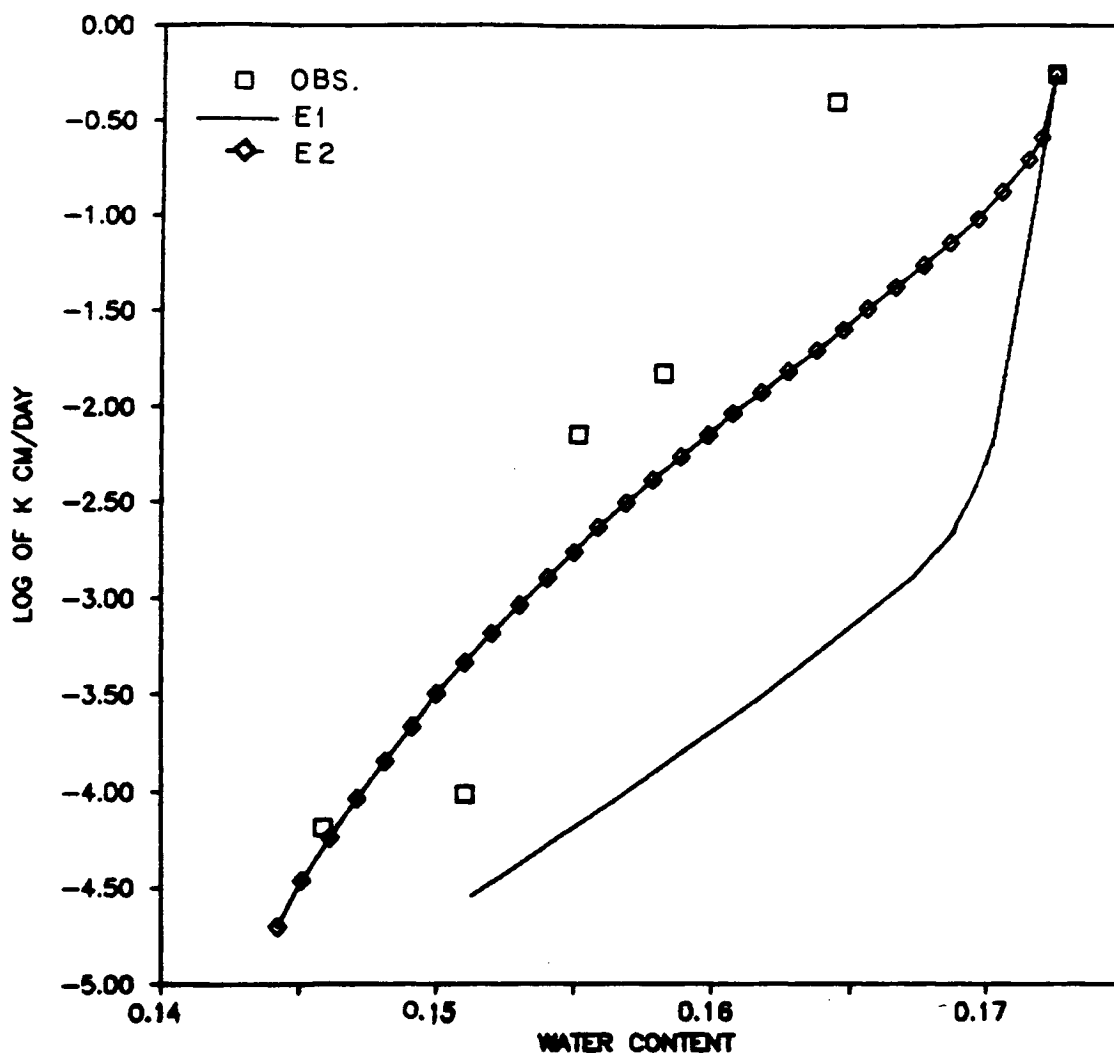


Figure 22. Observed and fitted hydraulic conductivity curves for tuff T5 (pressure extractor method).

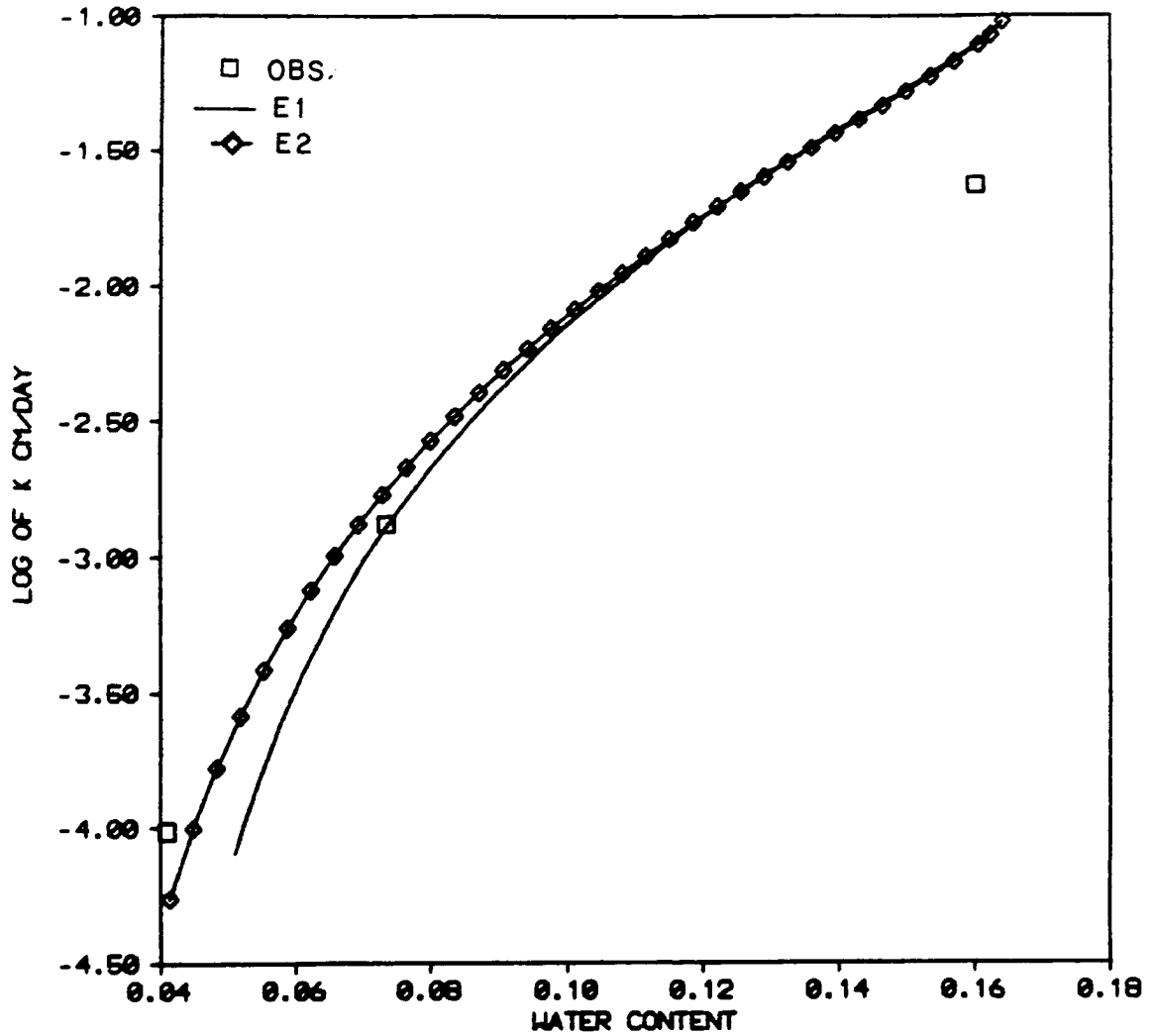


Figure 23. Observed and fitted hydraulic conductivity curves for sandstone S1 (pressure extractor method).

mentioned in Chapter 3, this section will be divided into two subsections. The first will discuss the results of using E1 optimization, and the second will be devoted to E2. Bear in mind that the parameters  $\theta_r$ ,  $\alpha$ , and  $n$  or  $m$  should be good enough to predict the observed water retention curve (using equation 20) and  $K$  vs  $\theta$  curve (using equation 21). Hence, the optimization functions will be evaluated according to their ability to produce a set of parameters that are good to predict the two curves.

#### Calculation of $K$ Using the Water Retention and $K_s$ Data

Hydraulic conductivity was calculated by equation 21, where the unknown parameters,  $\theta_r$ ,  $\alpha$ , and  $n$  or  $m$  were determined by the optimization function E1 (equation 25). The calculated  $K$  deviated from the measured  $K$  for almost all the samples studied.

The curves labeled E1 in Figures 18-23 are the results of this computational method for the tuffaceous samples. There is no consistent deviation from the experimental data (i.e., the computed  $K$  is higher than the observed data in one instance and lower in the other). But generally the calculated value seems to converge to the observed one as  $\theta$  goes to  $\theta_r$ . The water retention data used in the calculation of these figures were obtained by the pressure plate extractor method.

One sandstone sample was studied for its  $K$ , and the results are shown in Figure 23. There is fairly good fit between the model (E1) and the observed data.

The conductivity deviates even more from the observed data when the water retention data from the psychrometer is used (Figures 24 and 25, curves labeled E1 Psych).

However, when equation 20 is used to reproduce the moisture retention data using E1 derived parameters, the results were good when compared to the observed data (see curves E1 in Figures 5 to 11).

The deviation of calculated K from the observed data may be caused by the term  $(S_e^{0.5})$  in equation 21. The exponent 0.5 was empirically determined for soils by Mualem (1976). The term is meant to account for partial correlation between interconnected pores and for tortuosity.

For porous media, the higher the tortuosity, the lower is the conductivity (Carman, 1939). Wyllie and Spangler (1954) concluded that tortuosity of a consolidated medium is several orders of magnitude higher than that of nonconsolidated media. Therefore, it seems reasonable to use a larger exponent than 0.5 in equation 21 when using it for consolidated materials.

Since the samples studied have predicted K that is either higher or lower than the observed K, and not always higher, this conclusion cannot be viewed with high confidence. However, for the two sets of retention data obtained from the psychrometer, predicted K was higher than the observed K. By changing the exponent from 0.5 to 50 for sample T1 and to 25 for sample T2, it was possible to improve the fit to the experimental data (Figures 26 and 27). More studies are

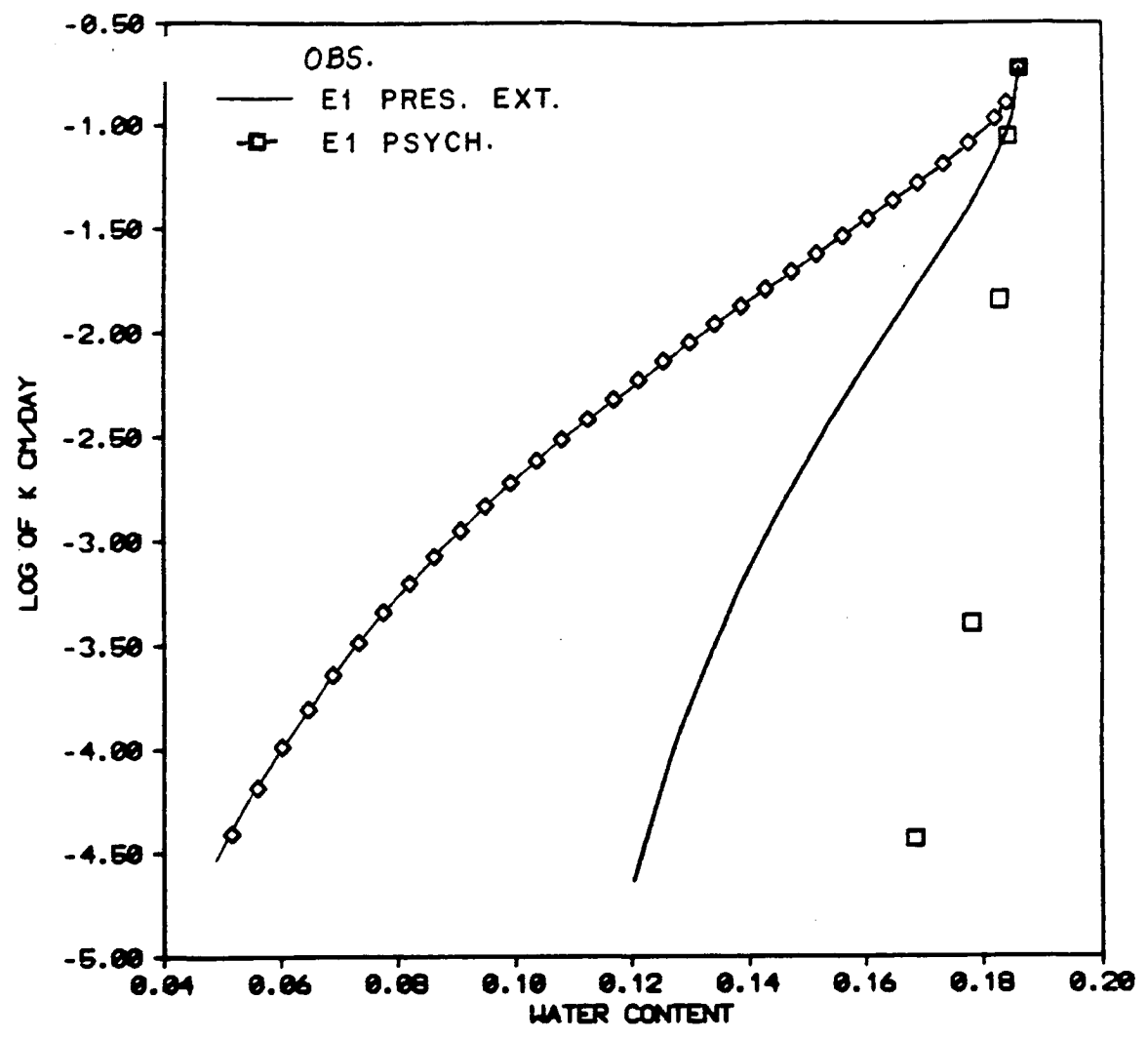


Figure 24. Comparison of fitted hydraulic conductivity curves from pressure extractor and from the psychrometer methods to the observed data for tuff T1.

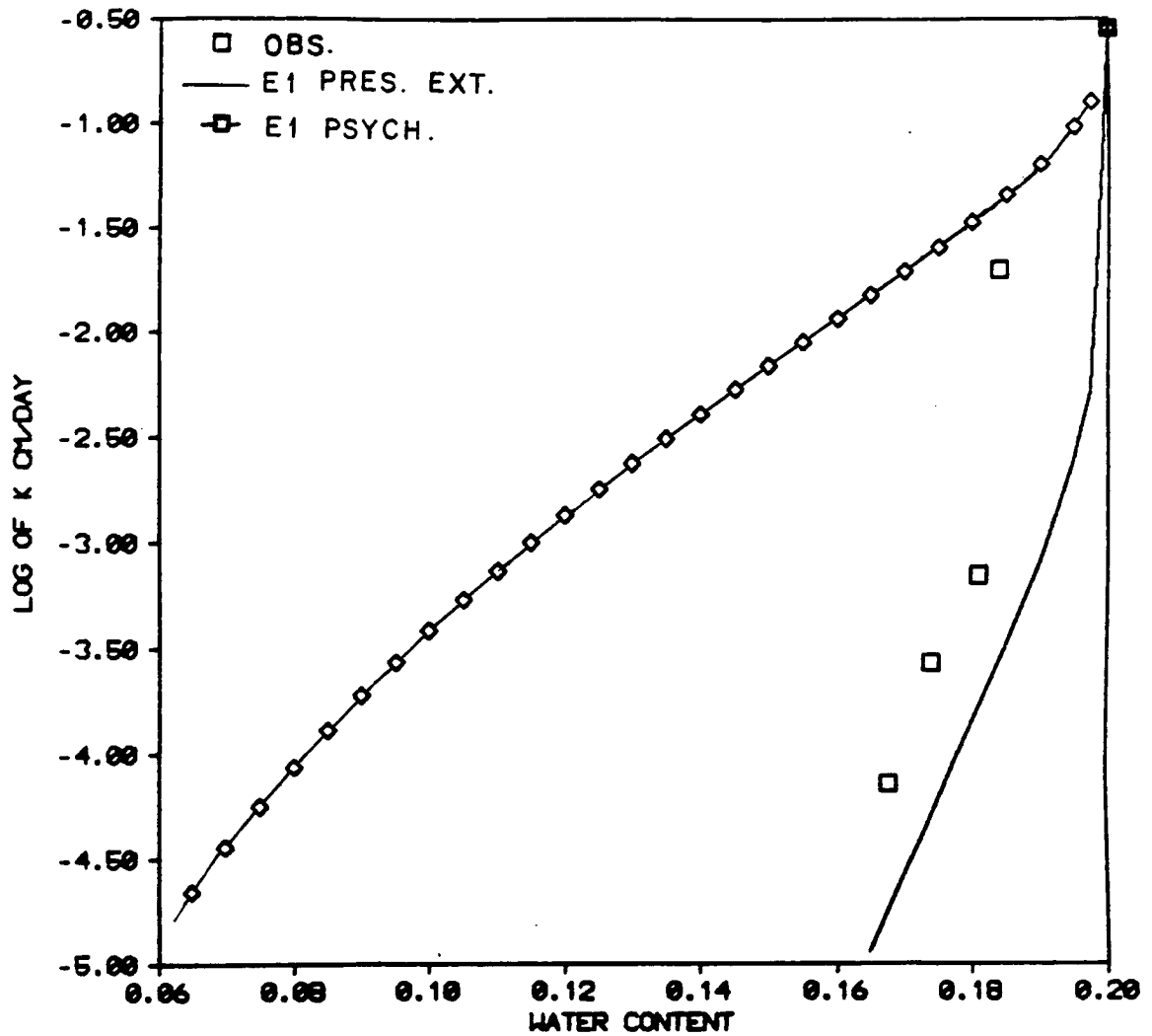


Figure 25. Comparison of fitted hydraulic conductivity curves from pressure extractor and from the psychrometer methods to be observed data for tuff T4.

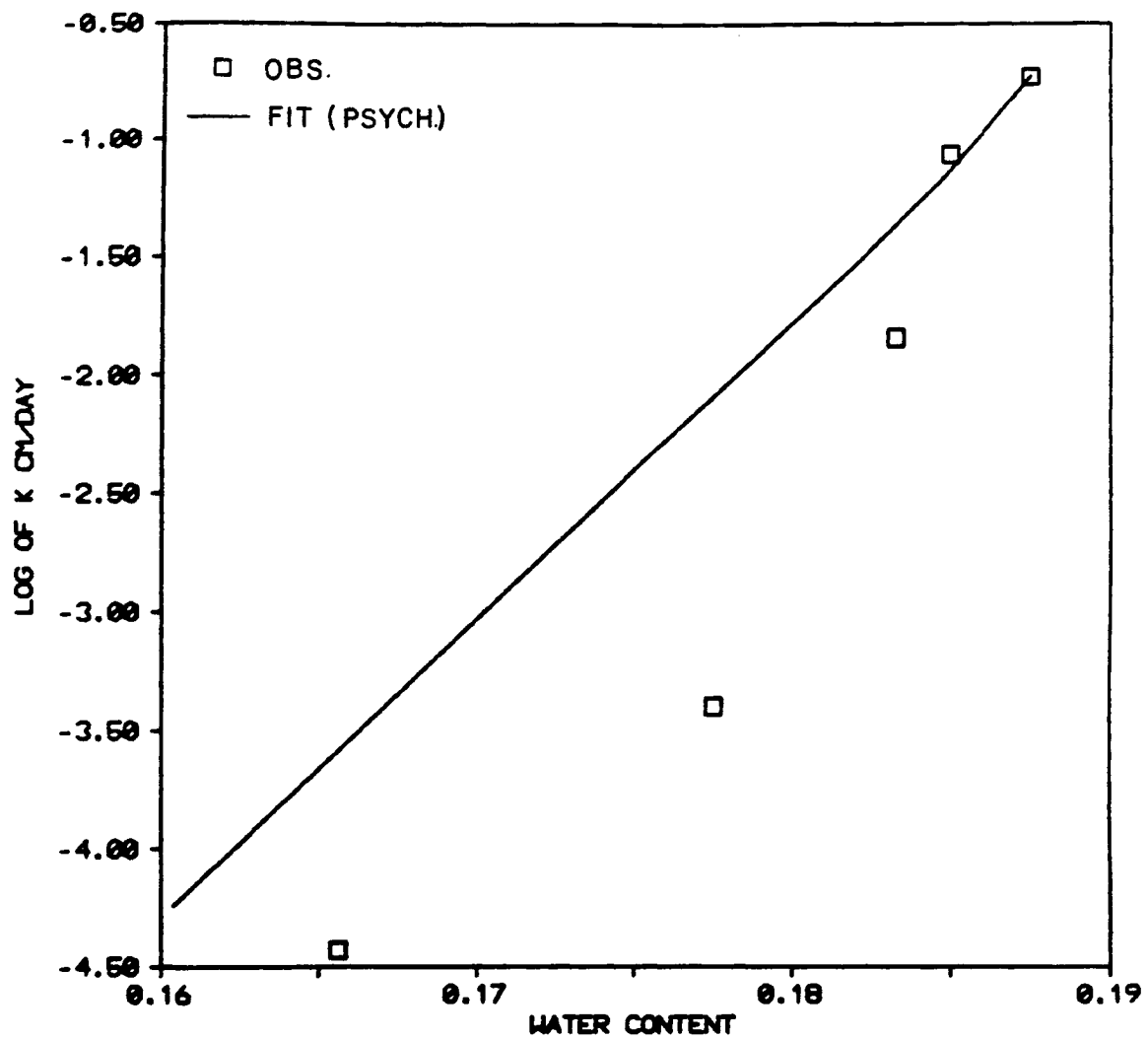


Figure 26. Observed and fitted hydraulic conductivity (by modifying equation 21) for tuff T1.

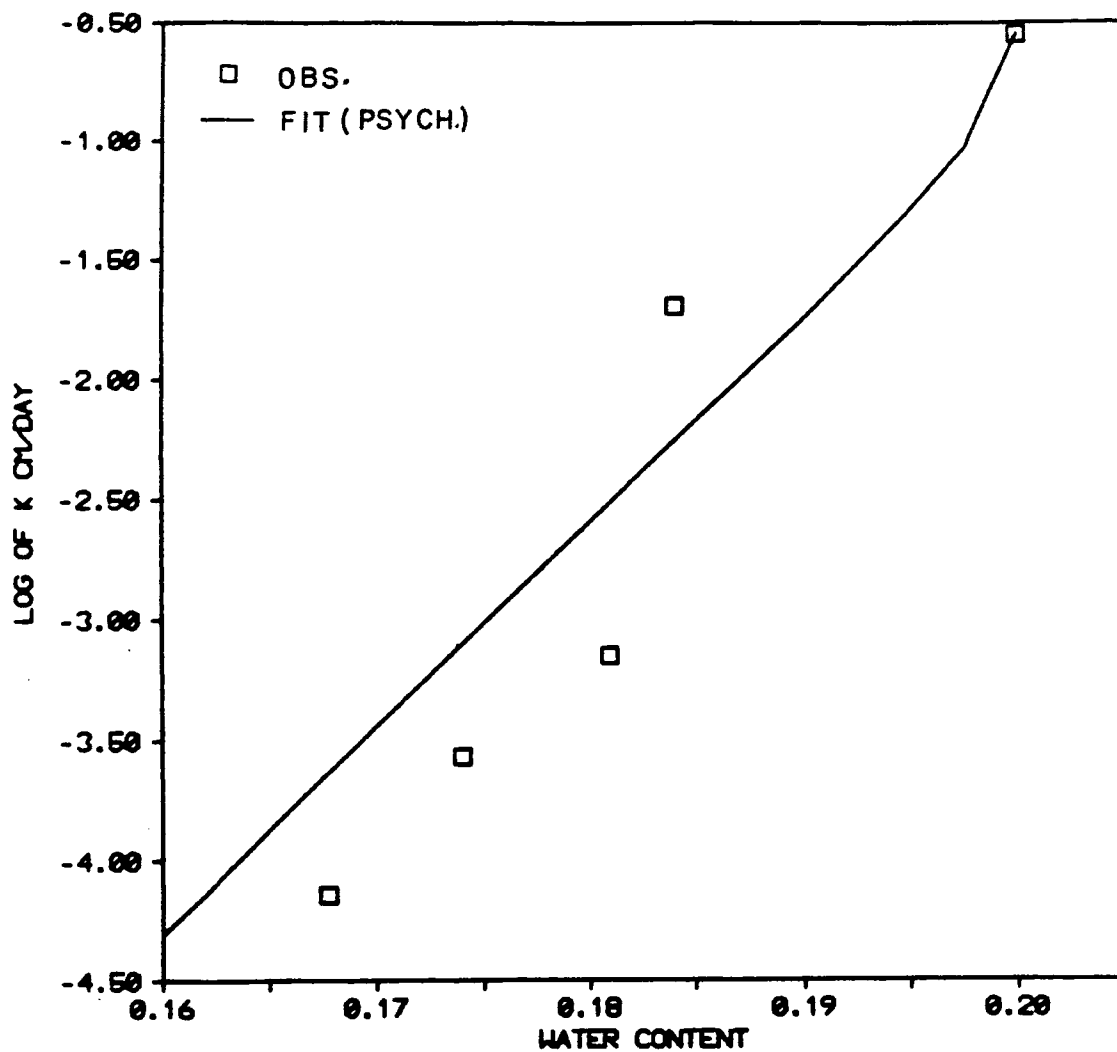


Figure 27. Observed and fitted hydraulic conductivity (by modifying equation 21) for tuff T4.

needed to draw any reliable conclusion about the exponent of the term  $S_e^{0.5}$  in equation 21.

Further examination of equation 21 requires an easy and yet reliable method to measure K for model verification. The outflow method appeared to give satisfactory results. Nevertheless, the method could be improved by extending the measurement to 2000 cm (2 bars) of pressure head using a more precise method for measuring outflow. Also, some of the theoretical limitations of the method could be eliminated by solving the inverse problem (Gardner, 1956) numerically rather than analytically.

#### Calculation of K Using Measured Water Retention, K, and $K_s$ Data

In this approach, K is calculated by equation 21, but the unknown parameters were estimated by the optimization function E2 (equation 26). Equation 26 incorporates the measured water retention and conductivity data to estimate the model parameters. The resulting curve of K matches the observed data better than the E1 method. Also, the observed water retention curve was reasonably reproduced by equation 20 using the parameters estimated by this approach. but the results are not as good as those from E1 as far as the retention curve is concerned (Figures 5 to 10, curves E2).

Figures 18 to 23 show the calculated K (curves E2) by this method.

When the overall results are considered, that is, the ability of the model to reproduce the observed water retention and K data, this

approach is preferred over the previous one. In other words, when the observed conductivity data are incorporated with the retention data to estimate the parameters, the calculation model will be more reliable in predicting K than in the case of using the water retention data only. Yates et al. (1984) have arrived at the same conclusion for unconsolidated media.

### Prediction of Diffusivity

Diffusivity, D, is also an important hydraulic property to characterize a porous medium. Any computation model for K should be applicable for D, since D and K are related by the equation:

$$D(\theta) = K \frac{dh}{d\theta} \quad (32)$$

Solving equation 20 for h will give:

$$h = \frac{1}{\alpha} \left( S_e^{-\frac{1}{m}} - 1 \right)^{\frac{1}{n}} \quad (33)$$

and K is given by equation 21. Therefore, by differentiating equation 33 and substituting the resultant along with equation 21 into equation 32 will give the following relation for D:

$$D = \frac{(1-m)K_s}{\alpha m(\theta_s - \theta_r)} S_e^{\frac{1}{2} - \frac{1}{m}} \left[ \left(1 - S_e^{\frac{1}{m}}\right)^{-m} + \left(1 - S_e^{\frac{1}{m}}\right)^m - 2 \right] \quad (34)$$

The diffusivity was measured by the outflow method for five tuff samples. The calculated D (equation 34) is compared to the

measured one (Figures 28 to 32). The computed curves E1 and E2 are distinguished from each other by the method of estimating the parameters  $\theta_r$ ,  $\alpha$ , and  $m$  in equation 34 (see Section 3.2 for explanation of E1 and E2). As was the case with the hydraulic conductivity, E2 predicted the observed D data better than E1 did. Notice that the slope of the curve E2 goes to infinity as  $\theta$  goes to  $\theta_s$  for all the samples, which is consistent with equation 32. E1, on the other hand, has a finite slope in three out of five cases (see Figures 29, 31 and 32). Therefore, based on the results of the limited number of samples studied, we conclude again that if it is at all possible, using the measured K along with the measured water retention data would give a better estimation for the parameters  $\theta_r$ ,  $\alpha$ , and  $n$  or  $m$  for the equations 20, 21, and 34.

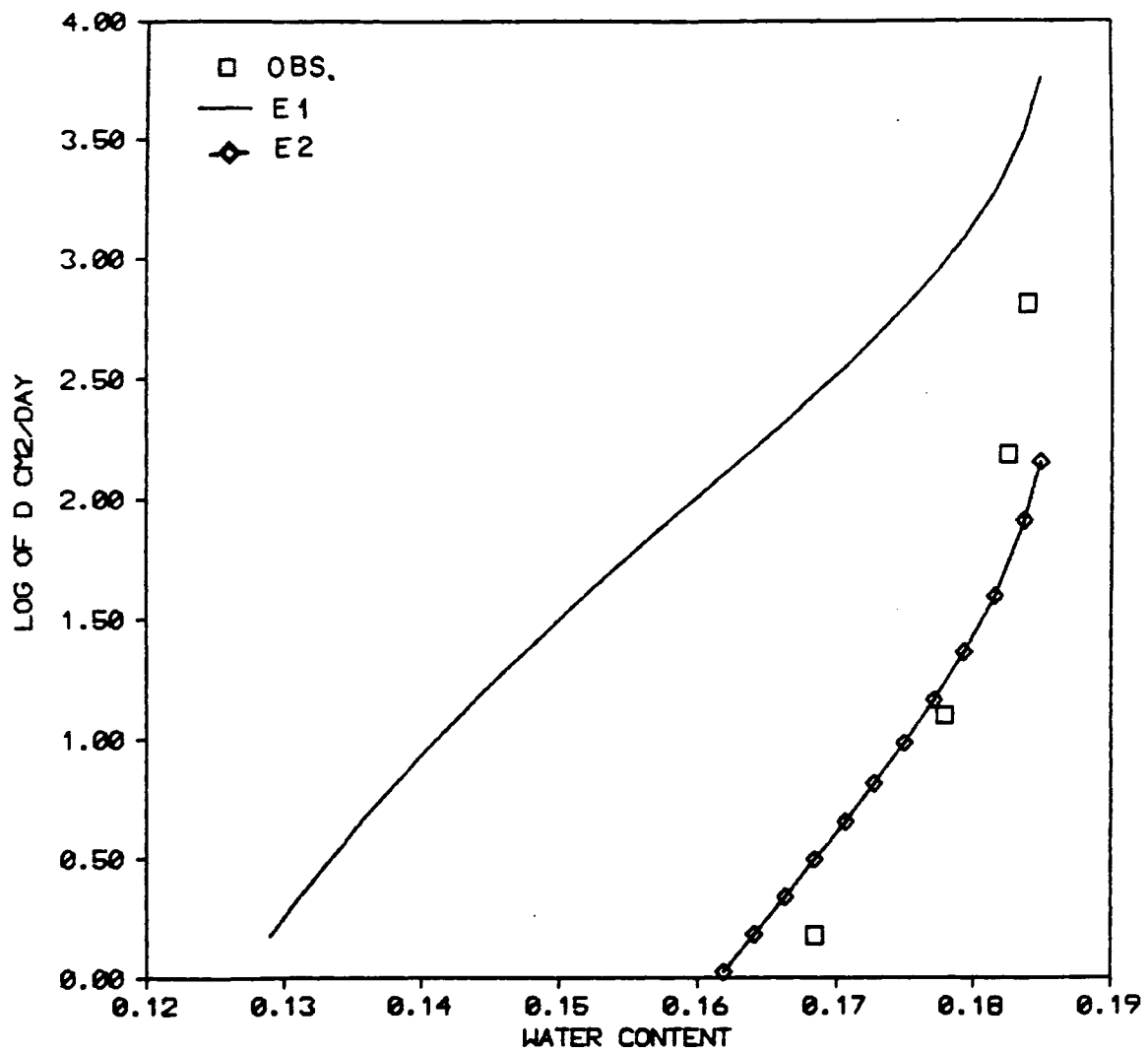


Figure 28. Observed and fitted diffusivity curves for tuff T1.

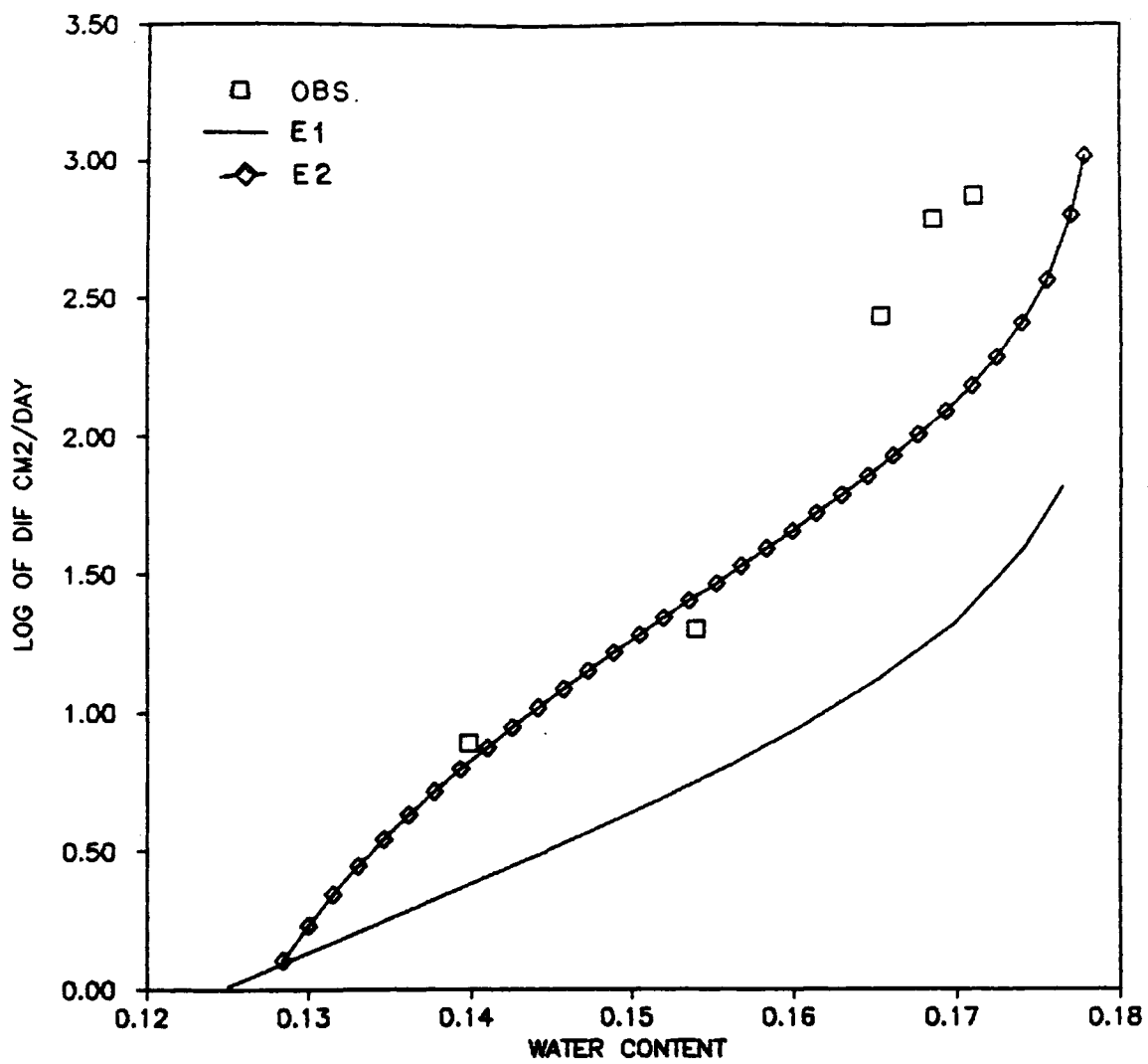


Figure 29. Fitted and observed diffusivity curves for tuff T2.

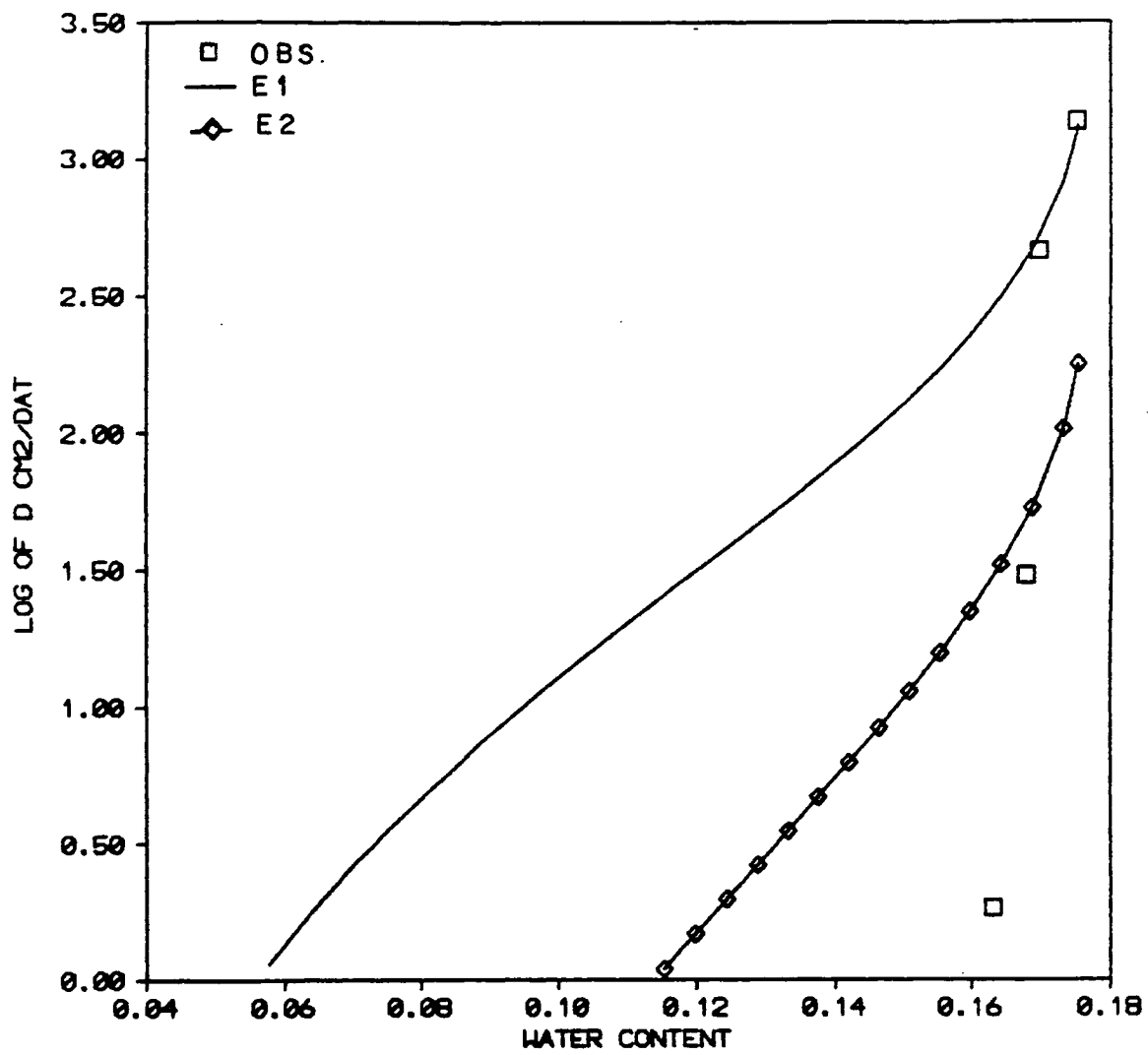


Figure 30. Fitted and observed diffusivity curves for tuff T3.

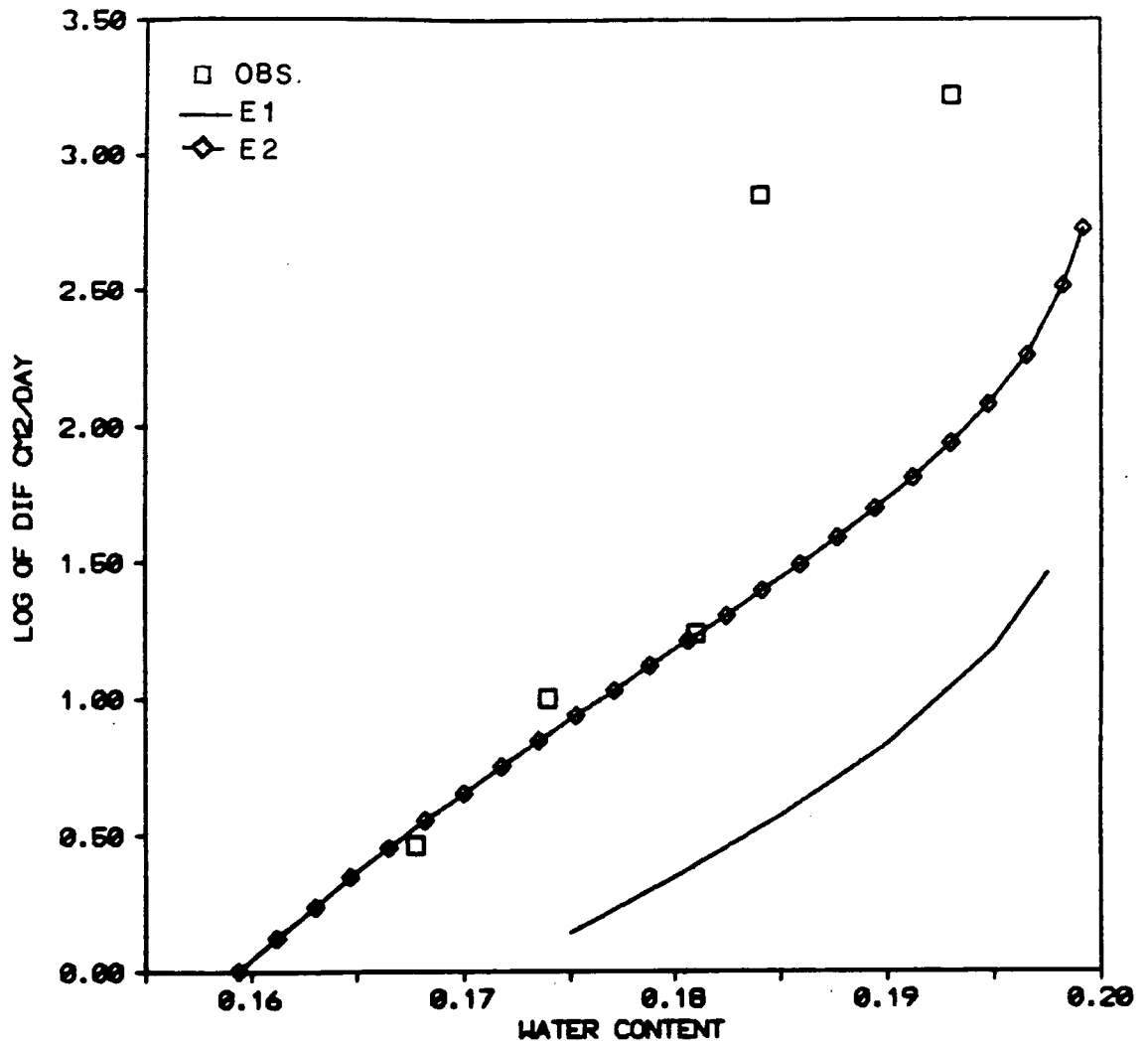


Figure 31. Observed and fitted diffusivity curves for tuff T4.

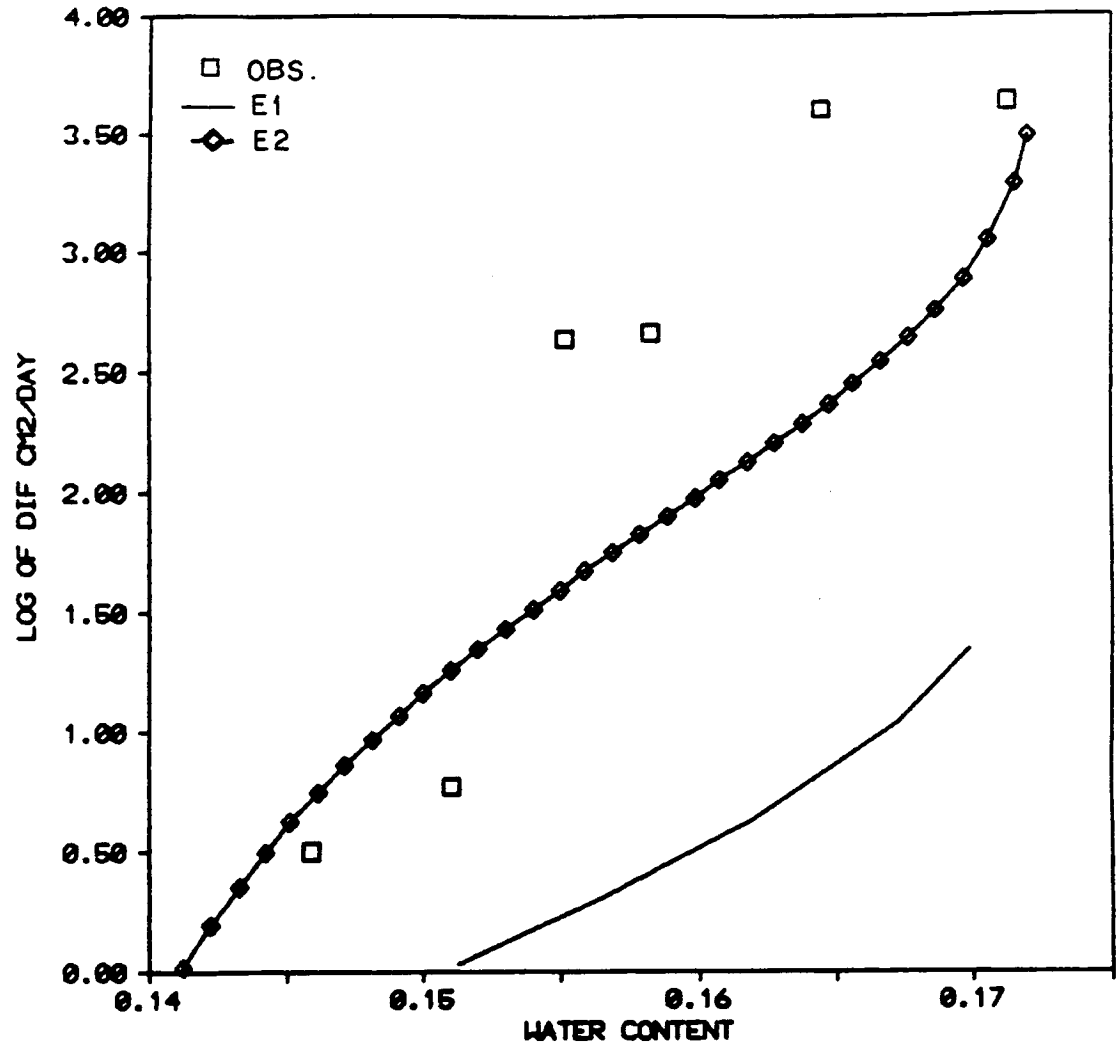


Figure 32. Fitted and observed diffusivity curves for tuff T5.

## CHAPTER 5

### SUMMARY AND CONCLUSIONS

The objective of this study is to assess the applicability of the predictive models for the unsaturated hydraulic conductivity  $K$  to a consolidated rock matrix. The models which were considered are those which make use of water retention data of the rock to predict  $K$ . Most of these models were derived for soils.

The most reliable model (van Genuchten and Nielsen, 1985) is that of Mualem (1976) which is given by equation (19). The successful prediction of  $K$  from rock retention data requires a reliable descriptive model of the retention curve. Equation (20) appeared to be a good way to predict retention curves (Peters et al, 1984, and Van Genuchten and Nielsen, 1985). Equation (20) is assumed, for the purpose of this study, to include three unknown parameters;  $\theta_r$ ,  $\alpha$ , and  $n$  or  $m$ , to be determined by fitting the model to experimental data.

In order to verify the calculated  $K$  curves, some experimental measurement of  $K$  were needed. Since, until now there is no known tested procedure to measure  $K$  for rocks, a method from the field of soil physics was used. The method, commonly known as the outflow method, was pioneered by Gardner (1956).

The water retention data were determined by two methods: the pressure plate extractor and the thermocouple psychrometer. The samples that were examined were cores from tuff and sandstone rocks.

The findings of the study are summarized as follows:

The water retention data obtained by the pressure extractor method are more accurate when compared to data from the psychrometer method near saturation. The psychrometer method overestimated the air entry value and did not predict the expected broad pore-size distribution for the tuffaceous materials. However, the pressure extractor method is very time consuming and its application is limited to a relatively small range of pressures. The psychrometer method, on the other hand, can be used to define the entire water retention curve of the sample in a matter of several hours.

The outflow method appeared to be suitable to measure  $K$ . The method is a relatively simple laboratory procedure and requires inexpensive instruments (Tempe pressure cell or similar equipment). But it also has its limitation. Besides the long time required to achieve the measurements, its application is limited to low pressures (2000 cm of pressure head at most). In addition, the method has inherent theoretical limitations, because it is based on analytical solution of the nonlinear inverse flow problem. Several assumptions (see Chapter 2) had to be made to linearize the problem and make it accessible to an analytical solution. Nevertheless, given the present situation where no method is available to measure unsaturated hydraulic conductivity for rocks, the method is considered adequate. In fact, with some improvements, the method could be used with little, if any, reservations.

The predicted K by equation (21) deviated from the observed K when the unknown parameters of the equation were estimated by fitting the water retention data alone to the model. Although the same parameters, when used in equation (20), predicted the water retention curve very well. The deviation from the observed data was more prominent when the psychrometer derived water retention data were used.

Considerable improvement in the predicted K was achieved when the unknown parameters of equation (21) were estimated by simultaneous fit of the observed conductivity and water retention data to the model. However, when these parameters were used in equation (20) to predict the water retention curve, the results, although acceptable, were not as good as those obtained from the parameters estimated from the water retention data alone.

The diffusivity of the rock matrix was also investigated. Again, the diffusivities calculated by equation (34), with its unknown parameters estimated by the simultaneous fit discussed above, approximated the observed data and the general expected shape of the diffusivity curve better than the case when the parameters from the water retention data alone were used.

Finally, it is concluded that the water retention model (equation (20)) is reliable in predicting the water retention curve for a rock matrix. However, the unsaturated hydraulic conductivity model (equation (21)) is yet to be improved to be considered reliable. The conductivity model weakness appeared to lie within the term  $(S_e^{0.5})$  which is assumed to account for partial correlation between adjacent

pores, and for tortuosity. Further examinations of the conductivity model are needed to assure its safe application for consolidated porous media.

## APPENDIX A

### DERIVATION OF MUALEM'S EQUATION

Equation 19 was developed by Mualem (1976) for homogeneous porous media, having interconnected pores defined by their radius  $r$ . The contribution of water-filled pores of radii  $r \rightarrow r + dr$  to  $\theta$  is

$$f(r) dr = d\theta \quad (\text{A.1})$$

where  $f(r)$  is the pore-size distribution. Integrating Equation 1 over the domain of water filled pores will give the water content,  $\theta$ , of the porous medium. Thus,

$$\theta = \int_{R_{\min}}^{R_f} f(r) dr \quad (\text{A.2})$$

where  $R_{\min}$  is the radius of the smallest pore and  $R_f$  is the radius of the largest of the pores filled with water. From A.2,  $\theta_s$  is given by

$$\theta_s = \int_{R_{\min}}^{R_{\max}} f(r) dr \quad (\text{A.3})$$

where  $R_{\max}$  is the radius of the largest pore in the porous medium.

Consider a porous media slab (Figure A.1) of length  $L$ . Assume that the areal porosity is equal to the volume porosity, so  $f(r) dr$  represents the ratio between the pore area of radii  $r \rightarrow r + dr$  and the total area of the cross-section of the porous media slab. The

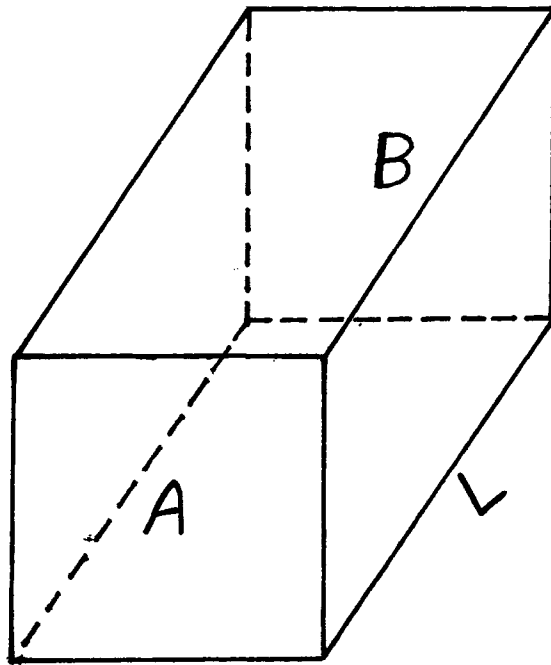


Figure A.1. Porous media slab for  
Mualem's equation.

probability of pores of radii  $r \rightarrow r + dr$  at face A encountering pores of radii  $\rho \rightarrow \rho + d\rho$  at face B is

$$F(r, \rho) = f(r) f(\rho) dr d\rho \quad (\text{A.4})$$

Equation A.4 is valid for the extreme case of  $L \gg R_{\max}$  (i.e., no direct connection between the pores  $r$  and  $\rho$  exists). The other extreme case is when  $L \rightarrow 0$ ; then, the correlation between the two faces is complete. For any length  $L$  between the above extreme cases the two pores in the sequence are assumed to be partially connected to each other. Mathematically, this partial connection is expressed by

$$F(r, \rho) = G f(r) f(\rho) dr d\rho \quad (\text{A.5})$$

where  $G$  is a correction accounting for partial correlation between the two pores.

The hydraulic conductivity through the porous media is controlled by the product  $r\rho$  (see Mualem, 1976, Appendix 1). The contribution of the  $r \rightarrow \rho$  element to the relative permeability is given by

$$dk_r = \frac{T G r \rho f(r) f(\rho) dr d\rho}{\int_{R_{\min}}^{R_{\max}} \int_{R_{\min}}^{R_{\max}} T G r \rho f(r) f(\rho) dr d\rho} \quad (\text{A.6})$$

where  $T$  is tortuosity factor. For a given water content  $\theta$ ,

$$k_r = \frac{\int_{R_{\min}}^{R_f} \int_{R_{\min}}^{R_f} T G r \rho f(r) f(\rho) dr d\rho}{\int_{R_{\min}}^{R_{\max}} \int_{R_{\min}}^{R_{\max}} T G r \rho f(r) f(\rho) dr d\rho} \quad (\text{A.7})$$

Assuming that  $T$  and  $G$  are functions of the effective saturation  $S_e$  (Burdine, 1953; Millington and Qurik, 1960), A.7 becomes

$$k_r = S_e^{\ell} \left[ \frac{\int_{R_{\min}}^{R_f} r f(r) dr}{\int_{R_{\min}}^{R_{\max}} r f(r) dr} \right]^2 \quad (\text{A.8})$$

Applying the capillary law  $r = c/h$  and A.1 to A.8, and using  $K_s$  as matching factor the unsaturated conductivity  $K$  is given by

$$K = K_s S_e^{\ell} \left[ \frac{\int_0^{S_e} \frac{1}{h(x)} dx}{\int_0^1 \frac{1}{h(x)} dx} \right]^2 \quad (\text{A.9})$$

where  $\theta$  is replaced by  $S_e$ . Equation A.9 is the same as Equation 19 in Chapter 2.

APPENDIX B

RETC COMPUTER CODE LISTING

```

C *****
C *
C *      ANALYSIS OF SOIL HYDRAULIC PROPERTIES      RETC      *
C *
C *      AUGUST, 1985
C *
C *****
C
C SUBROUTINE MAIN
C   IMPLICIT REAL*8 (A-H,O-Z)
C   DIMENSION X(100),Y(100),R(100),F(100),DELZ(100,7),W(100),B(14),
1E(7),P(7),PHI(7),Q(7),TB(14),A(7,7),D(7,7),INDEX(7),TH(14)
C   CHARACTER BI(14)*5,TITLE*60
C   DATA STOPCR/.00010/
C   DATA BI(8)/' WCR '/,BI(9)/' WCS '/,BI(10)/'ALPHA'/,BI(11)/' N '/
C   DATA BI(12)/' M '/,BI(13)/'EXPO '/,BI(14)/'CONDS'/
C
C   ----- OPEN I/O FILES -----
C   OPEN(5,FILE='RETC.IN')
C   OPEN(6,FILE='RETC.OUT')
C   CLOSE(6,STATUS='DELETE')
C   OPEN(6,FILE='RETC.OUT',STATUS='NEW')
C
C   ----- READ NUMBER OF CASES CONSIDERED -----
C   READ(5,1000) NC,NSTART,KP
C   IF(KP.NE.6) KP=1
C   DO 100 NCASE=1,NC
C   READ(5,1002) TITLE
C
C   ----- READ INPUT PARAMETERS -----
C   READ(5,1000) KEX,NWC,NOB,MTYPE,METHOD,KWATER,KIN,KOUT,KITER,MIT
C   IF(NOB.EQ.0) MIT=0
C   IF(NOB.EQ.0) KOUT=1
C   IF(MTYPE.LT.1.OR.MTYPE.GT.6) MTYPE=3
C
C   ----- READ INITIAL ESTIMATES -----
C   READ(5,1004) (B(I),I=8,14),W1
C   IF(NOB.GT.0) READ(5,1000) (INDEX(I),I=1,7)
C   IF(KWATER.EQ.1) INDEX(6)=0
C   IF(KWATER.EQ.1) INDEX(7)=0
C
C   ----- READ EXPERIMENTAL DATA -----
C   IF(NOB.GT.0) READ(5,1006) (X(I),Y(I),W(I),I=1,NOB)
C   IF(KEX.LE.0.OR.NCASE.LT.NSTART) GO TO 100
C   WRITE(KP,1008) TITLE
C   GO TO (5,5,1,2,3,3) MTYPE
1 B(11)=DMAX1(1.05D0,B(11))
C   B(12)=1.-1./B(11)
C   GO TO 4

```

```

2 B(11)=DMAX1(2.05D0,B(11))
  B(12)=1.-2./B(11)
  GO TO 4
3 B(12)=1.0
4 INDEX(5)=0
5 CONTINUE
  IF(MTYPE.EQ.1) WRITE(KP,1010)
  IF(MTYPE.EQ.2) WRITE(KP,1011)
  IF(MTYPE.EQ.3) WRITE(KP,1012)
  IF(MTYPE.EQ.4) WRITE(KP,1014)
  IF(MTYPE.EQ.5) WRITE(KP,1015)
  IF(MTYPE.EQ.6) WRITE(KP,1016)
  KLOG=0
  IF(2*(METHOD/2).EQ.METHOD) KLOG=1
  IF(KWATER.EQ.1) KLOG=0
  IF(MIT.EQ.0) GO TO 6
  IF(KWATER.EQ.1) WRITE(KP,1018)
  IF(KWATER.EQ.0.AND.METHOD.LE.4) WRITE(KP,1020)
  IF(KWATER.EQ.0.AND.METHOD.GT.4) WRITE(KP,1021)
  IF(KLOG.EQ.1) WRITE(KP,1022)
6 WRITE(KP,1023) MTYPE, METHOD
  IF(NOB.GT.0) WRITE(KP,1024) (I,BI(I+7),B(I+7),INDEX(I),I=1,7)
  NP=0
  IF(NOB.EQ.0) WRITE(KP,1024) (I,BI(I+7),B(I+7),NP,I=1,7)
  IF(NOB.EQ.0) GO TO 12

C
C ----- WRITE EXPERIMENTAL DATA -----
  IF(KIN.EQ.1) WRITE(KP,1025)
  WA=0.
  DO 7 I=1,NWC
    X(I)=DMAX1(X(I),1.D-5)
    IF(W(I).LT.1.D-3) W(I)=1.0
    WA=WA+DABS(W(I)*Y(I))
    IF(KIN.EQ.0) GO TO 7
  WRITE(KP,1026) I,X(I),Y(I),W(I)
7 CONTINUE
  WA=WA/FLOAT(NWC)
  IF(KWATER.EQ.1) GO TO 11
  IF(KIN.EQ.0) GO TO 8
  IF(METHOD.EQ.1) WRITE(KP,1027)
  IF(METHOD.EQ.2) WRITE(KP,1028)
  IF(METHOD.EQ.3) WRITE(KP,1029)
  IF(METHOD.EQ.4) WRITE(KP,1030)
  IF(METHOD.EQ.5) WRITE(KP,1031)
  IF(METHOD.EQ.6) WRITE(KP,1032)
8 WB=0.0
  NWC1=NWC+1
  DO 9 I=NWC1,NOB
    IF(METHOD.EQ.3.OR.METHOD.EQ.4) X(I)=DMAX1(X(I),1.D-5)
    IF(KLOG.EQ.1) Y(I)=DLOG10(Y(I))

```

```

IF(W(I).LT.1.D-3) W(I)=1.0
WB=WB+DABS(W(I)*Y(I))
IF(KIN.EQ.0) GO TO 9
IF(KLOG.EQ.0) WRITE(KP,1033) I,X(I),Y(I),W(I)
IF(KLOG.EQ.1) WRITE(KP,1034) I,X(I),Y(I),W(I)
9 CONTINUE
IF(MIT.EQ.0) GO TO 12
IF(W1.LT.1.D-2) W1=1.0
WB=WB/FLOAT(NOBS-NWC)
W2=WA/WB
W12=W1*W2
WRITE(KP,1036) W1,W2,W12
DO 10 I=NWC1,NOB
10 W(I)=W12*W(I)
11 CONTINUE
C
C ----- INITIALIZE UNKNOWN PARAMETERS -----
12 NP=0
DO 14 I=8,14
TB(I)=B(I)
IF(INDEX(I-7).EQ.0) GO TO 14
NP=NP+1
BI(NP)=BI(I)
B(NP)=B(I)
TB(NP)=B(I)
TH(NP)=B(I)
14 TH(I)=B(I)
IF(NOBS.EQ.0) GO TO 92
GA=0.05
DERL=0.002D0
NEXP=1+INDEX(1)+INDEX(2)+INDEX(3)+INDEX(4)+INDEX(5)
IF(KWATER.EQ.1) NOBS=NWC
C
C ----- START LEAST-SQUARES ANALYSIS -----
CALL MODEL(TH,F,X,NWC,NOBS,MTYPE,METHOD,INDEX,IOR)
IF(IOR.EQ.1) GO TO 94
IF(MIT.EQ.0) GO TO 83
SSQ=0.
DO 16 I=1,NOBS
R(I)=W(I)*(Y(I)-F(I))
16 SSQ=SSQ+R(I)*R(I)
NIT=0
WRITE(KP,1038) (BI(I),I=1,NP)
WRITE(KP,1040) NIT,SSQ,(B(I),I=1,NP)
C
C ----- BEGIN OF ITERATION -----
18 NIT=NIT+1
GA=0.05*GA
DO 22 J=1,NP
TEMP=TH(J)

```

```

TH(J)=(1.DO+DERL)*TH(J)
Q(J)=0
CALL MODEL(TH,DELZ(1,J),X,NWC,NOB,MTYPE,METHOD,INDEX,IOR)
IF(IOR.EQ.1) GO TO 94
DO 20 I=1,NOB
DELZ(I,J)=W(I)*(DELZ(I,J)-F(I))
20 Q(J)=Q(J)+DELZ(I,J)*R(I)
Q(J)=Q(J)/(TH(J)*DERL)

C
C ----- STEEPEST DESCENT -----
22 TH(J)=TEMP
DO 28 I=1,NP
DO 26 J=1,I
SUM=0.0
DO 24 K=1,NOB
24 SUM=SUM+DELZ(K,I)*DELZ(K,J)
D(I,J)=SUM/(TH(I)*TH(J)*DERL**2)
26 D(J,I)=D(I,J)
28 E(I)=DSQRT(D(I,I))
30 DO 32 I=1,NP
DO 32 J=1,NP
32 A(I,J)=D(I,J)/(E(I)*E(J))

C
C ----- A IS THE SCALED MOMENT MATRIX -----
DO 34 I=1,NP
P(I)=Q(I)/E(I)
PHI(I)=P(I)
34 A(I,I)=A(I,I)+GA
CALL MATINV(A,NP,P)

C
C ----- P/E IS THE CORRECTION VECTOR -----
STEP=1.0
36 DO 38 I=1,NP
38 TB(I)=P(I)*STEP/E(I)+TH(I)
DO 40 I=1,NP
IF(TH(I)*TB(I))44,44,40
40 CONTINUE
CALL MODEL(TB,F,X,NWC,NOB,MTYPE,METHOD,INDEX,IOR)
IF(IOR.EQ.1) GO TO 94
SUMB=0.0
DO 42 I=1,NOB
R(I)=W(I)*(Y(I)-F(I))
42 SUMB=SUMB+R(I)*R(I)
44 SUM1=0.0
SUM2=0.0
SUM3=0.0
DO 46 I=1,NP
SUM1=SUM1+P(I)*PHI(I)
SUM2=SUM2+P(I)*P(I)

```

```

46 SUM3=SUM3+PHI(I)*PHI(I)
   ARG=SUM1/DSQRT(SUM2*SUM3)
   ARG1=0.
   IF(NP.GT.1) ARG1=DSQRT(1.-ARG*ARG)
   ANGLE=57.29578*DATAN2(ARG1,ARG)
C
C   -----
   DO 48 I=1,NP
   IF(TH(I)*TB(I)) 50,50,48
48 CONTINUE
   IF((SUMB-SSQ)/SSQ.LT.1.D-5) GO TO 56
50 IF(ANGLE-30.D0) 52,52,54
52 STEP=0.5*STEP
   GO TO 36
54 GA=20.*GA
   GO TO 30
C
C   ----- PRINT COEFFICIENTS AFTER EACH ITERATION -----
56 CONTINUE
   DO 58 I=1,10
58 TH(I)=TB(I)
   IF(NIT.LT.KITER) WRITE(KP,1040) NIT,SUMB,(TH(I),I=1,NP)
   IF(INDEX(1).EQ.0) GO TO 60
   IF(NIT.LE.4.OR.TH(1).GT.0.001) GO TO 60
   INDEX(1)=0
   B(8)=0.0
   IF(NIT.GE.KITER) WRITE(KP,1040) NIT,SUMB,(TH(I),I=1,NP)
   WRITE(KP,1046)
   GO TO 12
60 IF(INDEX(6).EQ.0) GO TO 64
   EXPO=TH(NEXP)
   IF(EXPO.GT.1.D-3) GO TO 64
   IF(EXPO.LT.-1.D-3) GO TO 64
   IF(EXPO.LT.0.) GO TO 62
   B(13)=-0.2
   GO TO 12
62 B(13)=0.0001
   INDEX(6)=0
   WRITE(KP,1050) B(13)
   GO TO 12
64 DO 66 I=1,NP
   IF(DABS(P(I)*STEP/E(I))/(1.0D-20+ABS(TH(I)))-STOPCR) 66,66,68
66 CONTINUE
   GO TO 70
68 SSQ=SUMB
   IF(NIT.LE.MIT) GO TO 18
C
C   ----- END OF ITERATION LOOP -----
70 CONTINUE
   IF(NIT.GE.KITER) WRITE(KP,1040) NIT,SUMB,(TH(I),I=1,NP)

```

```

      CALL MATINV(D,NP,P)
C
C      ----- WRITE CORRELATION MATRIX -----
      DO 72 I=1,NP
72  E(I)=DSQRT(DMAX1(D(I,I),1.D-20))
      IF(NP.EQ.1) GO TO 78
      WRITE(KP,1052) (I,I=1,NP)
      DO 76 I=1,NP
      DO 74 J=1,I
74  A(J,I)=D(J,I)/(E(I)*E(J))
76  WRITE(KP,1054) I,(A(J,I),J=1,I)
C
C      ----- CALCULATE R-SQUARED OF FITTED VS OBSERVED VALUES -----
78  SUM=0.0
      SUMY=0.0
      SUMF=0.0
      SUMY2=0.0
      SUMF2=0.0
      SUMYF=0.0
      DO 80 I=1,NOB
      SUM=SUM+W(I)
      SUMY=SUMY+Y(I)*W(I)
      SUMF=SUMF+F(I)*W(I)
      SUMY2=SUMY2+Y(I)**2*W(I)
      SUMF2=SUMF2+F(I)**2*W(I)
80  SUMYF=SUMYF+Y(I)*F(I)*W(I)
      RSQ=(SUMYF-SUMY*SUMF/SUM)**2/((SUMY2-SUMY**2/SUM)*(SUMF2-SUMF**2/
1SUM))
      WRITE(KP,1056) RSQ
C
C      ----- CALCULATE 95% CONFIDENCE INTERVAL -----
      Z=1./FLOAT(NOB-NP)
      SDEV=DSQRT(Z*SUMB)
      WRITE(KP,1058)
      TVAR=1.96+Z*(2.3779+Z*(2.7135+Z*(3.187936+2.466666*Z**2)))
      DO 82 I=1,NP
      SECOEF=E(I)*SDEV
      TVALUE=TH(I)/SECOEF
      TSEC=TVAR*SECOEF
      TMCOE=TH(I)-TSEC
      TPCOE=TH(I)+TSEC
      IF(NP.EQ.1) WRITE(KP,1060) BI(I),TH(I),SECOEF,TMCOE,TPCOE
82  IF(NP.GT.1) WRITE(KP,1062) BI(I),TH(I),SECOEF,TVALUE,TMCOE,TPCOE
C
C      ----- GIVE FINAL OUTPUT -----
83  IF(MIT.GT.0) WRITE(KP,1064)
      IF(MIT.EQ.0) WRITE(KP,1065)
      SSQ1=0.0
      SSQW1=0.0
      DO 84 I=1,NWC

```

```

XLOG=DLOG10(DMAX1(1.D-5,X(I)))
R(I)=Y(I)-F(I)
SSQ1=SSQ1+R(I)**2
SSQW1=SSQW1+(R(I)*W(I))**2
84 WRITE(KP,1066) I,X(I),XLOG,Y(I),F(I),R(I)
   IF(KWATER.EQ.1) GO TO 90
C
C ----- WRITE CONDUCTIVITY OR DIFFUSIVITY DATA -----
IF(METHOD.EQ.1) WRITE(KP,1068)
IF(METHOD.EQ.2) WRITE(KP,1069)
IF(METHOD.EQ.3) WRITE(KP,1070)
IF(METHOD.EQ.4) WRITE(KP,1071)
IF(METHOD.EQ.5) WRITE(KP,1072)
IF(METHOD.EQ.6) WRITE(KP,1073)
SSQ2=0.0
SSQW2=0.0
DO 88 I=NWC1,NOB
R(I)=Y(I)-F(I)
SSQ2=SSQ2+R(I)**2
SSQW2=SSQW2+(R(I)*W(I))**2
RLX=DLOG10(DMAX1(1.D-30,X(I)))
RLY=DLOG10(DMAX1(1.D-30,Y(I)))
RPZ=10.**DMIN1(3.D1,Y(I))
RLF=DLOG10(DMAX1(1.D-30,F(I)))
RPF=10.**DMIN1(3.D1,F(I))
IF(METHOD.EQ.1.OR.METHOD.EQ.5) WRITE(KP,1074) I,X(I),Y(I),F(I),
1R(I),RLY,RLF
IF(METHOD.EQ.2.OR.METHOD.EQ.6) WRITE(KP,1075) I,X(I),Y(I),F(I),
1R(I),RPZ,RPF
IF(METHOD.EQ.3) WRITE(KP,1076) I,X(I),RLX,Y(I),F(I),R(I),RLY
IF(METHOD.EQ.4) WRITE(KP,1077) I,X(I),RLX,Y(I),F(I),R(I),RPZ
88 CONTINUE
SSQ=SSQ1+SSQ2
SSQW=SSQW1+SSQW2
WRITE(KP,1078) SSQ1,SSQW1,SSQ2,SSQW2,SSQ,SSQW
90 CONTINUE
92 IF(KOUT.EQ.1) CALL PRINT(KP,MTYPE,TH)
94 IF(IOR.EQ.1) WRITE(1080)
   WRITE(KP,1082)
   WRITE(KP,'(A)') CHAR(12)
100 CONTINUE
C
C ----- END OF PROBLEM -----
1000 FORMAT(10I5)
1002 FORMAT(A60)
1004 FORMAT(8F10.0)
1006 FORMAT(F10.0,F15.0,F10.0)
1008 FORMAT(5X,67(1H*)/5X,1H*,65X,1H*/5X,1H*,5X,'ANALYSIS OF SOIL HYDRA
1ULIC PROPERTIES',23X,1H*/5X,1H*,65X,1H*/5X,1H*,A60,5X,1H*/5X,1H*,
265X,1H*)

```

```

1010 FORMAT(5X,1H*,5X,'VARIABLE N AND M (MUALEM-THEORY FOR K)',22X,1H*)
1011 FORMAT(5X,1H*,5X,'VARIABLE N AND M (BURDINE-THEORY FOR K)',21X,1H*
1)
1012 FORMAT(5X,1H*,5X,'MUALEM-BASED RESTRICTION, M=1-1/N',27X,1H*)
1014 FORMAT(5X,1H*,5X,'BURDINE-BASED RESTRICTION, M=1-2/N',26X,1H*)
1015 FORMAT(5X,1H*,5X,'BROOKS AND COREY EQUIVALENT (MUALEM)',24X,1H*)
1016 FORMAT(5X,1H*,5X,'BROOKS AND COREY EQUIVALENT (BURDINE)',23X,1H*)
1018 FORMAT(5X,1H*,5X,'ANALYSIS OF RETENTION DATA ONLY',29X,1H*)
1020 FORMAT(5X,1H*,5X,'SIMULTANEOUS FIT OF RETENTION AND CONDUCTIVITY D
1ATA',9X,1H*)
1021 FORMAT(5X,1H*,5X,'SIMULTANEOUS FIT OF RETENTION AND DIFFUSIVITY DA
1TA',10X,1H*)
1022 FORMAT(5X,1H*,5X,'FIT ON LOG-TRANSFORMED K/D DATA',29X,1H*)
1023 FORMAT(5X,1H*,5X,'MTYPE=',I2,5X,'METHOD=',I2,38X,1H*/5X,1H*,65X,
11H*/5X,67(1H*))
1024 FORMAT(//5X,'INITIAL VALUES OF THE COEFFICIENTS'/5X,34(1H=)/5X,'NO
1',6X,'NAME',8X,'INITIAL VALUE',3X,'INDEX'/(4X,I3,5X,A6,4X,F12.4,7X
2,I3))
1025 FORMAT(///5X,'OBSERVED DATA'/5X,13(1H=)/5X,'OBS. NO.',4X,'PRESSURE
1 HEAD',5X,'WATER CONTENT',5X,'WEIGHTING COEFFICIENT')
1026 FORMAT(5X,I5,4X,F12.3,7X,F12.4,7X,F12.4)
1027 FORMAT(17X,'WATER CONTENT',6X,'CONDUCTIVITY',5X,'WEIGHTING COEFFIC
1IENT')
1028 FORMAT(17X,'WATER CONTENT',4X,'LOG-CONDUCTIVITY',3X,'WEIGHTING COE
1FFICIENT')
1029 FORMAT(/5X,'NO',5X,'PRESSURE',5X,'COND',7X,'WEIGHT')
1030 FORMAT(/5X,'NO',5X,'PRESSURE',5X,'LOG-COND',5X,'WEIGHT')
1031 FORMAT(/5X,'NO',5X,'WC',7X,'DIF',7X,'WEIGHT')
1032 FORMAT(/5X,'NO',5X,'WC',5X,'LOG-DIF',5X,'WEIGHT')
1033 FORMAT(5X,I5,4X,F12.4,8X,D12.4,7X,F12.4)
1034 FORMAT(5X,I5,4X,F12.4,7X,F12.4,7X,F12.4)
1036 FORMAT(/5X,'WEIGHTING COEFFICIENTS'/5X,22(1H=)/5X,'W1=',F9.5,4X,
1'W2=',F9.5,5X,'W12=',F9.5)
1038 FORMAT(//5X,'NIT',5X,'SSQ',2X,7(3X,A5))
1040 FORMAT(4X,I3,F11.5,7F8.4)
1042 FORMAT(//5X,'PARAMETER N IS TOO SMALL, THIS CASE IS NOT EXECUTED')
1046 FORMAT(//5X,'WCR IS LESS THEN 0.001: CHANGED TO FIT WITH WCR=0.0')
1050 FORMAT(40X,'EXPO FIXED AT ',F8.6)
1052 FORMAT(//5X,'CORRELATION MATRIX'/5X,18(1H=)/8X,10(4X,I2,4X))
1054 FORMAT(4X,I3,10(2X,F7.4,1X))
1056 FORMAT(//5X,'RSQUARED FOR REGRESSION OF OBSERVED VS FITTED VALUES
1=',F11.8/5X,65(1H=))
1058 FORMAT(//5X,'NONLINEAR LEAST-SQUARES ANALYSIS: FINAL RESULTS'/
25X,47(1H=)/50X,'95% CONFIDENCE LIMITS'/5X,'VARIABLE',5X,'VALUE',
25X,'S.E.COEFF.',3X,'T-VALUE',5X,'LOWER',7X,'UPPER')
1060 FORMAT(5X,A6,F13.5,F12.5,8X,'--',2X,2F11.4)
1062 FORMAT(5X,A6,F13.5,F12.5,4X,F8.2,2F11.4)
1064 FORMAT(//5X,'OBSERVED AND FITTED DATA'/5X,24(1H=)/5X,'NO',9X,'P',
19X,'LOG-P',4X,'WC-OBS',4X,'WC-FIT',4X,'WC-DIF')

```

```

1065 FORMAT(/5X,'OBSERVED AND CALCULATED VALUES (FOR CALCULATED VALUES
1'/5X,29(1H=),' USE THE FIT-LABELED ENTRIES)'/5X,'NO',9X,'P',9X,
2'LOG-P',4X,'WC-OBS',4X,'WC-FIT',4X,'WC-DIF')
1066 FORMAT(4X,I3,D14.4,4F10.4)
1068 FORMAT(/12X,'WC',6X,'K-OBS',7X,'K-FIT',7X,'K-DEV',6X,'LOGK-OBS',
12X,'LOGK-FIT')
1069 FORMAT(/12X,'WC',5X,'LOGK-OBS',2X,'LOGK-FIT',2X,'LOGK-DEV',
13X,'K-OBS',7X,'K-FIT')
1070 FORMAT(/15X,'P',7X,'LOG-P',4X,'K-OBS',7X,'K-FIT',7X,'K-DEV',
15X,'LOGK-OBS')
1071 FORMAT(/15X,'P',7X,'LOG-P',3X,'LOGK-OBS',2X,'LOGK-FIT',2X,
1'LOGK-DEV',4X,'K-OBS')
1072 FORMAT(/12X,'WC',6X,'D-OBS',7X,'D-FIT',7X,'D-DEV',6X,'LOGD-OBS',
12X,'LOGD-FIT')
1073 FORMAT(/12X,'WC',5X,'LOGD-OBS',2X,'LOGD-FIT',2X,'LOGD-DIF',
14X,'D-OBS',7X,'D-FIT')
1074 FORMAT(4X,I3,F9.4,3D12.4,2F10.4)
1075 FORMAT(4X,I3,F9.4,3F10.4,2D12.4)
1076 FORMAT(4X,I3,D13.4,F8.4,3D12.4,F10.4)
1077 FORMAT(4X,I3,D13.4,F8.4,3F10.4,D12.4)
1078 FORMAT(/5X,'SUM OF SQUARES OF OBSERVED VERSUS FITTED VALUES'/5X,
147(1H=)/22X,'UNWEIGHTED',3X,'WEIGHTED'/5X,'RETENTION DATA',2F12.5/
25X,'COND/DIFF DATA',2F12.5/11X,'ALL DATA',2F12.5)
1080 FORMAT(/5X,'PARAMETER N IS TOO SMALL, THIS CASE IS NOT EXECUTED')
1082 FORMAT(/5X,'END OF PROBLEM'/5X,14(1H=))
CLOSE(5)
CLOSE(6)
STOP
END

```

C  
C  
C  
C  
C

```

-----
SUBROUTINE MODEL(B,Y,X,NWC,NOB,MTYPE,METHOD,INDEX,IOR)

```

```

PURPOSE: TO CALCULATE THE HYDRAULIC PROPERTIES

```

```

IMPLICIT REAL*8 (A-H,O-Z)
DIMENSION B(14),Y(100),X(100),INDEX(7)
K=0
IOR=0
DO 2 I=8,14
IF(INDEX(I-7).EQ.0) GO TO 2
K=K+1
B(I)=B(K)
2 CONTINUE
WCR=B(8)
WCS=B(9)
ALPHA=B(10)
IND=INDEX(1)+INDEX(2)+INDEX(3)+INDEX(4)
B(11)=DMAX1(1.005DO,B(11))
IF(MTYPE.EQ.3) B(12)=1.-1./B(11)

```

```

IF(MTYPE.NE.4) GO TO 4
B(11)=DMAX1(2.005D0,B(11))
B(12)=1.-2./B(11)
4 IF(IND.GT.0) B(IND)=B(11)
RN=B(11)
RM=B(12)
EXPO=B(13)
CONDS=B(14)
RMN=RM*RN
DLGA=DLOG10(ALPHA)
RMT=FLOAT(MTYPE-2*((MTYPE-1)/2))
IF(NOB.EQ.NWC) GO TO 12
C
C -----CALCULATE COMPLETE BETA FUNCTION-----
IF(MTYPE.GT.2) GO TO 10
AA=RM+RMT/RN
BB=1.-RMT/RN
IF(BB.GT.0.004) GO TO 8
IOR=1
GO TO 60
8 BETA=GAMMA(AA)*GAMMA(BB)/GAMMA(RM+1.)
WCL=DMAX1(2./(2.+RM),0.2D0)
DLG1=(3.0-RMT)*DLOG10(RN/(BETA*(RMN+RMT)))
10 DLG2=3.0-RMT+EXPO+2.0/RMN
DLG3=DLOG10(RMN*ALPHA*(WCS-WCR))
DLG4=DLOG10(CONDS)
DLGC=-35.0
DLGD=-35.0
C
C ----- CALCULATE FUNCTIONAL VALUES Y(I) -----
12 DO 54 I=1,NOB
IF(METHOD.EQ.3.OR.METHOD.EQ.4) GO TO 13
IF(I.GT.NWC) GO TO 28
13 AX=ALPHA*X(I)
IF(AX.LT.1.D-20) GO TO 16
EX=RN*DLOG10(AX)
IF(MTYPE.LT.5) GO TO 14
IF(AX.LE.1.) GO TO 16
IF(EX.GT.10.) GO TO 20
GO TO 22
14 IF(EX.GT.-10.) GO TO 18
16 RWC=1.0
GO TO 26
18 IF(EX.LT.10.) GO TO 24
EX=RM*EX
IF(EX.LT.30.) GO TO 22
20 RWC=0.0
GO TO 26
22 RWC=AX**(-RM*RN)
GO TO 26

```

```

24 RWC=(1.+AX**RN)**(-RM)
26 Y(I)=WCR+(WCS-WCR)*RWC
   IF(I.LE.NWC) GO TO 54
   GO TO 30

```

C  
C

```

----- CONDUCTIVITY DATA -----
28 RWC=(X(I)-WCR)/(WCS-WCR)
30 IF(RWC.GT.1.D-10) GO TO 31
   DLGC=-30
   DLGD=-30
   COND=1.D-30
   DIF=1.D-30
   GO TO 50
31 IF(RWC.LT.0.999999D0) GO TO 32
   DLGC=DLG4
   COND=CONDS
   DLGD=30.0
   DIF=1.D30
   GO TO 50
32 DLGW=DLOG10(RWC)
   DLGC=DLG2*DLGW+DLG4
   DLGD=DLGC-DLG3-(RMN+1)*DLGW/RMN
   IF(DLGC.LT.-30..OR.DLGW.LT.(-15.*RM)) GO TO 48
   IF(MTYPE.GT.4) GO TO 46
   DW=RWC**(1./RM)
   IF(MTYPE.GT.2) GO TO 42

```

C  
C

```

----- MTYPE = 1 OR 2 (VARIABLE M,N) -----
IF(DW.GT.1.D-06) GO TO 34
DLGC=DLGC+DLG1
DLGD=DLGC-DLG3-(RMN+1.)*DLGW/RMN
GO TO 48
34 IF(RWC-WCL) 36,36,38
36 TERM=BINC(DW,AA,BB,BETA)
   GO TO 44
38 TERM=1.-BINC(1.-DW,BB,AA,BETA)
   GO TO 44

```

C  
C

```

----- MTYPE = 3 OR 4 (RESTRICTED M,N) -----
42 A=DMIN1(0.999999D0,DMAX1(1.D-7,1.-DW))
   TERM=1.DO-A**RM
   IF(DW.LT.1.D-04) TERM=RM*DW*(1.-0.5*(RM-1.)*DW)
44 RELK=RWC**EXPO*TERM
   IF(RMT.LT.1.5) RELK=RELK*TERM
   DLGC=DLOG10(RELK)+DLG4
   DLGD=DLGC-DLG3-(RMN+1.)*DLGW/RMN-(RN-1.)*DLOG10(1.-DW)/RN
   GO TO 48

```

C  
C

```

----- MTYPE = 5 OR 6 -----
46 DLGD=DLG4-DLG3+(2.0-RMT+EXPO+1./RN)*DLGW

```

```

48 DLGC=DMAX1(-30.DO,DLGC)
   DLGD=DMAX1(-30.DO,DLGD)
   DLGD=DMIN1(30.DO,DLGD)
   COND=10.**DLGC
   DIF=10.**DLGD
50 IF(METHOD.EQ.1.OR.METHOD.EQ.3) Y(I)=COND
   IF(METHOD.EQ.2.OR.METHOD.EQ.4) Y(I)=DLGC
   IF(METHOD.EQ.5) Y(I)=DIF
   IF(METHOD.EQ.6) Y(I)=DLGD
1000 FORMAT(I5,6D13.5)
54 CONTINUE
60 CONTINUE
   RETURN
   END

```

C

C

```
-----
SUBROUTINE MATINV(A,NP,B)
```

C

C

```
PURPOSE: TO INVERT THE MATRIX FOR PARAMETER ESTIMATION
```

C

```

IMPLICIT REAL*8 (A-H,O-Z)
DIMENSION A(7,7),B(7),INDEX(7,2)
DO 2 J=1,7
2 INDEX(J,1)=0
  I=0
4 AMAX=-1.0
  DO 12 J=1,NP
    IF(INDEX(J,1)) 12,6,12
6 DO 10 K=1,NP
  IF(INDEX(K,1)) 10,8,10
8 P=ABS(A(J,K))
  IF(P.LE.AMAX) GO TO 10
  IR=J
  IC=K
  AMAX=P
10 CONTINUE
12 CONTINUE
  IF(AMAX) 30,30,14
14 INDEX(IC,1)=IR
  IF(IR.EQ.IC) GO TO 18
  DO 16 L=1,NP
  P=A(IR,L)
  A(IR,L)=A(IC,L)
16 A(IC,L)=P
  P=B(IR)
  B(IR)=B(IC)
  B(IC)=P
  I=I+1
  INDEX(I,2)=IC

```

```

18 P=1./A(IC,IC)
   A(IC,IC)=1.0
   DO 20 L=1,NP
20  A(IC,L)=A(IC,L)*P
   B(IC)=B(IC)*P
   DO 24 K=1,NP
   IF(K.EQ.IC) GO TO 24
   P=A(K,IC)
   A(K,IC)=0.0
   DO 22 L=1,NP
22  A(K,L)=A(K,L)-A(IC,L)*P
   B(K)=B(K)-B(IC)*P
24  CONTINUE
   GO TO 4
26  IC=INDEX(I,2)
   IR=INDEX(IC,1)
   DO 28 K=1,NP
   P=A(K,IR)
   A(K,IR)=A(K,IC)
28  A(K,IC)=P
   I=I-1
30  IF(I) 26,32,26
32  RETURN
   END

```

C  
C  
C  
C  
C

-----  
FUNCTION GAMMA(Z)

PURPOSE: TO CALCULATE THE GAMMA FUNCTION FOR POSITIVE Z

```

IMPLICIT REAL*8 (A-H,O-Z)
IF(Z.LT.33.) GO TO 2
GAMMA=1.D36
RETURN
2  X=Z
   GAMMA=1.0
   IF(X-2.0) 10,10,8
6  IF(X-2.0) 14,14,8
8  X=X-1.0
   GAMMA=GAMMA*X
   GO TO 6
10 IF(X-1.0) 12,16,14
12 GAMMA=GAMMA/X
   X=X+1.0
14 Y=X-1.0
   FY=1.0-Y*(.5771017-Y*(.985854-Y*(.8764218-Y*(.8328212-Y*(.5684729-
2Y*(.2548205-.0514993*Y))))))
   GAMMA=GAMMA*FY
16 RETURN
   END

```

```

C
C -----
C FUNCTION BINC(X,A,B,BETA)
C
C PURPOSE: TO CALCULATE THE INCOMPLETE BETA-FUNCTION
C
C IMPLICIT REAL*8 (A-H,O-Z)
C DIMENSION T(100)
C DATA NT/10/
C NT1=NT+1
C T(1)=- (A+B)*X/(A+1.0)
C DO 2 I=2,NT,2
C Y=FLOAT(I/2)
C Y2=FLOAT(I)
C T(I)=Y*(B-Y)*X/((A+Y2-1.0)*(A+Y2))
2 T(I+1)=- (A+Y)*(A+B+Y)*X/((A+Y2)*(A+Y2+1.0))
C BINC=1.0
C DO 4 I=1,NT
C K=NT1-I
4 BINC=1.+T(K)/BINC
C BINC=X**A*(1.-X)**B/(BINC*A*BETA)
C RETURN
C END

```

```

C
C -----
C SUBROUTINE PRINT(KP,MTYPE,TH)
C
C PURPOSE: TO PRINT THE SOIL-HYDRAULIC PROPERTIES
C
C IMPLICIT REAL*8(A-H,O-Z)
C DIMENSION TH(14)
C DATA NW/42/,DWC/.025/
C WRITE(KP,1000) MTYPE
C WCR=TH(8)
C WCS=TH(9)
C ALPHA=TH(10)
C RN=TH(11)
C RM=TH(12)
C EXPO=TH(13)
C CONDS=TH(14)
C COND=0.0
C DIF=0.0
C RMN=RM*RN
C DLGA=DLOG10(ALPHA)
C RMT=FLOAT(MTYPE-2*((MTYPE-1)/2))
C IF(MTYPE.GT.2) GO TO 4
C AA=RM+RMT/RN
C BB=1.-RMT/RN
C IF(BB.GT.0.004) GO TO 2
C WRITE(KP,1002) RN

```

```

GO TO 28
2 BETA=GAMMA(AA)*GAMMA(BB)/GAMMA(RM+1.)
  WCL=DMAX1(2./(2.+RM),0.2D0)
  DLG1=(3.0-RMT)*DLOG10(RN/(BETA*(RMN+RMT)))
4 DLG2=3.0-RMT+EXPO+2.0/RMN
  DLG3=DLOG10(RMN*ALPHA*(WCS-WCR))
  DLG4=DLOG10(CONDS)
C
C ----- CALCULATE CURVE -----
DO 24 I=1,NW
  RWC=FLOAT(I-2)*DWC
  IF(I.EQ.1) RWC=0.25*DWC
  IF(I.EQ.2) RWC=0.5*DWC
  IF(I.EQ.NW) RWC=1.-0.5*DWC
  WC=WCR+(WCS-WCR)*RWC
  DLGW=DLOG10(RWC)
  DLGC=DLG2*DLGW+DLG4
  DLGP=-DLGA-DLGW/RMN
  IF(DLGW.GT.(-6.*RM).AND.MTYPE.LT.5) DLGP=DLGP+DLOG10(1.-RWC**(1./
1RM))/RN
  IF(DLGP.GT.20..OR.DLGC.LT.-30..OR.DLGW.LT.(-15.*RM)) GO TO 24
  PP=10.**DLGP
  IF(MTYPE.GT.4) GO TO 18
  DW=RWC**(1./RM)
  IF(MTYPE.GT.2) GO TO 14
  IF(DW.GT.1.D-06) GO TO 6
  DLGC=DLGC+DLG1
  DLGD=DLGC-DLG3-(RMN+1.)*DLGW/RMN
  GO TO 20
6 IF(RWC-WCL) 8,8,10
8 TERM=BINC(DW,AA,BB,BETA)
  GO TO 16
10 TERM=1.-BINC(1.-DW,BB,AA,BETA)
  GO TO 16
14 TERM=1.-RWC*(ALPHA*PP)**RMN
  IF(DW.LT.1.D-04) TERM=RM*DW*(1.-0.5*(RM-1.)*DW)
16 RELK=RWC**EXPO*TERM
  IF(RMT.LT.1.5) RELK=RELK*TERM
  DLGC=DLOG10(RELK)+DLG4
  DLGD=DLGC-DLG3-(RMN+1.)*DLGW/RMN-(RN-1.)*DLOG10(1.-DW)/RN
  GO TO 20
18 DLGD=DLG4-DLG3+(2.0-RMT+EXPO+1./RN)*DLGW
20 IF(ABS(DLGC).LT.35.) COND=10.**DLGC
  IF(ABS(DLGD).LT.35.) DIF=10.**DLGD
22 WRITE(KP,1004) WC,PP,DLGP,COND,DLGC,DIF,DLGD
24 CONTINUE
  IF(MTYPE.GT.4) GO TO 26
  PP=0.
  WRITE(KP,1006) WCS,PP,CONDS,DLG4
  GO TO 28

```

```
26 PP=1./ALPHA
   DLGP=DLOG10(PP)
   DLGD=DLG4-DLG3
   DIF=10.**DIF
   WRITE(KP,1004) WCS,PP,DLGP,CONDS,DLG4,DIF,DLGD
28 CONTINUE
```

```
C
C
```

```
-----
1000 FORMAT(//5X,'SOIL HYDRAULIC PROPERTIES (MTYPE =',I2,')'/5X,37(1H=)
   1/8X,'WC',8X,'P',8X,'LOGP',5X,'COND',7X,'LOGK',7X,'DIF',7X,'LOGD')
1002 FORMAT(//5X,'PARAMETER N IS TOO SMALL (N=',F8.5,'): THIS CASE IS N
   10T EXECUTED')
1004 FORMAT(4X,F7.4,D13.4,F7.3,2(D13.4,F8.3))
1006 FORMAT(4X,F7.4,D13.4,7X,D13.4,F8.3)
   RETURN
   END
```

## REFERENCES

- Blake, F. C., The resistance of packing to fluid flow. Trans. Amer. Inst. Chem. Engrs., 14, 415-421, 1922.
- Blake, G. R., Particle density, In Methods of soil analysis, eds. C. A. Black, D. D. Evans, J. L. White, L. E. Emsminger, and F. E. Clark, Agronomy 9, 371-373, 1965.
- Brooks, R. H., and A. T. Corey, Hydraulic properties of porous media, Hydrol. Pap. 3, Colo. State Univ., Fort Collins, 1964.
- Brooks, R. A., and A. T. Corey, Hydraulic properties of porous media affecting fluid flow, J. Irrig. Drain. Div. Amer. Soc. Civil. Eng., 92(IR2), 61-88, 1966.
- Burdine, N. T. Relative permeability calculation from size distribution data, Trans. AIME, 198, 71-78, 1953.
- Carman, P. G., Fluid flow through granular beds, Trans. Instn. Chem. Engrs., Lond., 15, 150-166, 1937.
- Carman, P. G., Flow of gases through porous media, Academic Press Inc., Publ., New York, 1956.
- Childs, E. C., and Collis-George, The permeability of porous materials, Proc. Roy. Soc., Ser. A. 201, 392-405, 1950.
- Gardner, W. R., Calculation of capillary conductivity from pressure plate outflow data, Soil Sci. Soc. Amer. Proc. 20, 317-320, 1956.
- Green, R. E., and J. C. Corey, Calculation of hydraulic conductivity: A further evaluation of some predictive methods, Soil Sci. Soc. Amer. Proc., 35, 3-8, 1950.
- Jackson, Ray D., On the calculation of hydraulic conductivity, Soil Sci. Soc. Amer. Proc., 36, 380-382, 1972.
- Jackson, R. D., R. J. Reginato, and C. H. M. Van Bavel, Comparison of measured and calculated hydraulic conductivities of unsaturated soils, Water Resour. Res., 1(3), 375-380, 1965.
- Klute, A., The determination of the hydraulic conductivity and diffusivity of unsaturated soils, Soil Sci., 113(4), 264-276, 1972.

- Kozeny, J., Uber-Kaillare leitang des wassers in Boden, Cited in Carman, P. C., Flow of gases through porous media, Academic Press Inc. Publ., N.Y., 1956.
- Kunze, R. J., and Don Kirkham, Simplified accounting for membrane impedance in capillary conductivity determination, Soil Sci. Soc. Amer. Proc., 26, 421-426, 1962.
- Kunze, R. J., G. Uehara, and K. Graham, Factors important in the calculation of hydraulic conductivity, Soil Sci. Soc. Amer. Proc., 32, 760-765, 1968.
- Marshal, T. J., A relation between permeability and size distribution of pores, J. Soil Sci., 9, 1-8, 1958.
- Millington, R. J., and J. P. Qurik, Transport in porous media, Int. Congr. Soil Sci., Trans. 7th (Madison, Wis.) 1.3:97-106, 1960.
- Millington, R. J., and J. P. Qurik, Permeability of porous solids, Trans. Faraday Soc., 57, 1200-1206, 1961.
- Miller, E. E., and D. E. Elrick, Dynamic determination of capillary conductivity extended for non-negligible membrane impedance, Soil Sci. Soc. Amer. Proc., 22, 483-486, 1958.
- Mualem, Y., A new model for predicting the hydraulic conductivity of unsaturated porous media, Water Resour. Res., 12(3), 513-522, 1976.
- Mualem, Y., and A. Klute, A predictor-corrector method for measurement of hydraulic conductivity and membrane conductance, Soil Sci. Soc. Am. J., 48, 993-1000, 1984.
- Nielsen, D. R., D. Kirkham, and E. R. Perrier, Soil capillary conductivity: Comparison of measured and calculated values, Soil Sci. Soc. Amer. Proc., 24, 157-160, 1960.
- Peters, R. R., E. A. Klaveter, I. J. Hall, S. C. Blair, P. R. Heller, and G. W. Gee, Fracture and matrix hydrologic characteristics of tuffaceous materials from Yucca Mountain, Nye County, Nevada, Sandia Report, Sand 84-1471, 188 pp., Sandia Nat. Lab., Albuquerque, N.M., 1984.
- Richards, L. A., Physical condition of water in soil, In Methods of soil analysis, eds. C. A. Black, D. D. Evans, J. L. White, L. E. Emsinger, and F. E. Clark, Agronomy 9, 128-152, 1965.
- Rijtema, P. E., Calculation of capillary conductivity from pressure plate outflow data with non-negligible membrane impedance, Netherlands J. Agric. Sci., 7, 209-215, 1959.

- Tucson Water, CAP water quality impacts, SAWARA, 3(12), 1985.
- Van Genuchten, M. Th., Calculating the unsaturated hydraulic conductivity with a new closed-form analytical model, Research Report 78-WR-08, Dept. of Civil Eng., Princeton Univ., Princeton, New Jersey, 63 pp., 1978.
- Van Genuchten, M. Th., A closed-form equation for predicting the hydraulic conductivity of unsaturated soils, Soil Sci. Soc. Am. J., 44, 892-898, 1980.
- Van Genuchten, M. Th., Program: REWTC.F77, Unpublished manuscripts, 1985.
- Van Genuchten, M. Th., and D. R. Nielsen, On describing and predicting the hydraulic properties of unsaturated soils, Annales Geophysicae 3(5), 615-628, 1985.
- Wyllie, M. R. J. and M. B. Spangler, Application of electrical resistivity measurements to problem of fluid flow in porous media, Bull. Amer. Assoc. Petrol. Geol., 36(2), 359-403, 1952.
- Yates, S. R., M. Th. Van Genuchten, and A. W. Warrick, Fitting closed-form equation to unsaturated soil hydraulic properties, Dept. of Soils, Water and Engr., Univ. of Arizona, Unpublished manuscripts, 1985.